Active fault hazards in the Taupō District

NJ Litchfield
RJ Van Dissen
R Morgenstern
DB Townsend
P Villamor
SD Kelly

GNS Science Consultancy Report 2020/31
August 2020

DISCLAIMER

This report has been prepared by the Institute of Geological and Nuclear Sciences Limited (GNS Science) exclusively for and under contract to Taupō District Council. Unless otherwise agreed in writing by GNS Science, GNS Science accepts no responsibility for any use of or reliance on any contents of this report by any person other than Taupō District Council and shall not be liable to any person other than Taupō District Council, on any ground, for any loss, damage or expense arising from such use or reliance.

Use of Data:

Date that GNS Science can use associated data: May 2020

BIBLIOGRAPHIC REFERENCE

Litchfield NJ, Morgenstern R, Villamor P, Van Dissen RJ, Townsend DB, Kelly SD. 2020. Active faults in the Taupō District. Lower Hutt (NZ): GNS Science. 114 p. Consultancy Report 2020/31.

CONTENTS

FIGURES

TABLES

APPENDICES

APPENDIX FIGURES

APPENDIX TABLES

EXECUTIVE SUMMARY

Taupō District Council have identified a need to update active faults in their District Plan and gain a better understanding of the risks associated with active fault hazards. Taupō District Council commissioned GNS Science to provide this information, with the specific tasks of: 1) compiling existing information, 2) developing Fault Avoidance Zones for active faults within existing Light Detection and Ranging (LiDAR) areas, 3) developing Fault Awareness Areas for active faults outside of existing LiDAR areas and 4) providing advice on active fault hazards and incorporation into the Taupō District Plan. This report summarises these findings and is accompanied by GIS data of active faults, Fault Avoidance Zones and Fault Awareness Areas.

Ground-surface rupture hazard is the permanent breakage and buckling of ground along an active fault during an earthquake and causes considerable damage to any infrastructure upon or crossing it. However, compared with earthquake shaking, which can be widespread, the likely location of ground-surface rupture hazard can often be located accurately (within a few metres) and potential damage could be avoided or mitigated. Risk-based land-use planning tools developed for this purpose are based on three key parameters: 1) fault location (i.e. the likely rupture zone – Fault Avoidance Zones and Fault Awareness Areas); 2) fault activity, as measured by its average recurrence interval (RI) of surface rupture (how often on average it ruptures the ground surface); and 3) building type.

The Taupō District is crossed by many active faults, most of which are in the Taupō Rift, a zone of closely spaced normal faulting accommodating tectonic extension and volcanism. The eastern edge of the district just crosses the predominantly strike-slip North Island Dextral Fault Belt (NIDFB). There have been no large ground-surface-rupturing earthquakes in the Taupō District since 1840, but there has been centimetre- to decimetre-scale ground-surface rupture during earthquake swarms in 1895, 1922–1923 and 1983 in the Taupō Rift. Paleoseismic data are sparse, confined to just a few Taupō Rift faults, and show centimetre- to metre-scale ruptures of the ground surface during earthquakes that do not always rupture every trace of a specific fault and recurrence intervals that vary through time and space. These data and recent New Zealand historical earthquakes show that ground-surface ruptures in medium to large earthquakes are likely to form centimetre- to metre-scale steps and cracks on multiple traces. Impacts of ground surface ruptures on infrastructure in the 1987 Edgecumbe, 2010 Darfield and 2016 Kaikōura earthquakes show that engineering mitigation strategies could be considered for particular planning circumstances.

Fault Avoidance Zones are fault rupture zones and setback zones around detailed (~≤1:20,000 scale) fault mapping, as outlined in the Ministry for the Environment ‘Planning for development of land on or close to active faults’ guidelines (MfE Active Fault Guidelines; Kerr et al. 2003). New Fault Avoidance Zones have been developed for 21 faults in the Taupō District from an updated fault map that combines recent and new mapping using LiDAR data. Several new fault traces have been mapped, with almost all assigned to existing faults. Most of the Fault Avoidance Zones have a fault complexity classification of ‘well-defined’ (where faults are accurately mapped using LiDAR data), with interpolated zones connecting gaps where faults have been eroded by rivers or landslides classified as ‘well-defined extended’ and faults extrapolated beyond their mapped lengths classified as ‘uncertain constrained’.

Fault Awareness Areas are zones around active faults that have been mapped at a lower resolution (typically 1:50,000–1:250,000 scale), aiming to highlight areas where potential fault rupture hazards may be present and further work should be undertaken. They were originally developed in the Canterbury Region and are outlined in the Environment Canterbury report ‘Guidelines for using regional-scale earthquake fault information in Canterbury’ (ECan FFA

Guidelines; Barrell et al. 2015). Fault Awareness Areas are developed for the first time in the Taupō District, developed from existing fault mapping, and include recent detailed mapping using Bay of Plenty Regional Council LiDAR data in the Rangitaiki–Wairapukau area. The Fault Awareness Areas are classified as 'Definite', 'Likely' and 'Possible', with the buffer widths determined for these based on the surface expression of the fault trace.

Recurrence interval information has been compiled for the active faults of the Taupō District but, because of the challenges with using the sparse data, we have recommended categories of: 1) >10,000 to ≤20,000 years (RI Class V) and >5000 to ≤10,000 years (RI Class IV) for the Wheao and Te Whaiti faults, respectively, in the NIDFB; 2) ≤2000 years (RI Class I) as a conservative minimum for the named Taupō Rift faults (noting that some traces will have longer RIs); and 3) no categories have been assigned for newly mapped unnamed faults with no recurrence interval data. Based on these RI Classifications, we make recommendations of use for planning purposes based on the MfE Active Fault Guidelines for faults that have Fault Avoidance Zones defined and the ECan FAA Guidelines for faults that have Fault Awareness Areas defined. Recommendations are also made for work that would need to be undertaken for an individual wanting to build in a Fault Avoidance Zone or Fault Awareness Area.

Based on the findings in this report, GNS Science recommends that Taupō District Council:

- Replace any active fault datasets currently held and being used by Taupō District Council with those from this study.
- Include all Fault Avoidance Zones and Fault Awareness Areas developed in this study in the Taupō District Plan and in any other planning or hazard information maps for Taupō District.
- Develop planning provisions using the information provided in this report, including guiding principles and the risk-based decision-making tools of the MfE Active Fault Guidelines and ECan FAA Guidelines.
- Consider if engineering mitigation options are allowed for buildings, and under what general circumstances.
- Consider ground-surface rupture hazard for assessing lifeline developments that cross active faults in the district.
- Encourage consultants to follow the recommendations and methodologies presented in this report for assessing active fault ground-surface rupture hazard.
- When LiDAR data are obtained in areas not currently covered, update the fault map and, where possible, replace Fault Awareness Areas with Fault Avoidance Zones.
- Obtain better constraints on RI Class, in particular for faults where future population growth is expected. This could be achieved through a combination of site-specific paleoseismic (trenching) studies and more detailed analysis of fault scarp height and morphology using LiDAR data.

1.0 INTRODUCTION

1.1 Background and Context (from the Project Brief)

Taupō District Council has active fault maps in its District Plan, which are thought to be from 1998 and to reflect the information in GNS Science's New Zealand Active Faults Database at that time. These maps are out of date with regards to modern fault mapping practices and do not adequately reflect the uncertainty of fault location. For example, pencil thin lines are shown on the District Plan, and a 20 m avoidance zone is applied throughout the District Plan (Rule 4e.10 – Fault Line Hazard Area) when, in actuality, due to mapping simplification and uncertainty, the fault may be up to 200 m from the indicated line.

Taupō District Council also has several areas where the location of faults have been explored in recent years, either by the Council or developers, and for which Fault Avoidance Zones have been identified. This includes significant mapping in the Mapara Valley area (Villamor and Wilson 2007).

Taupō District Council have identified that they do not have a good understanding of the risks associated with active faults in the Taupō District. In particular:

- the likely recurrence intervals;
- what degree of single-event displacement is possible or likely; and
- what level of deformation is possible or likely, taking into account Taupō District soil structures.

Taupō District Council commissioned GNS Science to provide updated active fault information and advice on active fault hazards in the Taupō District, which are summarised in this report.

1.2 Scope, Objectives and Deliverables

The project objectives were to:

1. Assist Taupō District Council to understand the risks associated with active faults to facilitate the development of rules for the District Plan.
2. Develop updated hazard area maps for use in the District Plan.

The scope of work included the following tasks:

1. Compile existing information.
2. Develop Fault Avoidance Zones for active faults within all existing Light Detection and Ranging (LiDAR[1]) areas (Figure 1.1).
    - Review existing active fault mapping and Fault Avoidance Zone mapping (orange in Figure 1.1) within or adjacent to these areas.[2]

1 LiDAR is a high-resolution surveying method using laser light and a sensor. The raw data are used to develop Digital Surface or Elevation Models and, for simplicity, we refer to all of these as LiDAR data.

2 GNS Science and Taupō District Council agreed that Fault Avoidance Zones would not be developed for the Bay of Plenty Regional Council LiDAR area shown in dark grey on Figure 1.1.

- Accurately map the location of active faults and classify each fault in terms of accuracy of location according to the classification in the Ministry for the Environment 'Planning for development of land on or close to active faults' guidelines (MfE Active Fault Guidelines; https://www.mfe.govt.nz/sites/default/files/media/RMA/planning-development-faults-graphics-dec04%20(1).pdf).
- Develop Fault Avoidance Zones based on the accuracy and location according to the classification in the MfE Active Fault Guidelines.

3. Develop Fault Awareness Areas for active faults outside existing LiDAR areas.
   - Review existing active fault mapping (green in Figure 1.1) and update if necessary.
   - Develop Fault Awareness Areas according to the classifications in the Environment Canterbury Guidelines (ECan FAA Guidelines; http://opendata.canterburymaps.govt.nz/datasets/1bb8e14fdc240edb4545967ed8aec48_0).
4. Provide advice on active fault hazards and their incorporation into the Taupō District Plan.
   - Review and summarise existing recurrence interval information and make some general recommendations for planning purposes.
   - Review and summarise existing ground-surface rupture deformation information from historical earthquakes and Taupō Rift paleoseismic data. Based on these, make some general recommendations regarding:
     - Possible single-event displacements.
     - The level of deformation possible, considering Taupō District soil structures.
     - Potential impacts for small- to medium-sized timber-framed houses.
   - Estimate how many faults may not be active faults using the certainty classifications and briefly discuss potential other origins.
   - Provide recommendations of work needed for an individual wishing to:
     - Build in a Fault Awareness Area and to have an expert define a Fault Avoidance Zone.
     - Build in a Fault Avoidance Zone and to determine specific risks and whether building there is acceptable.

The deliverables are this report and the Geographic Information System (GIS) map data – specifically, shapefiles of:

- Fault Avoidance Zone lines
- Fault Avoidance Zone polygons
- Fault Awareness Area lines, and
- Fault Awareness Area polygons.

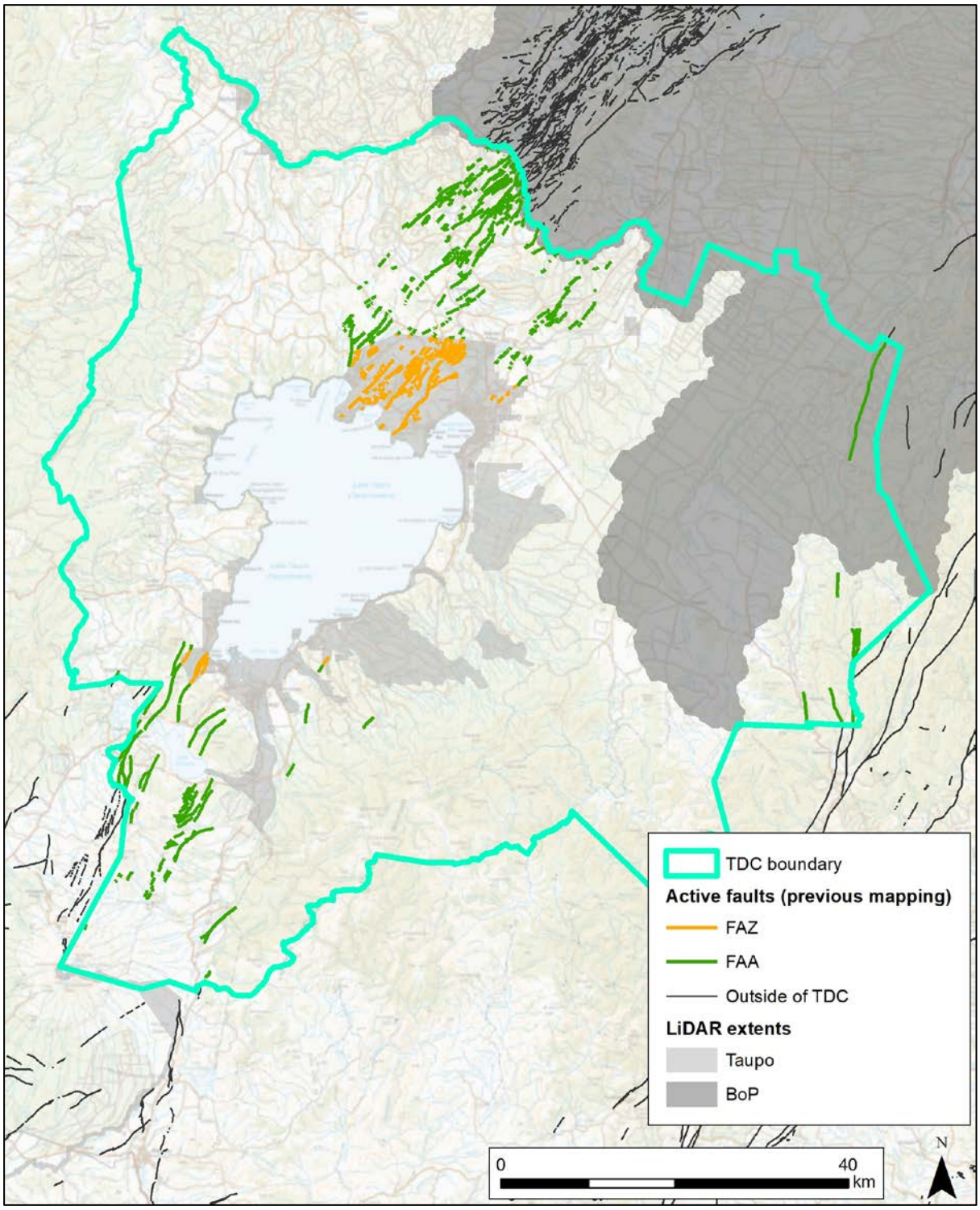

Figure 1.1 Active faults in the high-resolution version of the New Zealand Active Faults Database (as mapped prior to this study), colour-coded according to the work undertaken. BoP = Bay of Plenty, FAA = Fault Awareness Area, FAZ = Fault Avoidance Zone, TDC = Taupō District Council.

1.3 Fault Avoidance Zones and Fault Awareness Areas for District Plan Purposes

Ground-surface rupture hazard is the permanent breakage and buckling of ground along an active fault during an earthquake and causes considerable damage to any infrastructure upon or crossing it. However, compared with earthquake shaking, which can be widespread, the likely location of ground-surface rupture hazard can often be located accurately to within a few metres, and so potential damage could be avoided or mitigated. Risk-based land-use planning tools have been developed for this purpose, and we describe below the main points of the two tools used in this study, Fault Avoidance Zones and Fault Awareness Areas.

1.3.1 Fault Avoidance Zones

Fault Avoidance Zones are a recommended risk-based tool to mitigate surface rupture hazard for land-use planning purposes, as described in the MfE Active Fault Guidelines (Kerr et al. 2003). The aim of the MfE Active Fault Guidelines is to assist resource management planners tasked with formulating land-use policy and making decisions about development of land on, or near, active faults. The MfE Active Fault Guidelines provide information about active faults, specifically fault rupture hazard, and promote a risk-based approach when dealing with development in areas subject to ground-surface fault rupture hazard. In the MfE Active Fault Guidelines, the surface rupture hazard of an active fault at a specific site is characterised by two parameters:

1. the location/complexity of surface rupture of the fault; and
2. the activity of the fault, as measured by its average recurrence interval of surface rupture.

The MfE Active Fault Guidelines also advance a hierarchical relationship between fault recurrence interval and building importance, such that the greater the importance of a structure with respect to life safety, the longer the recurrence interval of the fault required before a plan should enable construction. For example, only low-occupancy structures, such as farm sheds and fences (i.e. Building Importance Category 1 structures), should be allowed to be built across active faults with average recurrence intervals of surface rupture less than 2000 years (i.e. RI Class I). As another example, in a ‘greenfield’ (i.e. undeveloped) setting, more significant structures such as schools, airport terminals and large hotels (i.e. Building Importance Category 3 structures) should not be sited across faults with average recurrence intervals shorter than 10,000 years (i.e. RI Class ≤IV).

In practice, Fault Avoidance Zones are created by defining a 20 m setback buffer around the fault complexity zones, which defines the likely rupture zone of faults. The fault complexity zones are themselves generated from buffers surrounding the detailed fault mapping linework, with the width of fault complexity zones generally determined by an expert assessment of fault location accuracy (or lack thereof) plus the resolution and georeferencing uncertainty of the data.

A key feature of Fault Avoidance Zones is that they are developed around accurate mapping of the surface expression of active faults. These maps are usually compiled at scales of 1:1000–1:18,000, which is appropriate for cadastral purposes. This is a key difference with the Fault Awareness Areas described below.

A description of the construction of Fault Avoidance Zones is contained in Section 3.3. Recommendations for utilising Fault Avoidance Zones in a planning and risk reduction context are provided in Section 5.2.

1.3.2 Fault Awareness Areas

Fault Awareness Areas were originally developed for districts within the Canterbury Region from 1:250,000 scale fault maps produced for each district within the region (e.g. Barrell and Townsend 2012; Barrell 2013). The scale of such maps is not appropriate to define Fault Avoidance Zones; however, Canterbury Regional Council requested an alternative way by which preliminary decisions could be made around those faults that were not mapped in detail.

The purpose of Fault Awareness Areas is *to show the general location of active faults and thereby highlight areas where a potential fault rupture hazard may be present*. Such information is intended to assist council authorities, existing and future landowners and developers, infrastructure managers and emergency managers with land-use planning.

Subsequent to the Canterbury Region fault mapping, Fault Awareness Areas have been developed for several other local authorities for faults mapped at 1:50,000 to 1:250,000 scale (e.g. Langridge and Morgenstern 2018; Barrell 2019) and/or in lower-priority areas for planning purposes (Litchfield et al. 2019). In the latter study, comparison of previously defined Fault Awareness Areas with the location and distribution of faults that ruptured in the 2016 M_W 7.8 Kaikōura Earthquake showed that they are both useful as an indicator of areas of future fault rupture and sufficiently wide to capture the distribution of rupture.

Fault Awareness Areas have not previously been generated for any active faults in the Taupō District. In this study, they have been developed for previously mapped active faults in areas not currently covered by LiDAR data (and thus not mapped in detail), as well as recently mapped faults in the area covered by the Bay of Plenty Regional Council LiDAR data (dark grey in Figure 1.1), which are not currently a priority for Taupō District Council. A description of how the Fault Awareness Areas were created for this project is contained in Section 4.2. Recommendations for using the Fault Awareness Areas in a planning context are provided in Section 5.2.

1.4 Report Contents and Layout

This report summarises the results of this project and describes the active fault (GIS) map data provided.

- Section 2 provides an overview of active faults in the Taupō District and summarises existing information. A general overview of active faults is contained in Appendix 1.
- Section 3 describes the Fault Avoidance Zones developed for active faults in areas with existing LiDAR data.
- Section 4 describes Fault Awareness Areas developed for active faults outside the areas with existing LiDAR data.
- Section 5 provides advice on active faults for incorporation into the District Plan. Further details of the impacts of surface ruptures on residential buildings are contained in Appendix 2.
- Section 6 provides recommendations for use of the information in this report and future work.

2.0 TAUPŌ DISTRICT ACTIVE FAULTS – EXISTING INFORMATION

2.1 Tectonic Setting

The Taupō District spans parts of the Taupō Volcanic Zone (TVZ) and the western margin of the North Island Dextral Fault Belt (NIDFB), both of which have formed in association with the westward subduction of the Pacific Plate beneath the North Island at the Hikurangi Trough (Figure 2.1A). The TVZ is a ~2-million-year-old volcanic arc characterised by andesitic and silicic volcanism, high crustal heat flow producing geothermal systems, numerous shallow earthquakes, and tectonic extension (Wilson and Rowland 2016). The tectonic extension is partly accommodated by a dense (closely spaced) system of NNE–SSW- to NE–SW-trending normal[3] faults that dip either NW or SE (e.g. Villamor and Berryman 2001, 2006; Litchfield et al. 2014; Gómez-Vasconcelos et al. 2017; McNamara et al. 2019). These faults collectively form the Taupō Rift (previously the Taupō Fault Belt) and, in the Taupō District, can be grouped into three domains – the Tongariro, Taupō and Whakamaru domains from south to north (Rowland and Sibson 2001; Figure 2.1B). Active faults are also likely to be present beneath Lake Taupō (e.g. Grindley and Hull 1986).

The NIDFB (also known as the North Island Fault System) is a series of NE–SW- to N–S-trending dextral[4] oblique-slip faults that variably bound or cut through the Axial Ranges (Figure 2.1). These extend from Cook Strait in the south to the Bay of Plenty in the north and include the Wellington, Wairarapa, Mohaka and Whakatane faults (e.g. Beanland and Haines 1998; Mouslopoulou et al. 2007; Litchfield et al. 2014; Bland et al. 2019). The NIDFB has formed in response to the oblique subduction of the Pacific Plate, accommodating some of the plate boundary-parallel component of motion; most of the plate boundary-perpendicular component of motion is accommodated by reverse[3] faults in the Hawke's Bay and Wairarapa coastal ranges and offshore and by the Hikurangi subduction fault (interface) at depth (Figure 2.1A). The eastern edge of the Taupō District encompasses part of the NIDFB (Figure 2.1B) and includes the Wheao and Te Whaiti faults.

When describing active faults in this report, and particularly those in the Taupō Rift, we follow the convention of describing an individual line as a fault trace and a fault as a collection of fault traces that are inferred to connect at depth. This concept is discussed further in Section 2.4.

3 See Appendix 1 for active fault definitions, including cartoons showing normal, reverse and strike-slip movement types.

4 Dextral is a strike-slip movement type.

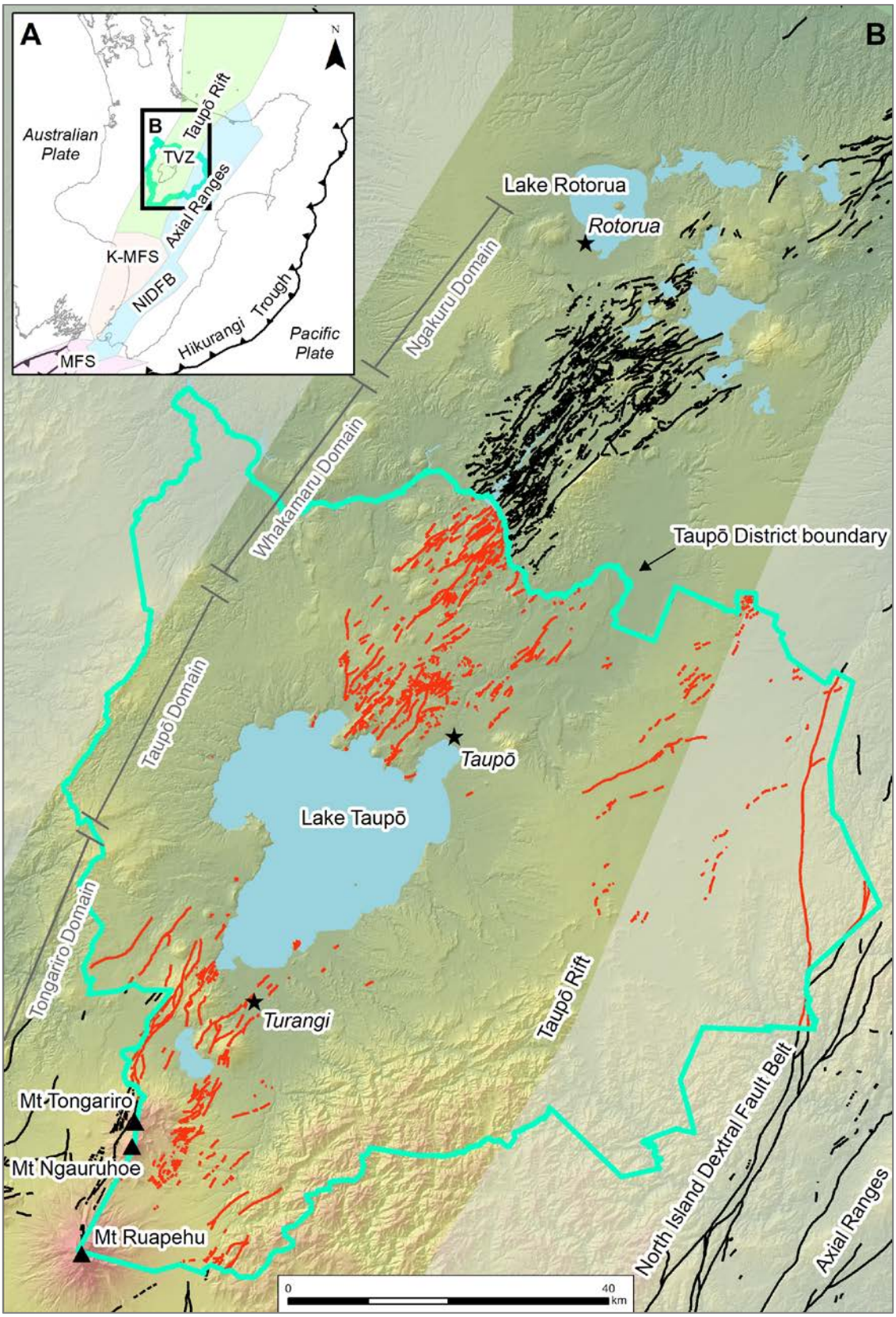

Figure 2.1 Tectonic setting of the Taupō District. (A) Major tectonic domains of the central North Island, from Litchfield et al. (2014). (B) Active faults in and around the Taupō District. Red lines are compiled in this study and the black lines are from the New Zealand Active Faults Database. K-MFS = Kapiti-Manawatu Fault System, MFS = Marlborough Fault System, NIDFB = North Island Dextral Fault Belt, TVZ = Taupō Volcanic Zone. All of the central, non-shaded area is the Taupō Rift.

2.2 Historical Seismicity

The Taupō District has a well-documented record of historical earthquakes. Figure 2.2 shows recorded earthquakes in and around the district of magnitude ≥M_W 2 and ≤40 km depth since 1850[5]. Deeper earthquakes do occur but are mainly on or within the Pacific Plate subducted beneath the district (i.e. within the Hikurangi Subduction Zone). There have been no historical Hikurangi Subduction Zone earthquakes that have caused damage in the Taupō District.

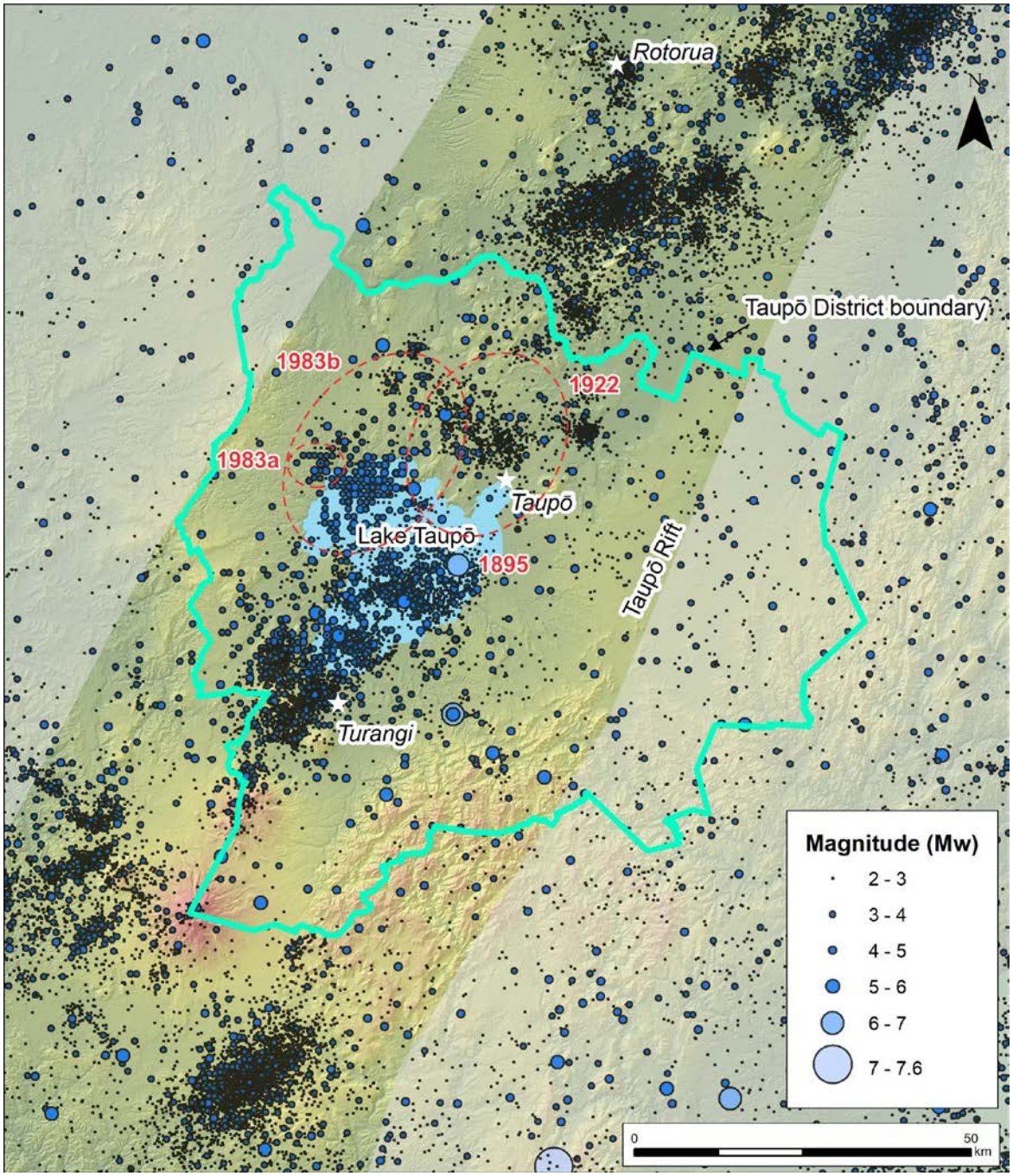

Figure 2.2 Epicentres of shallow (≤40 km) earthquakes of ≥M_W 2 since 1850 in the Taupō District. The locations of earthquake swarms discussed in the text are shown in red; from the GeoNet Earthquake Catalogue[5].

5 Figure 2.2 shows recorded earthquakes in the GeoNet earthquake catalogue and does not include *all* earthquakes >M_W 2 and ≤40 km depth since 1850, as the smallest earthquakes have only been recorded as the network has improved.

The majority of the shallow (≤40 km depth) earthquakes within the Taupō District are in the Taupō Rift and typically occur in clusters of small to moderate earthquakes. A poorly recorded cluster occurred in August 1895, for which only the largest, a ~M_W 6 earthquake on the east side of Lake Taupō, is shown in Figure 2.2. That earthquake caused landslides, ground cracking, subsidence and fissures "on a line of a concealed fault from Mt Tauhara to Earthquake Gully behind Rotongaio" (Grindley and Hull 1986). Villamor et al. (2001) suggest that the ~M_W 6 1895 earthquake could have been on the Kaingaroa Fault of Grindley (1960), although no active traces have been identified on this fault to date.

Better documented is the April 1922 to early 1923 swarm centred north of Lake Taupō (Figure 2.2). These earthquakes produced landslides, fissuring, ground-surface fault rupture and subsidence of the north shore of Lake Taupō (Grange 1932; Grindley and Hull 1986) (Figure 2.3A). Villamor et al. (2001) re-evaluated the evidence for ground-surface fault rupture and concluded that ~0.5 m average displacement occurred on a 3.2-km-long section of the Kaiapo Fault and 0.5 m average displacement occurred on the Whakaipo Fault for 3 km north of Mapara Road, 2 km north of Whangamatā Bay. Larger reported displacements (≤3.5 m subsidence) of the shoreline of Lake Taupō by the Whakaipo Fault were interpreted to be the result of landsliding. Minor displacements (≤0.1 m) of faults 300 m east of the Ngangiho Fault were considered to be triggered by earthquake shaking (Villamor et al. 2001).

The 1983 swarm is also well-documented and occurred in two phases northwest (1983a) and north of Lake Taupō (1983b; Figure 2.2) (Otway et al. 1984; Grindley and Hull 1986). Although these earthquakes were relatively small (≤M_W 4.3) they caused minor (≤0.5 m) deformation of the Lake Taupō shoreline and minor cracking (≤0.05 m displacement) along the Kaiapo Fault (Figure 2.3B).

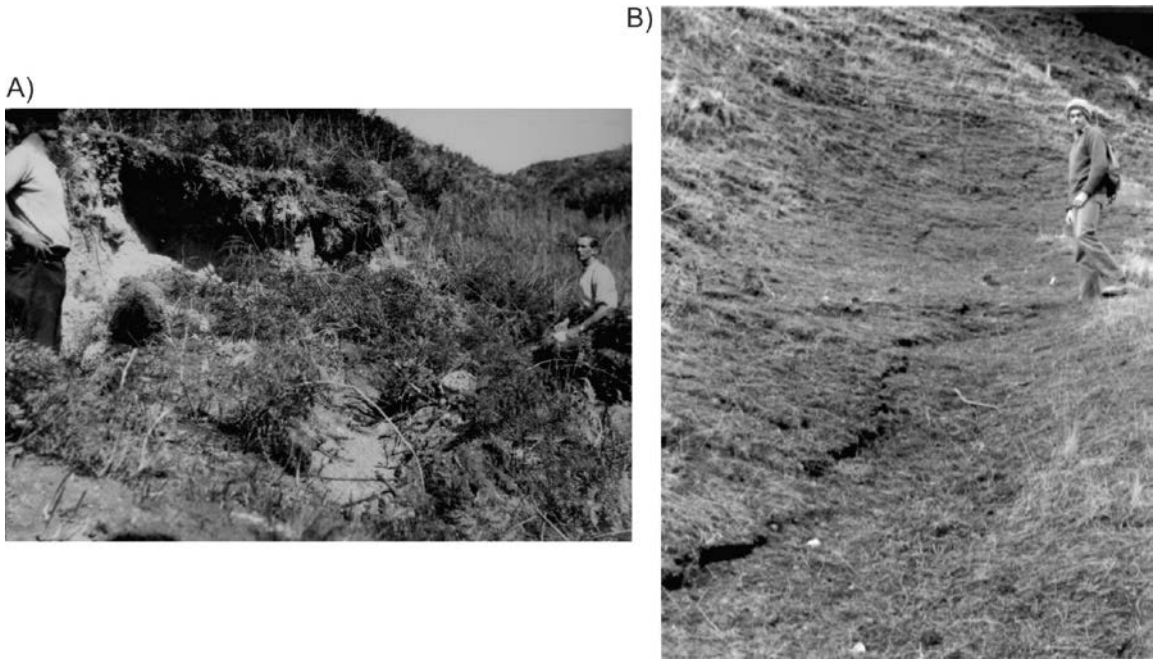

Figure 2.3 Ground-surface deformation from historical earthquake swarms in the Taupō District. (A) Deformation north of Whakaipo Bay, which is likely to primarily be from landsliding rather than fault rupture (Villamor et al. 2001); from the Gerrard Ward Collection, Taupō Museum. (B) Minor cracking along the Kaiapo Fault in the 1983 swarm, from Otway et al. (1984).

Appendix 2 also provides a description of the 1987 M_W 6.5 Edgecumbe earthquake, which, although outside the Taupō District, is a useful analogue of the types of ground-surface ruptures and impacts on residential buildings that could be expected within the district and is discussed further in Section 5.

2.3 Previous Active Fault Mapping

Active faults in the Taupō District have been mapped for many decades using a variety of techniques, including aerial photograph analysis, field mapping and, more recently, LiDAR analysis. Key datasets compiled and reviewed for this project were the:

- High-resolution version of the New Zealand Active Faults Database. This contains active faults mapped at a variety of scales (~1:1000–1:50,000), including those currently in the Taupō District Plan. Most of the faults in the New Zealand Active Faults Database were mapped from aerial photographs and the data are almost exclusively from prior to 2010.
- 1:250,000-scale version of the New Zealand Active Faults Database (https://data.gns.cri.nz/af/; Langridge et al. 2016). Most of the data in this version are from the 1:250,000 Geological Maps of New Zealand (QMAP) by Leonard et al. (2010) (Rotorua) and Lee et al. (2011) (Hawke's Bay). The QMAP datasets contain both active and inactive faults.
- Geology of the Tongariro National Park Area 1:60,000-scale geological map (Townsend et al. 2017), which also contains both active and inactive faults.
- Detailed (~1:16,000-scale) mapping and Fault Avoidance Zones developed for the Mapara Valley area. Active faults were mapped from aerial photographs (Villamor and Wilson 2007) in a desktop assessment (i.e. they were not ground-truthed, although four trenches had been excavated across one fault in another study – Villamor et al. (2007), described in Section 2.4.1).
- Detailed mapping of active faults using 1-m-resolution LiDAR data and orthophotographs in the Kinloch to Wairakei Village area for research purposes (McNamara et al. 2019).
- Detailed mapping using aerial photographs (generally 1:16,000) and 1–2-m-resolution LiDAR data for various fault location studies. Some faults have been ground-truthed with field inspections, geophysical data (Ground Penetrating Radar and Seismic Reflection) and trenches (e.g. Villamor et al. 2015).
- Compilation, review and some new mapping using LiDAR data for the upcoming 1:120,000-scale Taupō Rift geological map (GS Leonard and DB Townsend in preparation). The dataset contains both active and inactive faults.

2.4 Paleoseismic Data

Paleoseismic data are information about past earthquakes on active faults that tell us about the tectonic behaviour of a fault and its likely future behaviour, and therefore ground-surface rupture hazard. Key data include slip rate, single-event displacement, recurrence interval and the last event. Slip rate is a measure of the total number of ground-surface rupture displacements over time (e.g. accumulated displacement from several fault ruptures during the time interval when the ruptures occurred). It is a measure of relative fault activity and is determined from dated displaced landforms, such as river terraces. Single-event displacement is the amount of ground-surface rupture displacement in an individual earthquake and is ideally averaged from multiple ground-rupturing earthquakes determined from deformed landforms, such as river terraces. Recurrence interval is the time interval between large ground-surface-rupturing earthquakes and provides an indication of the likelihood of a fault rupturing in the near future. Recurrence interval can be obtained directly from the time between earthquakes (e.g. determined from trench information) or calculated by dividing single-event displacement by slip rate. The last event is the timing of the last ground-surface-rupturing earthquake, which is determined by dating of the displaced landform (e.g. a river terrace) or the youngest deformed layers (e.g. volcanic ash) exposed in a trench.

Paleoseismic data have only been obtained for a small proportion of the total number of active faults in the Taupō District (Figure 2.4). This is for a variety of reasons, including challenges with: 1) obtaining long paleoearthquake records in areas with thick, young, volcanic layers (e.g. the 1700-year-old Taupō ignimbrite); 2) obtaining permissions to excavate trenches in Tongariro National Park; and 3) accessibility, or lack thereof, in the North Island Axial Ranges (NIDFB). Trenches have been excavated across a few faults for fault location purposes (Figure 2.4), but limited paleoseismic interpretations have been undertaken and full details (e.g. surveyed fault locations) are not available.

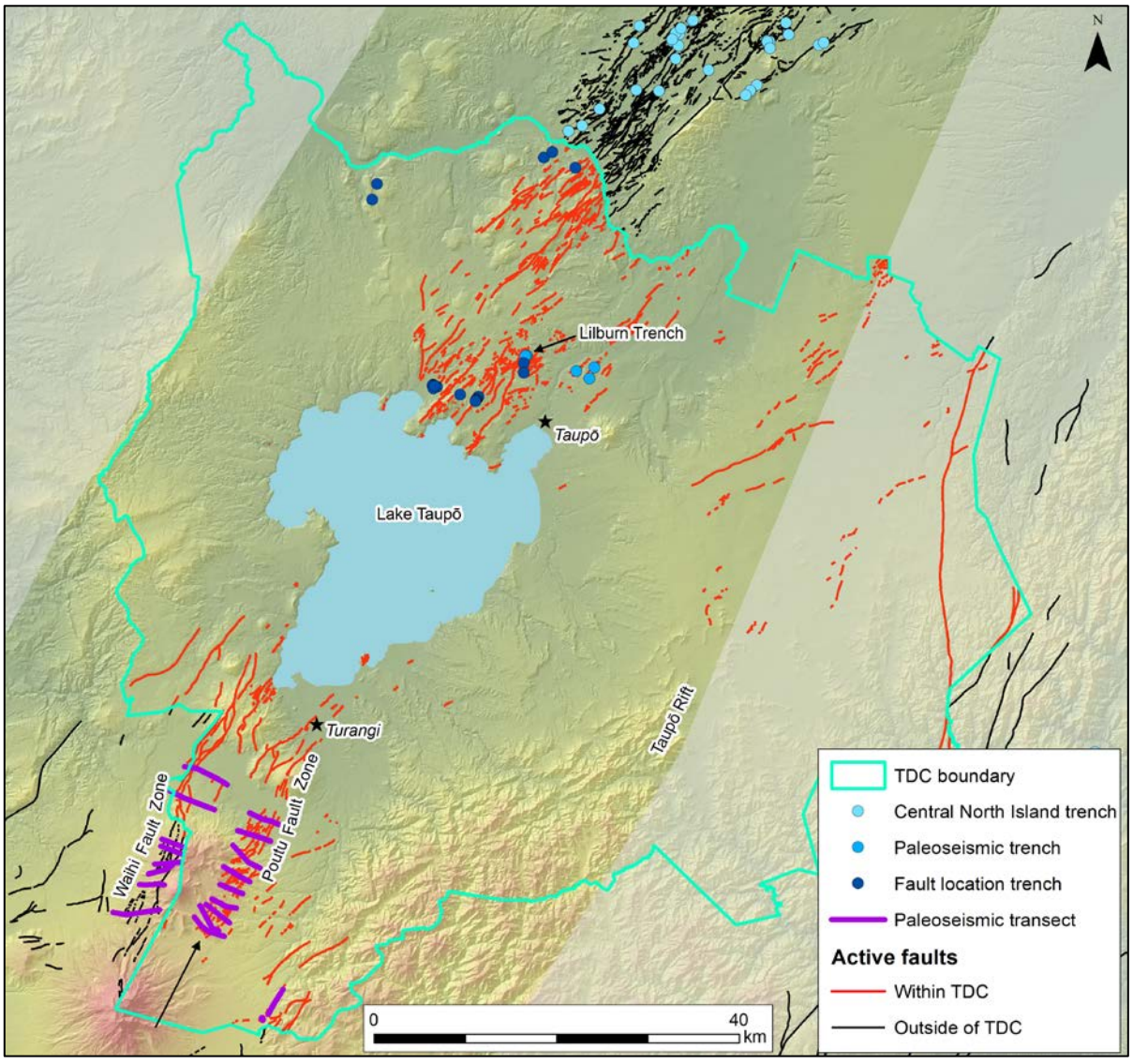

Figure 2.4 Paleoseismic and fault location (trench) sites in and surrounding the Taupō District. 'Central North Island trench' refers to paleoseismic sites outside of the Taupō District. Paleoseismic transects are compilations of data from natural exposures.

The existing paleoseismic data in the Taupō District are summarised in Table 2.1 and two datasets are described below to illustrate some general findings. It should be noted that these are data derived from field observations (from trenches and natural exposures) and that some paleoseismic data (e.g. recurrence interval) can and has also been calculated for some Taupō District active faults using other methodologies, such as single-event displacement divided by slip rate, as mentioned above. This method has been used to calculate recurrence intervals for some Taupō District faults and these are compiled together with the paleoseismic data and discussed in Section 5.

Table 2.1 Existing paleoseismic data for active faults in the Taupō District. 'Major' refers to large (metre-scale) displacements, 'minor' to small (centimetre-scale) displacements.

Fault Name	Slip Rate (mm/yr)	RI (Years)	Last Event (Calibrated Years Before Present)	Data	Data Source
Maleme	Variable Average ~3.5 mm/yr	3500 (one strand)	~900	Seven trenches north of Taupō District	Villamor and Berryman (2001); McClymont et al. (2009); Villamor et al. (2011)
Thorpe–Poplar	-	-	>13,800	Three trenches south and southwest of Ohakuri Dam	Villamor et al. (2003)
Kaiapo	-	3360–5000 (major; one strand) >10,000 (minor; one strand)	~1700 (minor)	Lilburn Trench, roadcut	Villamor et al. (2007, 2015)
Aratiatia	-	≤5000–7500 (major)	~1700 (both strands; minor) ~4000 (W strand; major) ~10,000 (E strand; major)	Three trenches south of the Aratiatia Dam	Berryman et al. (1994)
Waihi	2.6 ± 0.8	-	<3000	From natural exposures compiled across eight transects	Gómez-Vasconcelos et al. (2017)
Poutu	2.2 ± 1.9	-	<3000	From natural exposures compiled across nine transects	Gómez-Vasconcelos et al. (2017)
Upper Waikato Stream	0.5 ± 0.06	-	<3500	From natural exposures	Gómez-Vasconcelos et al. (2016)

2.4.1 Lilburn Trench

The Lilburn trench was excavated across a scarp of the Kaiapo Fault near the Te Mihi Geothermal Power Plant (Figure 2.4) as part of the planning investigations for the plant (Villamor et al. 2015). In the Te Mihi area, the Kaiapo Fault consists of multiple fault scarps/traces but, to the south, it is a single trace. The trench is excavated across just one of these traces and so the information from the Lilburn trench does not characterise the whole Kaiapo Fault.

The Lilburn trench, like others in the Taupō Rift, revealed that the scarp is underlain by several faults or fault strands (planes) (Figure 2.5). The faults displace volcanic ash and sedimentary layers by different amounts, ranging from centimetres to about one metre. The different amounts of displacements and the timing of fault ruptures for each fault strand suggest that not every fault strand exposed in the trench ruptures in every ground-rupturing earthquake, which has also been found elsewhere in the Taupō Rift (e.g. Berryman et al. 1998; Villamor et al. 2007, 2011; Canora-Catalán et al. 2008). This has important implications when extrapolating the value of a recurrence interval for fault rupture obtained from a trench to other strands within the same fault (see more below).

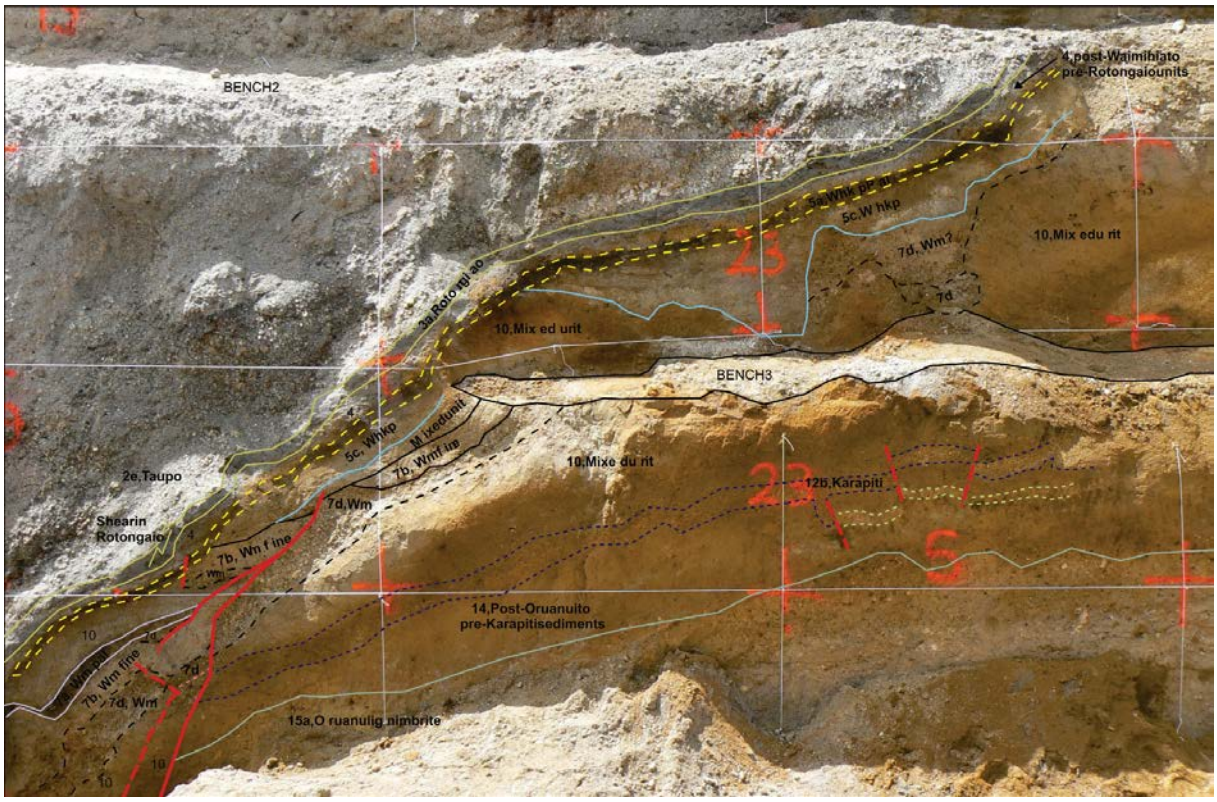

Figure 2.5 Interpreted photograph of part of the Lilburn trench across the Kaiapo Fault. Red lines mark active faults, other lines denote layers of volcanic ash, soil and materials with a mixed origin.

Another feature of the Lilburn trench, as well as others in the Taupō Rift (e.g. Villamor et al. 2007, 2011), are ground-surface-rupturing earthquakes associated with a volcanic eruption. In the Lilburn trench, the most recent earthquake occurred during the ~1700-year-old Taupō eruption. From a dataset of 50 trenches in the northern Taupō Rift, Villamor et al. (2011) found that 30% of ground-surface-rupturing earthquakes occurred immediately prior to, during or immediately after a volcanic eruption, whereas 70% were independent of volcanic eruptions. Up to three other earthquakes between ~11,500 and 1700 years ago revealed in the Lilburn trench are not associated with volcanic eruptions.

Based on the information from the Lilburn trench, a ground-penetrating radar profile and a nearby roadcut, it was interpreted that the Kaiapo Fault strands likely converge into a single fault at depth (Figure 2.6). The faults with small displacements are interpreted to be secondary (Figure 2.6) faults and to have a recurrence interval of >10,000 years. The faults with larger displacements are considered the primary faults and to have a recurrence interval of ~3360–5000 years (Table 2.1), as they likely rupture every time the master fault ruptures.

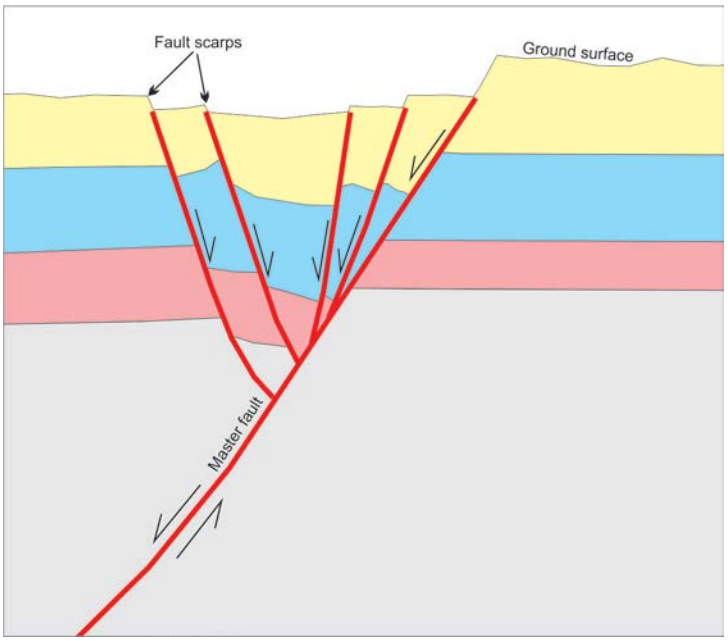

Figure 2.6 Schematic cross-section of a Taupō Rift fault showing multiple fault strands converging at depth onto a single master fault.

2.4.2 Waihi and Poutu Fault Zones Natural Exposure Transects

In the Tongariro Domain south of Lake Taupō (Figure 2.1B), active faults such as the Waihi and Poutu fault zones have been studied from natural exposures in streambanks (Gómez-Vasconcelos et al. 2016, 2017, 2019) (e.g. Figure 2.7). The natural exposures were interpreted in the same way as a trench and also revealed multiple faults with displacements ranging from centimetres to a few metres and evidence for surface-rupturing earthquakes during volcanic eruptions. These exposures, while very valuable to understanding fault activity, only accounted for a few fault strands and so the displacement values and rupture history in this area are very incomplete.

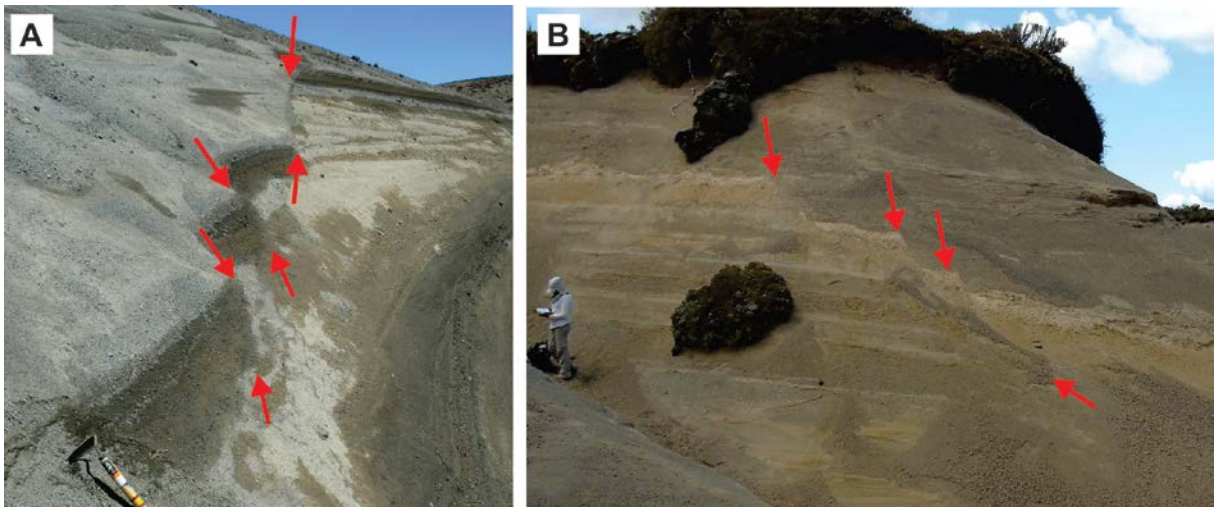

Figure 2.7 Examples of natural exposures of the Poutu Fault Zone. Active faults are marked by the red arrows; from Gómez-Vasconcelos et al. (2017).

To obtain a more complete and longer history of earthquakes on each fault zone, paleoseismic data have been compiled along transects crossing multiple fault strands (Figure 2.4). Ground-surface fault rupture displacements were measured across all fault strands within each transect, and the age of the rocks and sediments at the surface displayed by faults was used to assess the total activity (slip rate) of each strand, which was then summed across the transect. These showed that there are periods of more frequent earthquakes during times of volcanic eruptions and less frequent earthquakes during volcanic quiescence. This results in slip rate varying through time, which has also been documented for other Taupō Rift faults (e.g. Nicol et al. 2006; Villamor et al. 2007; Canora-Catalán et al. 2008). For the Waihi and Poutu fault zones, vertical slip rates range from 1.4 to 4 mm/yr and 1.4 to 5.3 mm/yr, respectively.

The Waihi and Poutu fault zones are also relatively long faults for the Taupō Rift (30 and 40 km, respectively) and so another likely explanation for surface-rupturing earthquakes varying in size, time and space is that faults are segmented and that some earthquakes may only rupture part of the fault (a fault segment). Gómez-Vasconcelos et al. (2019) suggest that each fault zone may consist of at least two segments (Figure 2.8) and that earthquakes may range from rupture of a single segment (e.g. Poutu South) to rupture of three segments (e.g. all Waihi plus other faults southwest of Lake Taupō). Variability in the rupture of different segments of other Taupō Rift faults has also been suggested (e.g. Villamor et al. 2007; Berryman et al. 2008).

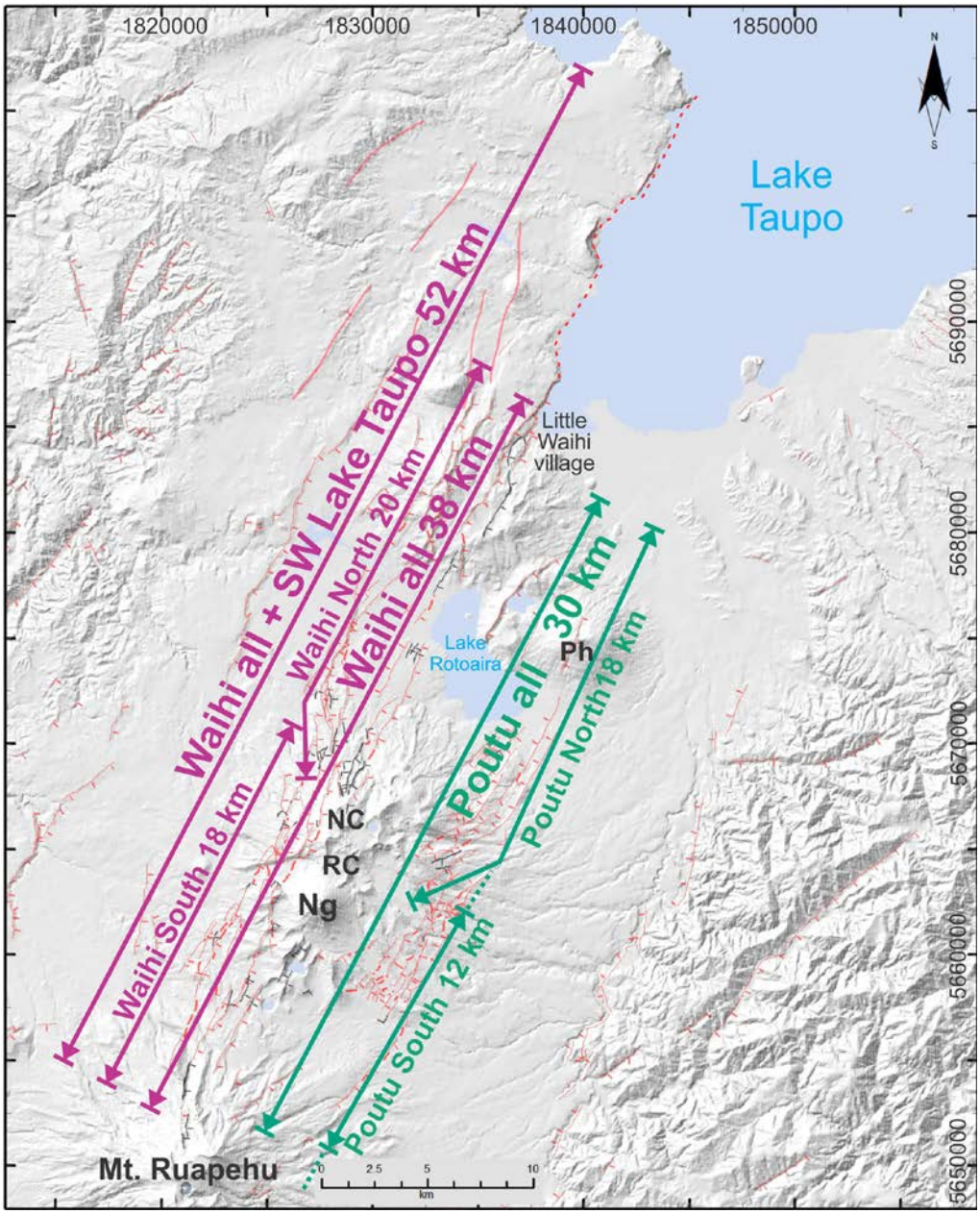

Figure 2.8 Potential surface-rupture segments for the Waihi and Poutu fault zones. From Gómez-Vasconcelos et al. (2019). NC = North Crater, Ng = Ngauruhoe, RC = Red Crater, Ph = Pīhanga.

3.0 FAULT AVOIDANCE ZONES

3.1 Fault Mapping Methodology

The updated fault map for developing Fault Avoidance Zones in the Taupō District was developed in two main ways:

- For areas where fault mapping using LiDAR data had already been undertaken, such as the Te Mihi area (McNamara et al. 2019), that mapping was reviewed and updated where required.
- Areas covered by more recent LiDAR data were reassessed for surface fault traces. Previous mapping (especially for the upcoming 1:120,000-scale Taupō Rift geological map – GS Leonard and DB Townsend in preparation) was used as a guide, but all areas were examined, with particular attention being paid to areas noted for potential future development.

In addition, although the Taupō Rift faults are characteristically numerous, short and discontinuous, in some places the faults have been either eroded away by landslides or stream erosion or covered over by young volcanic ash and/or sediment. In these areas, mapped fault traces were either connected with inferred faults or extended beyond their mapped lengths (Figure 3.1). The decision whether to connect or extend faults or to leave gaps is based on: 1) our experience of fault mapping and 2) assessment of geological maps and topography (landforms) to identify where fault rupture has likely continued between traces in past earthquakes and is likely to in the future. The lengths faults have been extended is determined from geological units or landforms or, if they are buried by younger layers, they were extended by 10%. Although we cannot rule out ground-surface rupture occurring beyond the mapped and inferred faults, we are confident that we have identified faults as best as is possible using the currently available evidence (e.g. LiDAR and geological maps).

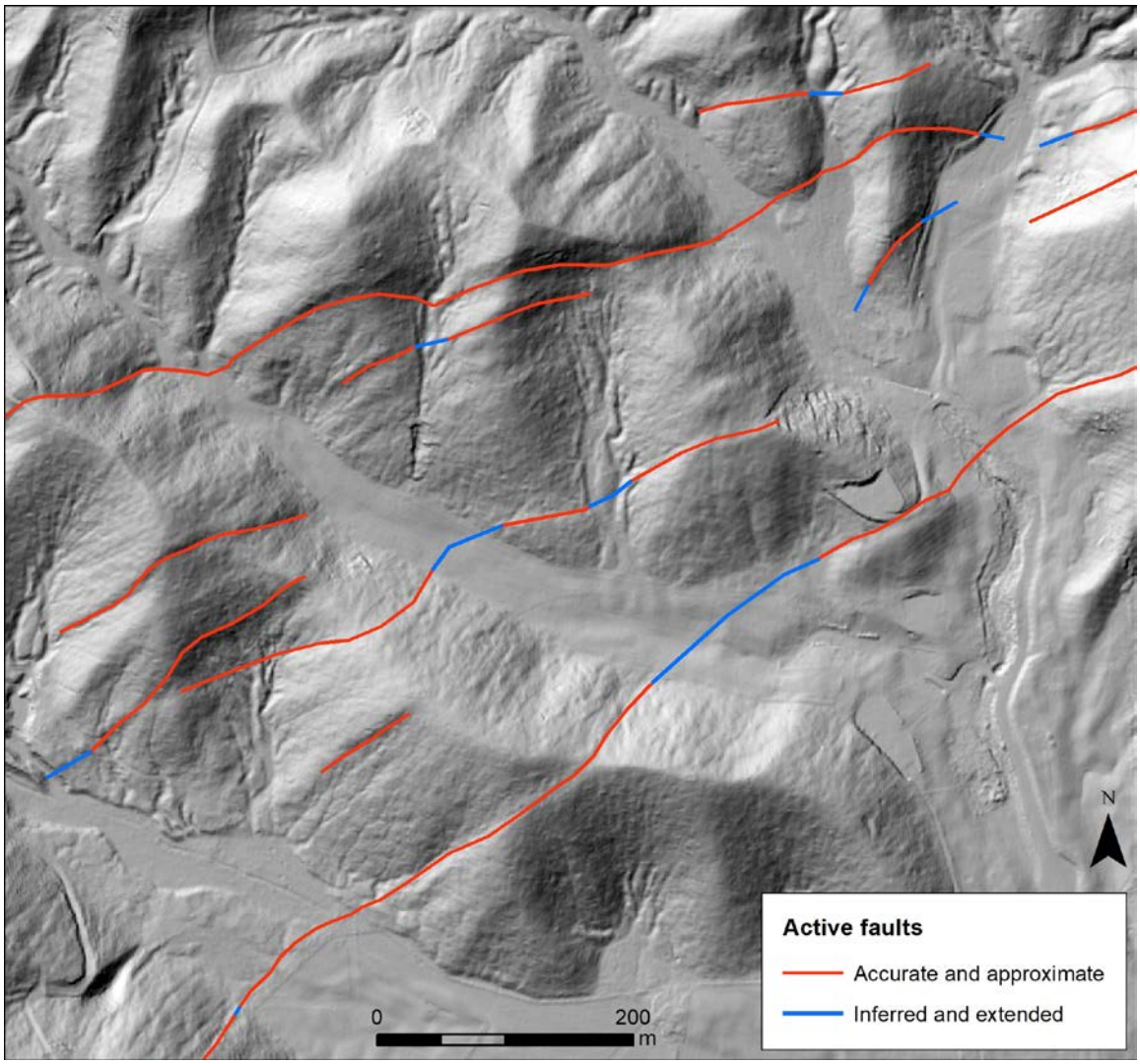

Figure 3.1 Examples of faults that have been extended or extrapolated (inferred) along-strike across areas where they have almost certainly been eroded away (e.g. by stream erosion) or buried by young stream sediments.

3.2 Fault Attributes

The attributes assigned to each fault are listed in Table 3.1. Key attributes for developing Fault Avoidance Zones are highlighted in bold and are discussed further in Section 3.3. Many of the attributes were missing from previous map datasets, so were added in this project.

Table 3.1 Attributes for mapped active faults in areas covered by LiDAR data in the Taupō District for the purposes of developing Fault Avoidance Zones. Key attributes for developing Fault Avoidance Zones are shown in bold.

Attribute	Name in Shapefile	Definition
Fault name	FAULT_NAME	The name given to an active fault.
Dominant sense	DOM_SENSE	Dominant or primary sense of movement on the fault (normal – see Appendix 1 for a full list and further details).
Down quadrant	DOWN_QUAD	The direction of the down-thrown side of the fault described in terms of compass quadrants.
Expression	EXPRESSION	Description of how a fault is expressed at the ground surface (surface trace, eroded scarp, no trace or concealed).
Tectonic origin	TECTONIC_O	Certainty that the feature is of tectonic (e.g. earthquake) origin (definite, likely or possible).
Accuracy	ACCURACY	Accuracy of the location of the fault on the ground surface (accurate, approximate, uncertain or inferred).
Deformation width	**Deformatio**	**Horizontal width of the visible fault feature or, for concealed faults or faults with no surface trace, the maximum width of where the deformation could be located. Value is in metres.**
Capture uncertainty	**Capture_un**	**Uncertainty associated with transferring the fault location onto a map (capture area). Value is in metres.**
Setback width	**Setback**	**An additional 20-metre-wide zone either side of a likely fault rupture zone (deformation width) to capture the area of intense ground deformation. Value is in metres.**
Fault complexity	**Fault_comp**	**The width and distribution of the deformed land around the fault trace (well-defined, well-defined extended or uncertain constrained – see Table 3.2 for a full list and further details).**
Recurrence interval class	**RI_Class** **RI_Years**	**The average time between surface-rupturing events on a fault, grouped into six classifications (RI Class I, IV or V – see Table 3.3 for a full list and further details).**

Table 3.2 Definitions of fault complexity terms. Adapted from the MfE Active Fault Guidelines (Kerr et al. 2003). In practise, all fault traces in the Taupō District were only classified as 'Well-defined', 'Well-defined extended' or 'Uncertain constrained'.

Fault Complexity	Definition
Well-defined	Fault rupture deformation is well-defined and of limited geographic width (e.g. metres to tens of metres wide).
Well-defined extended	Fault rupture deformation has been either buried or eroded over short distances, but its position is tightly constrained by the presence of nearby distinct fault features.
Distributed	Fault rupture deformation is distributed over a relatively broad, but defined, geographic width (e.g. tens to hundreds of metres wide), typically as multiple fault traces and/or folds.
Uncertain constrained	Areas where the location of fault rupture is uncertain because evidence has been either buried or eroded, but where the location of fault rupture can be constrained to a reasonable geographic extent (≤300 m).
Uncertain poorly constrained	The location of fault rupture deformation is uncertain and cannot be constrained to lie within a zone less than 300 m wide, usually because evidence of deformation has been either buried or eroded away, or the features used to define the fault's location are widely spaced and/or very broad in nature.

Table 3.3 Definition of Recurrence Interval (RI) classes, from the MfE Active Fault Guidelines. In practise, all faults in the Taupō District were only classified as RI Class I, IV or V.

RI Class	Average Recurrence Interval of Surface Rupture
I	≤2000 years
II	>2000 to ≤3500 years
III	>3500 to ≤5000 years
IV	>5000 to ≤10,000 years
V	>10,000 to ≤20,000 years
VI	>20,000 to ≤125,000 years

3.3 Fault Avoidance Zone Construction Methodology

Fault Avoidance Zones (polygons) were developed using the following steps (Figure 3.2):

1. Buffer the active fault trace (black lines in Figure 3.2A, C) by the Deformation Width (light orange in Figure 3.2A, C). This forms the 'Likely fault rupture zone' in the MfE Active Fault Guidelines (Kerr et al. 2003). In the Taupō Rift, the fault is considered to most likely be in the centre of the fault scarp, so the buffer zones are symmetrical about the fault lines.
2. Buffer fault extensions (Figure 3.1) by an additional ±10%, rounded to the nearest metre. This is to account for the greater, but unknown, location uncertainty.
3. Buffer the faults by the Capture Uncertainty (dark green in Figure 3.2A, C). This accounts for the uncertainty in the exact geographical coordinates of a point or line on a map, given the intrinsic location error derived from the map resolution. A single value of ±3 m was used, and this value takes into account both the resolution (1–2 m) and the uncertainty in georeferencing LiDAR data.

4. Buffer the Deformation Width and Capture Uncertainty by a further ±20 m to create what is sometimes referred to as the 'Setback Zone' (light green in Figure 3.2A, C). This additional 20 m accommodates the intense deformation and secondary ruptures that can occur close to primary mapped fault rupture.

The combined zone is the Fault Avoidance Zone (Figure 3.2B), which is classified with the recurrence interval class and fault complexity. Recurrence interval classes are defined in Table 3.3 and are discussed in Section 5.1. Fault complexities are defined in Table 3.2, although, in practise in the Taupō District, all faults were classified either as well-defined (for those with traces visible in the LiDAR data), well-defined extended (for those joining gaps), or uncertain constrained (for those extended beyond the mapped lengths).

It is important to note that representations of Fault Avoidance Zones obtained by a 20 m buffer around a fault line, e.g. around a fault from the National Active Fault Database, are not considered good practice, as they do not take into account the Deformation Width and Capture Uncertainty. Only in cases where the fault plane (or fault planes) has been exposed in the field, through paleoseismic trenches, can the Deformation Width can be substantially reduced and the Capture Uncertainty removed.

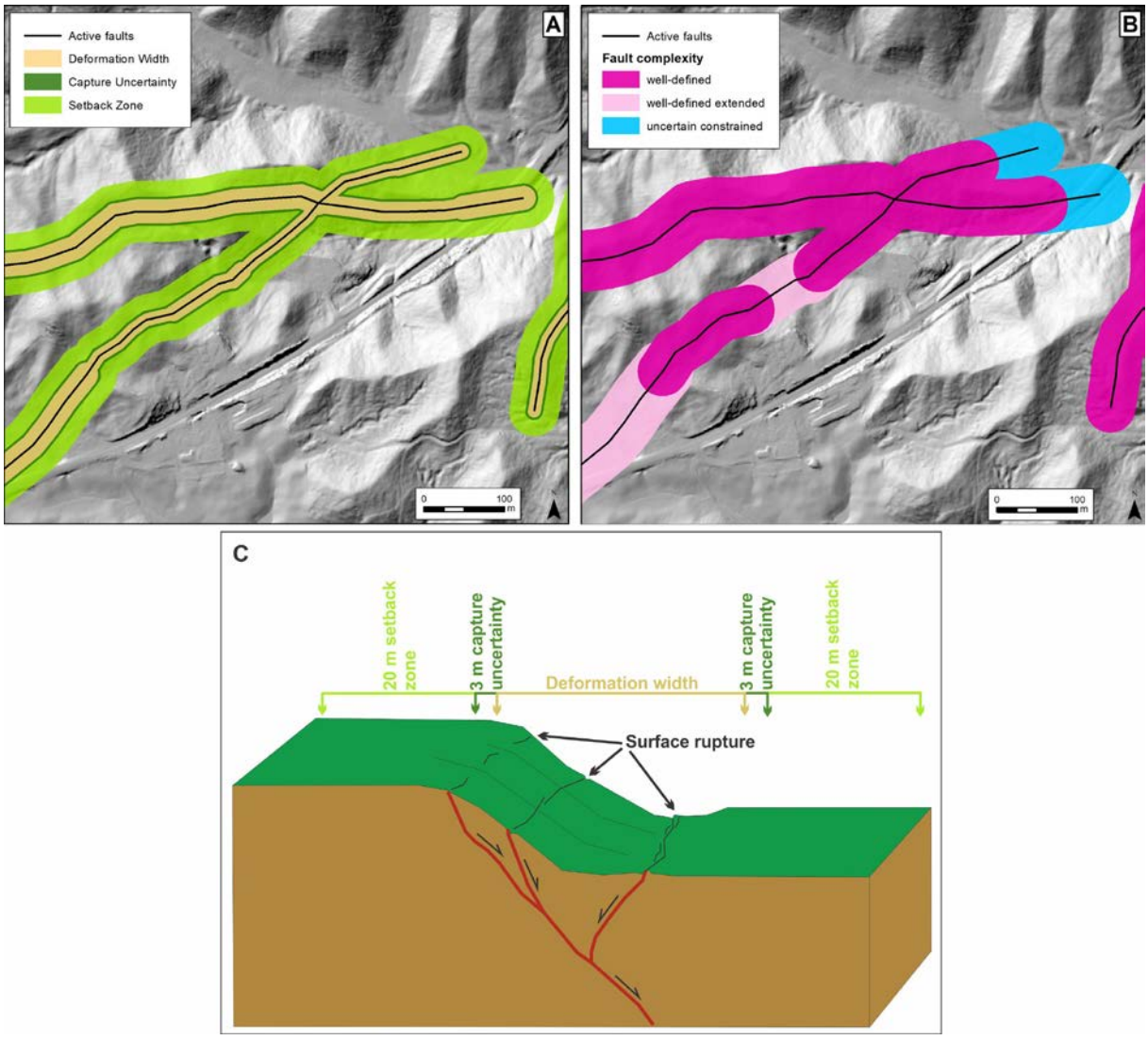

Figure 3.2 Components of the Fault Avoidance Zones. (A) Individual buffer zones used to create Fault Avoidance Zones. (B) The resulting Fault Avoidance Zones classified by fault complexity. (C) Schematic block diagram showing how the buffer zones relate to fault features in the field.

Fault Avoidance Zones developed for the Taupō District are shown in Figure 3.3. They are briefly described in Sections 3.4 and 3.5, from south to north, along with significant updates in the fault mapping and Fault Avoidance Zones developed previously. In our discussion of the fault mapping, we follow the convention of describing an individual line as a fault trace and a fault as a collection of fault traces that are inferred to connect at depth (Figures 2.6 and 3.2).

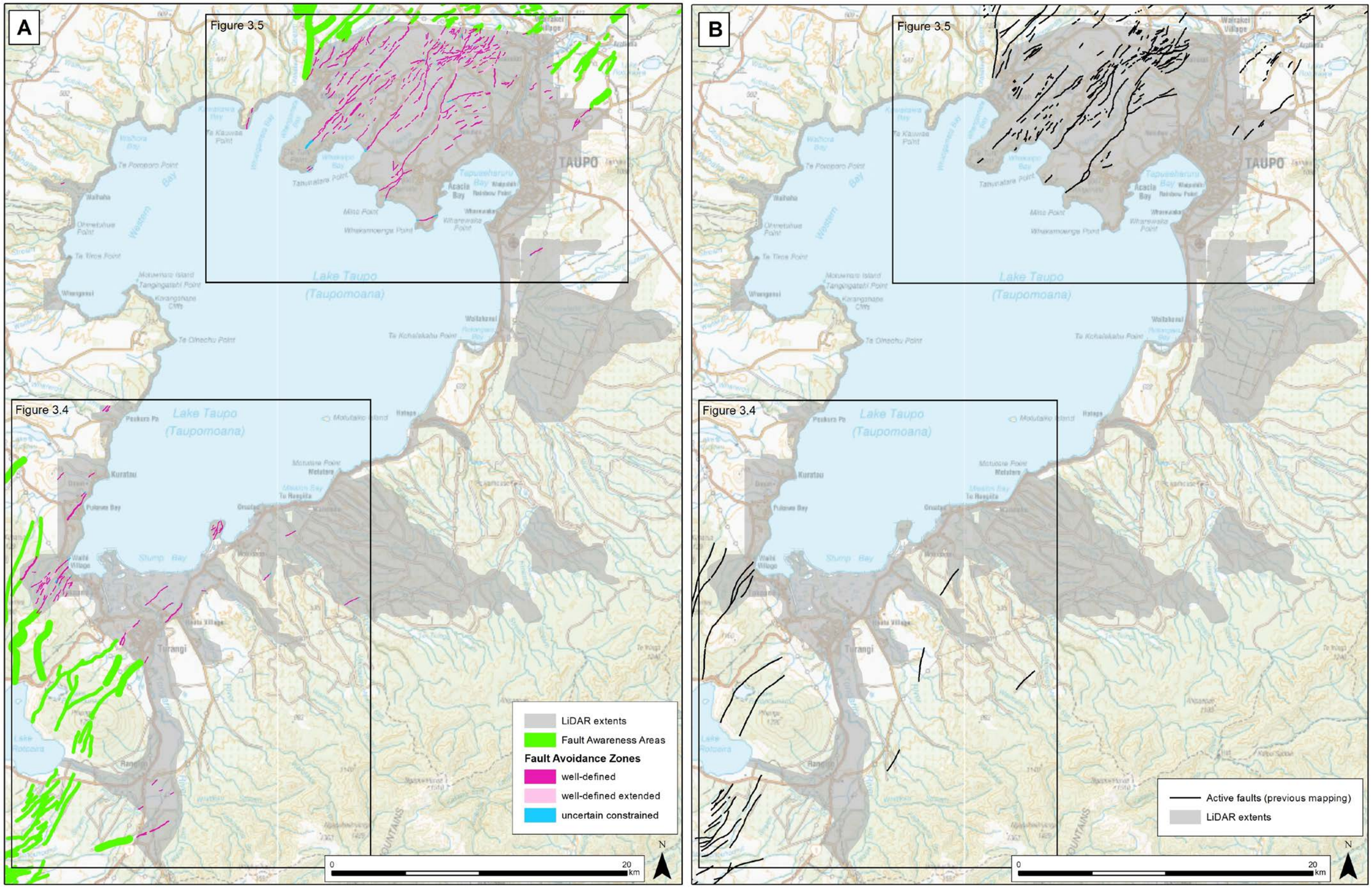

Figure 3.3 (A) Fault Avoidance Zones (pink and blue – classified by fault complexity) developed for the areas covered in LiDAR data (grey). (B) Previous active fault mapping from the high-resolution version of the New Zealand Active Faults Database.

This page left intentionally blank.

3.4 Fault Avoidance Zones in the Tongariro Domain

Analysis of the LiDAR data reveals many new fault traces in the Tongariro Domain (Figure 3.4). Almost all of these are inferred to belong to previously mapped faults (the Waihi, Taurewa, Rotopounamu and Poutu faults), with the addition of one new fault, the Treetrunk Fault, named after Treetrunk Gorge and the Treetrunk active fault earthquake source in the New Zealand National Seismic Hazard Model (NSHM; Stirling et al. 2012).

The Taurewa Fault is shown to have a greater density of traces (Figure 3.4A) than previously mapped (Figure 3.4B), although the tectonic origin of some of these traces is only 'likely' or 'possible' because some may alternatively be landslide features. Fault Avoidance Zone widths range from 55 to 116 m.

Other new fault traces have been mapped on both sides of the southern end of Lake Taupō, and, except for the dense faulting on the peninsula west of Motuoapa, are sparse (>500 m apart) and relatively short (<2 km). This may reflect the interpretation that they form the northeast ends of several previously mapped faults (Figure 3.4A). The Fault Avoidance Zones for these faults are generally classified as well-defined and they range in width from 56 to 126 m.

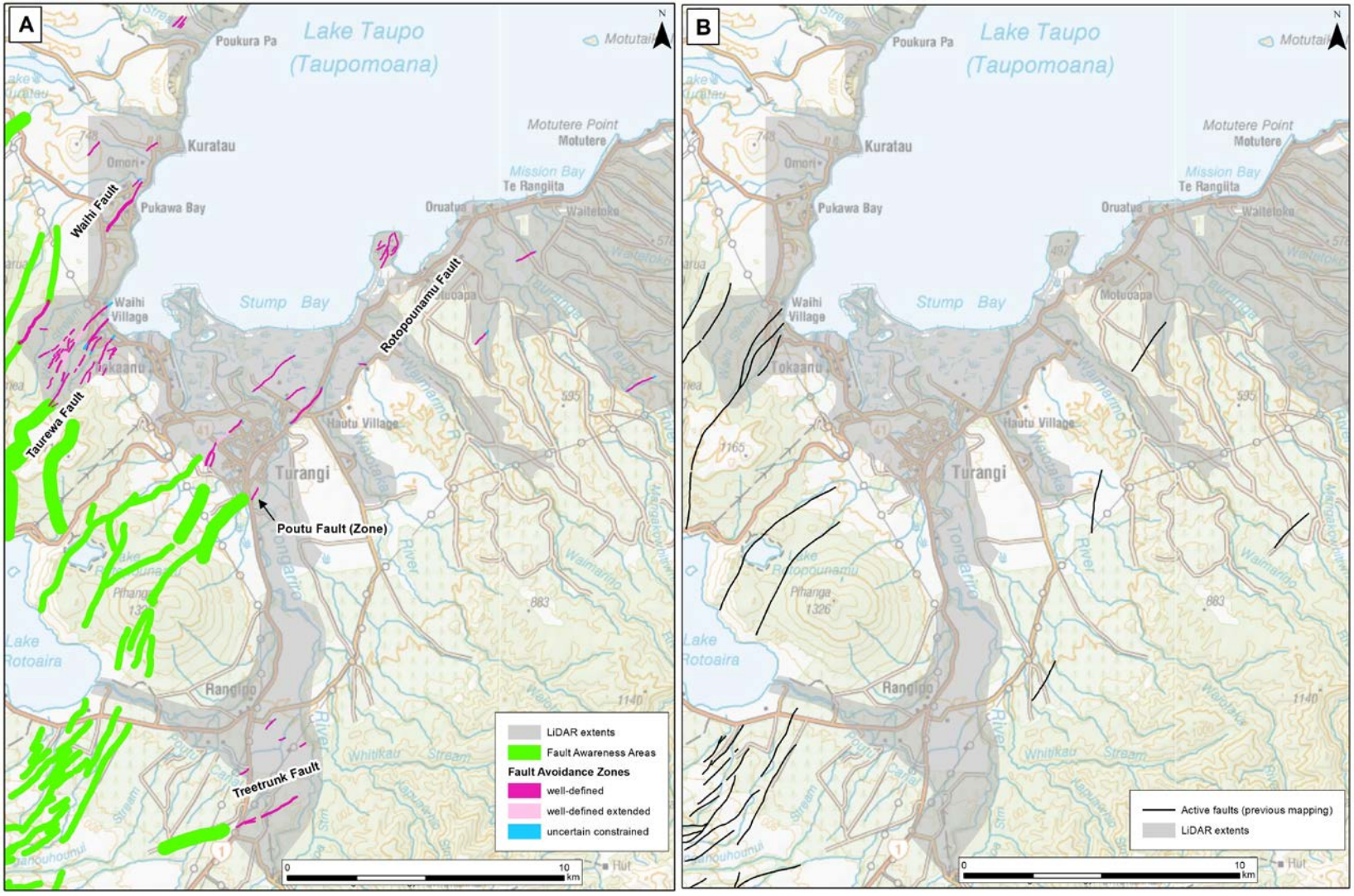

Figure 3.4 (A) Fault Avoidance Zones (pink and blue – classified by fault complexity) developed for the areas covered in LiDAR data in the Tongariro Domain (grey). (B) Previous active fault mapping in the Tongariro Domain from the high-resolution version of the New Zealand Active Faults Database.

3.5 Fault Avoidance Zones in the Southern Taupō Domain

The new mapping using LiDAR data in the southern Taupō Domain has led to the identification of some new fault traces, but also resulted in the removal of some previously mapped fault traces (Figure 3.5). This includes faults for which Fault Avoidance Zones had previously been defined using aerial photographs in the Mapara Valley area (Villamor and Wilson 2007). All newly mapped fault traces have been assigned to previously identified named faults.

The most complex faulting is in the area west of Wairakei, where the Te Mihi Fault cuts across the Whakaipo and Kaiapo faults (McNamara et al. 2019). To the south are some notably long, continuous traces, such as the 6–10-km-long traces of the Ngangiho, Whakaipo and Kaiapo faults. The tectonic origin for the majority of these faults is classified as ‘definite’ and ‘likely’, but about 15% are classified as ‘possible’ faults.

The Fault Avoidance Zone complexities are classified as well-defined, well-defined extended and uncertain constrained, and range in width from 52 to 146 m.

These new Fault Avoidance Zones differ from, and should replace, the Fault Avoidance Zones developed for the Mapara Valley area developed by Villamor and Wilson (2007).

This page left intentionally blank.

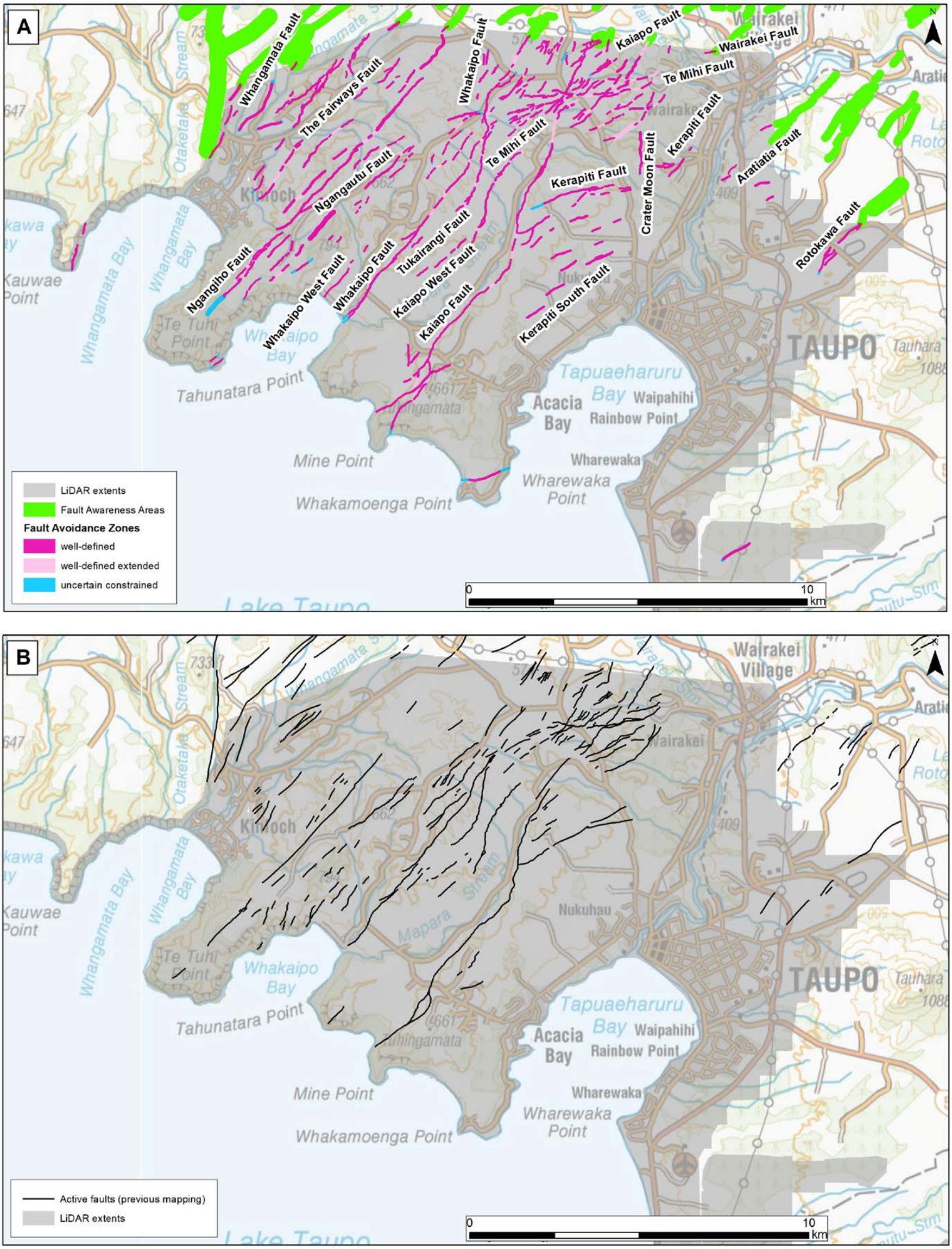

Figure 3.5 (A) Fault Avoidance zones (pink and blue – classified by fault complexity) developed for the areas covered in LiDAR data in the southern Taupō Domain (grey). (B) Previous active fault mapping from the high-resolution version of the New Zealand Active Faults Database.

This page left intentionally blank.

4.0 FAULT AWARENESS AREAS

4.1 Fault Mapping Methodology and Attributes

The fault map utilised for developing Fault Awareness Areas was derived using two main datasets:

- The upcoming 1:120,000-scale Taupō Rift geological map (GS Leonard and DB Townsend in preparation). This work has incorporated some detailed fault mapping using Bay of Plenty Regional Council LiDAR data in the eastern Taupō District (Villamor et al. 2017 and P Villamor unpublished data) and mapping using a 2-m-resolution Digital Surface Model in the Tongariro area.
- The high-resolution version of the New Zealand Active Faults Database. The scale varies from 1:16,000 in parts of the Taupō Rift to 1:250,000 in the NIDFB.

The attributes assigned to each fault are listed in Table 4.1. Key attributes for developing Fault Awareness Areas are highlighted in bold and are discussed further in Section 4.2. Many of the attributes were not populated for previously mapped faults, so were added in this study.

Table 4.1 Attributes for mapped active faults in areas not covered by LiDAR data in the Taupō District for the purposes of developing Fault Awareness Areas. Key attributes for developing Fault Awareness Areas are shown in bold.

Attribute	Name in Shapefile	Definition
Fault name	FAULT_NAME	The name given to an active fault.
Dominant sense	DOM_SENSE	Dominant or primary sense of movement on the fault (normal or dextral – see Appendix 1 for a full list and further details).
Subordinate sense	SUB_SENSE	Secondary sense of movement on the fault (normal – see Appendix 1 for a full list and further details).
Down quadrant	DOWN_QUAD	The direction of the down-thrown side of the fault described in terms of compass quadrants.
Accuracy	ACCURACY	Accuracy of the location of the fault on the ground surface (accurate, approximate, uncertain or inferred).
Certainty	**Certainty**	**The level of confidence that the mapped features are an active fault (definite, likely or possible – see Table 4.2 for further details).**
Surface form	**Surf_form**	**How clearly the mapped feature can be seen on the ground (well-expressed, moderately expressed or not expressed – see Table 4.3 for a full list and further details).**
Buffer distance	**BUFF_DIST**	**The buffer width used to create the Fault Awareness Area (125 or 250 m – see list in Section 4.2 for details).**
Recurrence interval class	**RI_Class** **RI_Years**	**The average time between surface-rupturing events on a fault, grouped into six classifications (RI Class I, IV and V – see Table 3.3 for a full list and further details).**

Table 4.2 Definitions of Certainty categories, from Barrell et al. (2015).

Category	Definition
Definite	The mapped feature is without doubt an active fault.
Likely	The mapped feature is probably an active fault, but other explanations for its origin cannot be ruled out (for example, it could have been formed by river erosion).
Possible	There is a possibility that the mapped feature is an active fault, but it is just as likely to be something else.

Table 4.3 Definitions of Surface Form categories, from Barrell et al. (2015). In practise, all faults in the Taupō District for which Fault Awareness Areas were defined are classified as 'Well-expressed', 'Moderately expressed' or 'Not expressed'.

Category	Definition
Well-expressed	The mapped feature should be able to be located on the ground to better than ±50 m – it can be clearly seen on the ground.
Moderately expressed	The mapped feature should be able to be located on the ground to better than ±100 m – it is not so easily seen on the ground.
Not expressed	The mapped feature cannot be seen at the ground surface and would require detailed investigation to locate it (for example, it has been covered by river gravels since the last movement on the fault.
Unknown	This term is applied where, for example, vegetation obscures the ground surface, or where the natural landscape has been heavily modified by humans and the degree of expression cannot be assessed using aerial or satellite photos, or where no photos of suitable scale, or other data such as LiDAR, are available for making an assessment.

4.2 Fault Awareness Areas Construction Methodology

The Fault Awareness Areas were developed by buffering the mapped faults according to the level of Certainty and their Surface Form. That is, buffers of 125 m either side (total width 250 m) were applied to faults characterised as:

- Definite (well-expressed)
- Definite (moderately expressed)
- Likely (well-expressed)
- Likely (moderately expressed)
- Possible (well-expressed).

Buffers of 250 m either side (total width 500 m) were applied to faults characterised as:

- Possible (moderately expressed)
- Possible (not expressed).

This generally follows the methodology developed by Barrell et al. (2015), except for buffering the Possible (well-expressed) faults by 125 m either side (they recommend buffering by 250 m either side). The difference is that the Barrell et al. (2015) methodology was developed for faults mapped at 1:250,000 scale, and in this present study the Possible (well-expressed) faults have been mapped using LiDAR or a detailed Digital Surface Model. They are therefore relatively accurately located, so the buffer does not need to incorporate the locational uncertainty inherent in a 1:250,000 scale dataset.

The Fault Awareness Areas developed for the Taupō District are shown in Figure 4.1. They are briefly described in Sections 4.3 to 4.5, along with significant updates in the fault mapping.

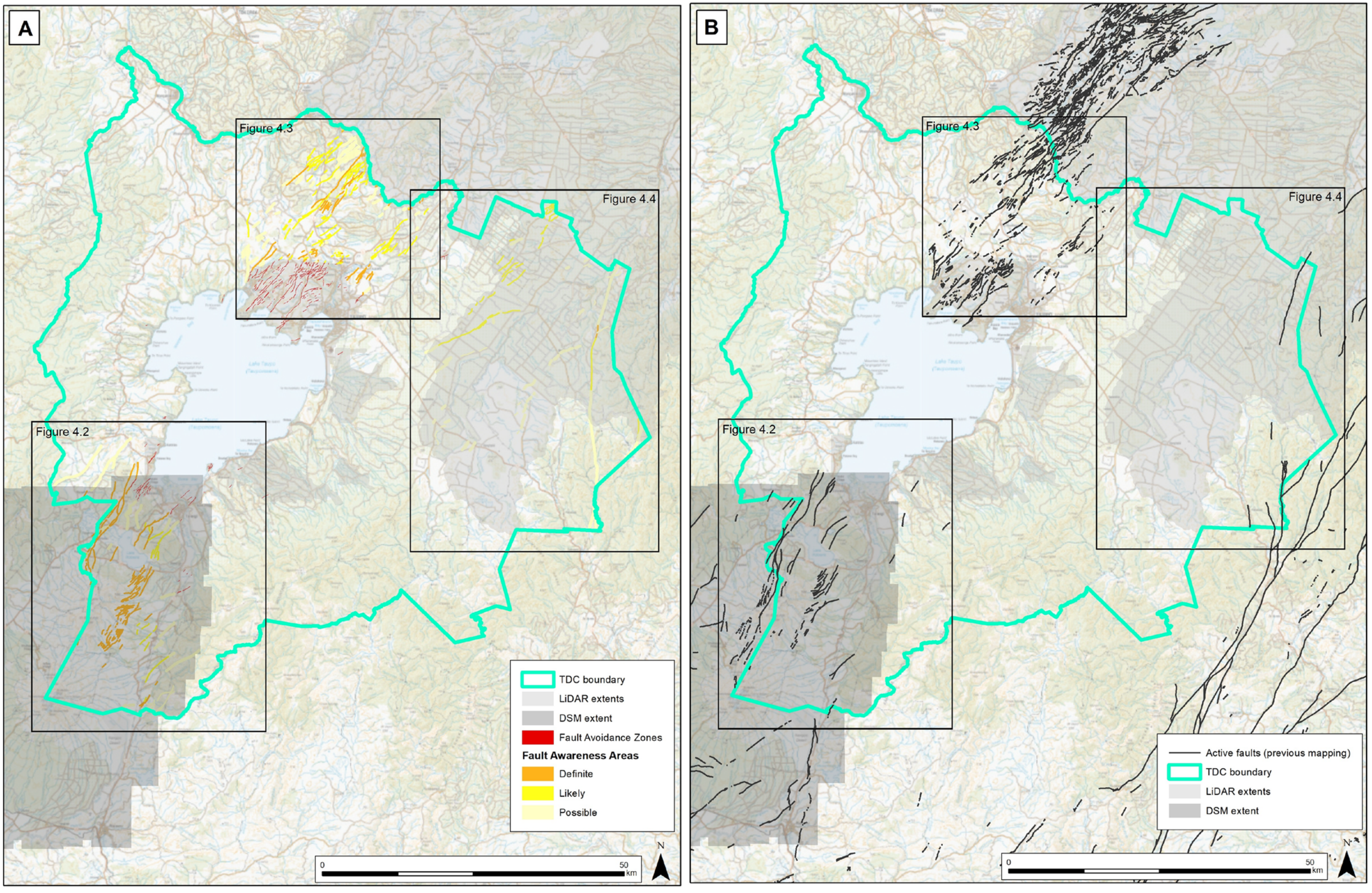

Figure 4.1 Fault Awareness Areas developed for the Taupō District Council (TDC). (A) Fault Awareness Areas (orange and yellow) developed for the Bay of Plenty Region LiDAR area and areas not covered by LiDAR data. (B) Previous active fault mapping from the high-resolution version of the New Zealand Active Faults Database.

This page left intentionally blank.

4.3 Fault Awareness Areas in the Tongariro Domain

The updated fault map in the Tongariro Domain (Figure 4.2) includes many new fault traces west and south of Tūrangi and the removal of some faults. The removed faults are because there is no evidence for them in aerial photographs or the 2-m-resolution Digital Surface Model.

Many of the new fault traces have been assigned to previously mapped faults (e.g. National Park, Waihi, Taurewa, Rotopounamu, Poutu and Wahianoa faults). Two new faults have been mapped, the Treetrunk and Upper Waikato Stream faults. The Treetrunk Fault is named after the Treetrunk active fault earthquake source in the New Zealand National Seismic Hazard Model (Stirling et al. 2012) and the Upper Waikato Stream Fault was named and characterised by Gómez-Vasconcelos et al. (2016, 2017, 2019).

Most (90%) of the traces are classified as ‘Definite’ (well-expressed), ‘Definite’ (moderately expressed), ‘Likely’ (well-expressed), ‘Likely’ (moderately expressed) or ‘Possible’ (well-expressed), so the Fault Awareness Areas are 250 m wide (that is, 125 m either side of the mapped fault). The remainder are ‘Possible’ (moderately expressed) and the Fault Awareness Areas are 500 m wide.

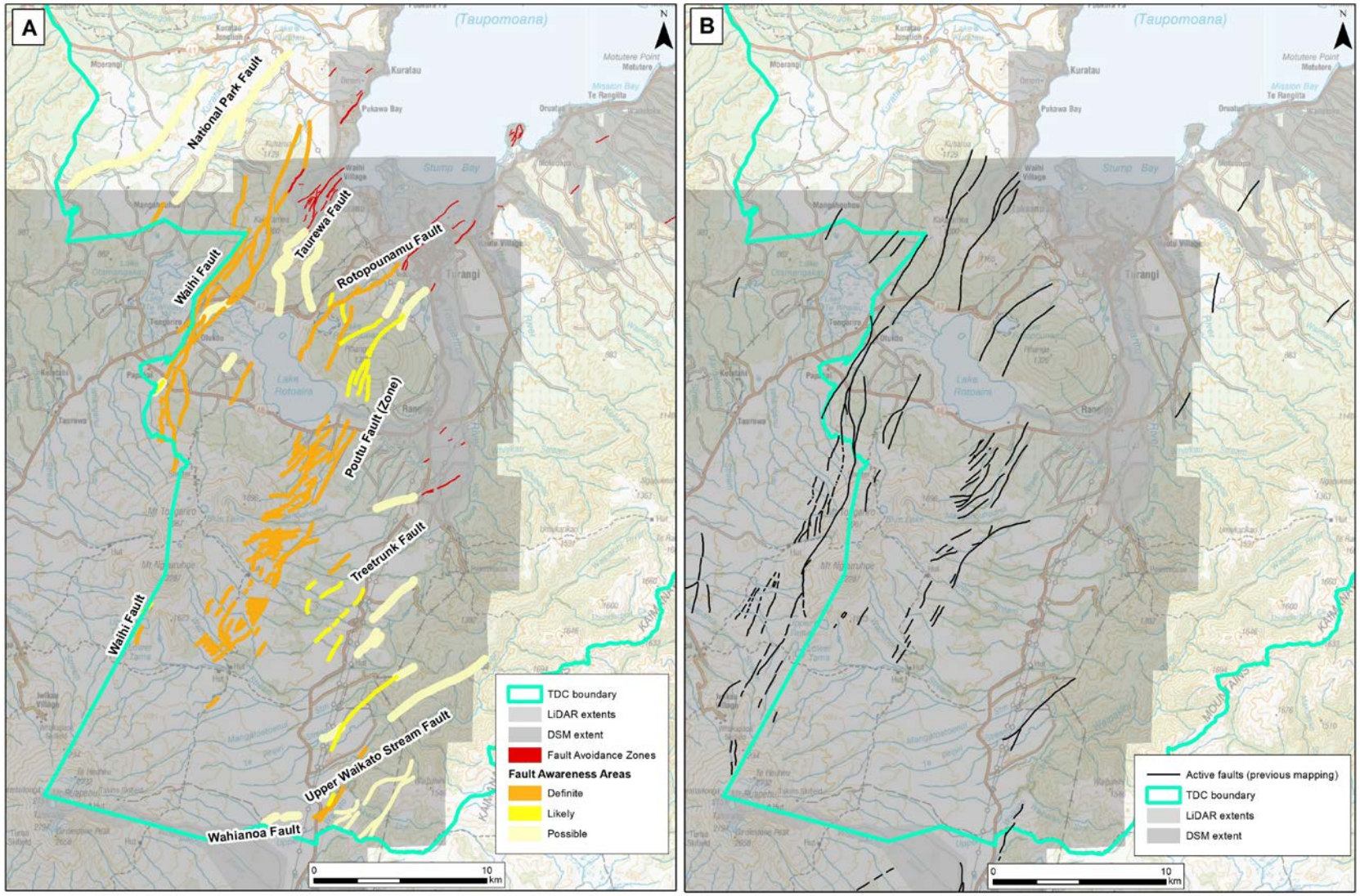

Figure 4.2 (A) Fault Awareness Areas (orange and yellow – classified by certainty) developed for areas not covered by LiDAR data in the Tongariro Domain. (B) Previous active fault mapping from the high-resolution version of the New Zealand Active Faults Database.

4.4 Fault Awareness Areas in the Northern Taupō and Whakamaru Domains

Most of the faults in the updated fault map in the northern Taupō and Whakamaru domains (Figure 4.3) are identified from the high-resolution version of the New Zealand Active Faults Database, but a few have been added (for example, west of Wairakei Village from the mapping of McNamara et al. 2019). All of the newly mapped faults are inferred to be traces of previously identified named faults.

The majority (75%) of the traces are classified as ‘Definite’ (well-expressed), ‘Definite’ (moderately expressed), ‘Likely’ (well-expressed) or ‘Likely’ (moderately expressed) and so the Fault Awareness Areas are 250 m wide. The remainder are classified as ‘Possible’ (moderately expressed) and the Fault Awareness Areas are 500 m wide.

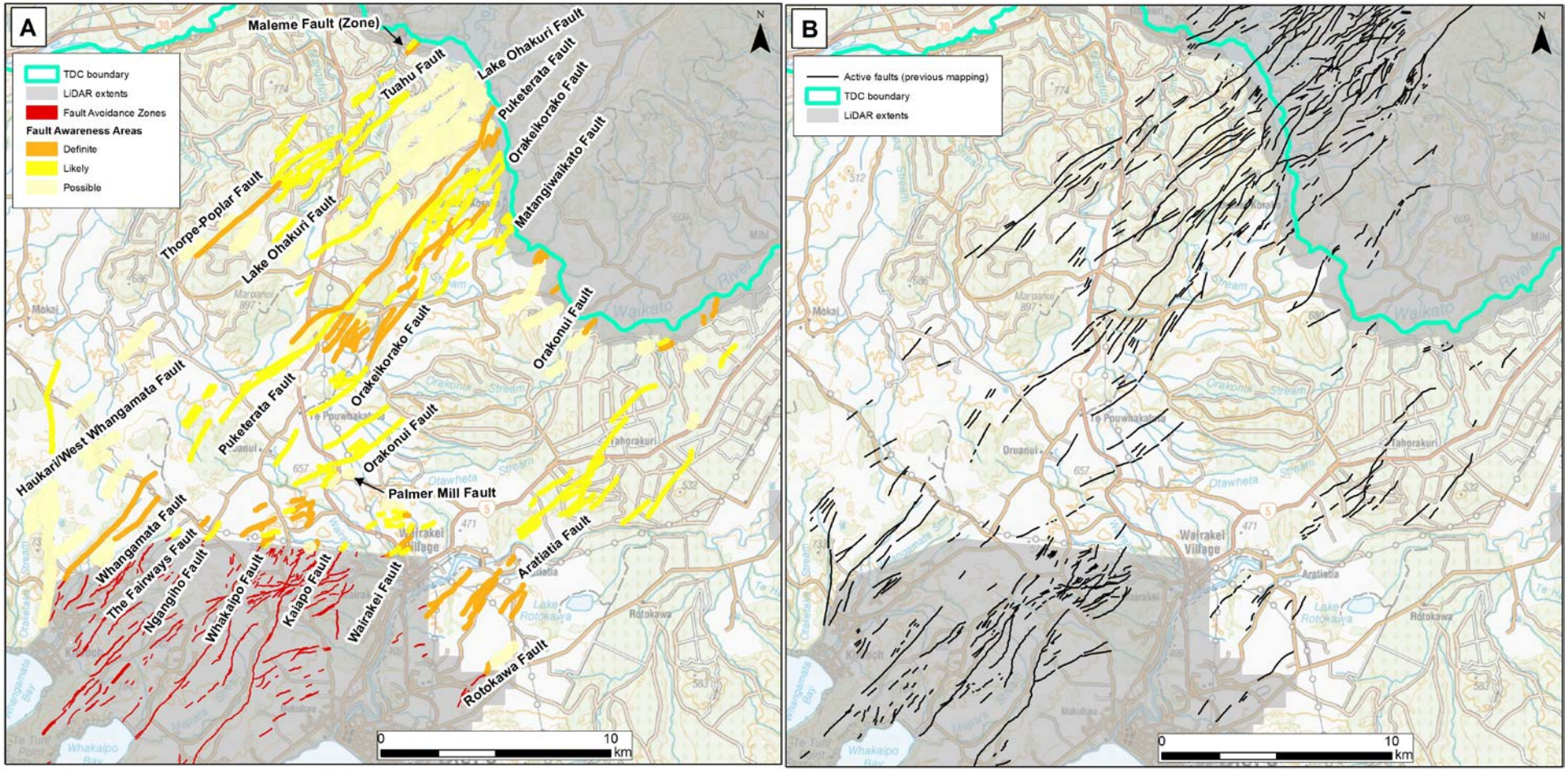

Figure 4.3 (A) Fault Awareness Areas (orange and yellow – classified by certainty) developed for areas not covered by LiDAR data in the Taupō and Whakamaru domains. (B) Previous active fault mapping from the high-resolution version of the New Zealand Active Faults Database.

4.5 Fault Awareness Areas in the Eastern Taupō District

The eastern part of the Taupō District, including part of the NIDFB, is partly covered by Bay of Plenty Regional Council LiDAR data (Figures 1.1, 4.1, 4.4). Recent fault mapping using these data (P Villamor and DB Townsend unpublished data) has identified many new traces (both likely and possible fault traces) in the Rangitaiki–Wairapukau area (Figure 4.4). Although the age and tectonic origin of many of these traces is currently unknown, it was judged prudent to develop Fault Awareness Areas for them.

The newly identified, unnamed traces (both likely and possible) generally trend northeast and the majority are thought to be normal faults. If movement on these faults has occurred in the last 25,000 years, this would suggest that the Taupō Rift may be wider than previously defined (e.g. Figure 2.1). It would also imply that the Taupō Rift overlaps the western edge of the NIDFB (Wheao Fault). None of the traces have been grouped into faults or given names and none have a Certainty classification of ‘Definite’. Instead they have been classified as ‘Likely’ (well-expressed), ‘Likely’ (moderately expressed), ‘Possible’ (well-expressed) and ‘Possible’ (moderately expressed). Only the latter have Fault Awareness Areas of 500 m wide, the remainder are 250 m wide.

The updated fault map for the part of the NIDFB in the Taupō District includes two faults, the Wheao and Te Whaiti faults (Figure 4.4). The LiDAR data reveal clear traces along the central Wheao Fault and a western strand of the Te Whaiti Fault. These traces have been classified as ‘Definite’ (moderately expressed) and ‘Likely’ (well-expressed) and the Fault Awareness Areas are accordingly 250 m wide. The remaining fault traces are classified as ‘Possible’ (moderately expressed) and ‘Possible’ (not expressed) and Fault Awareness Areas are 500 m wide. Three north-trending traces west of the Wheao Fault have been removed as there is no clear basis (e.g. features visible on aerial photographs) for their inclusion.

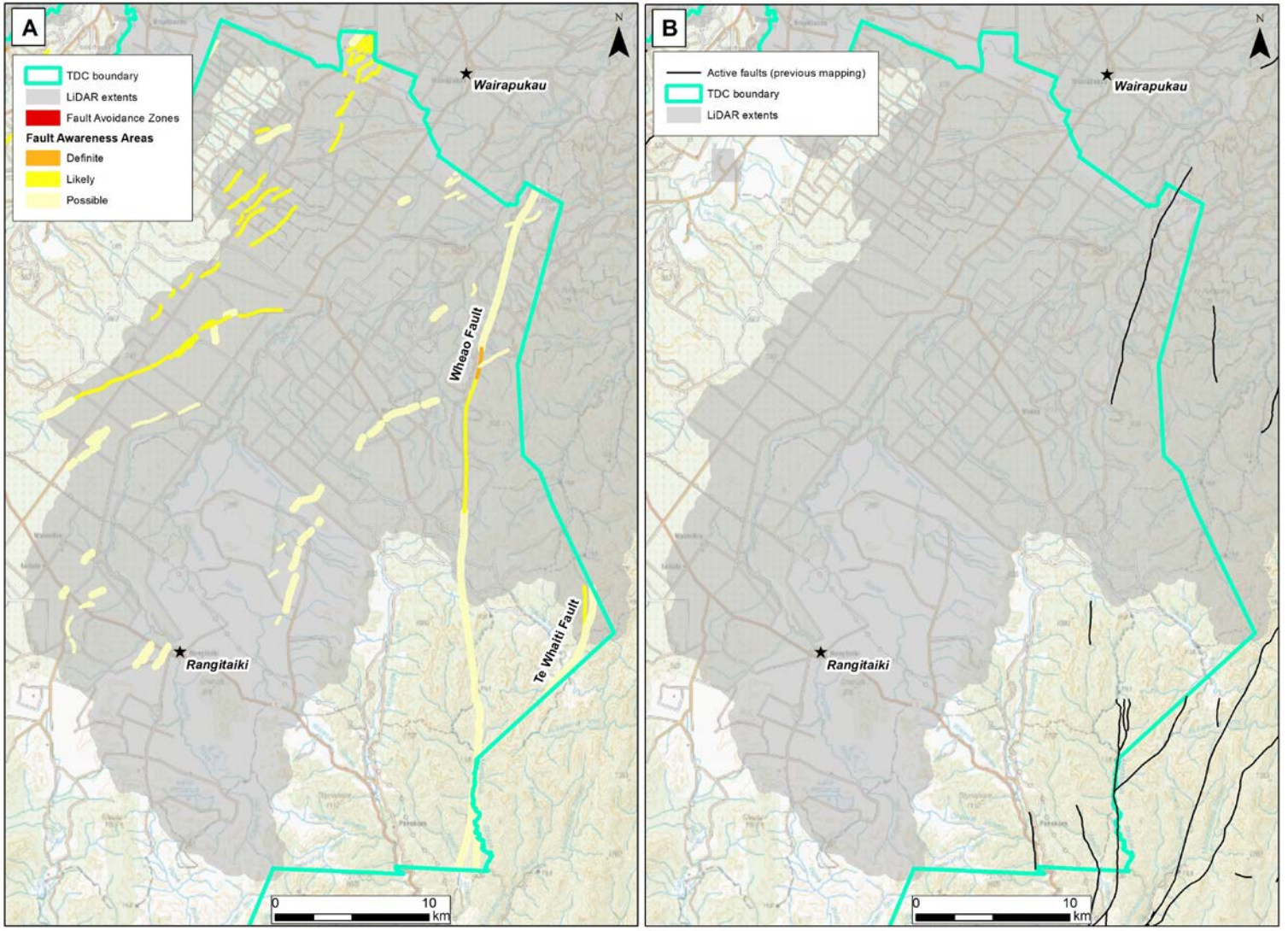

Figure 4.4 (A) Fault Awareness Areas (orange and yellow – classified by certainty) developed for the eastern Taupō District. (B) Previous active fault mapping from the high-resolution version of the New Zealand Active Faults Database.

5.0 ADVICE ON ACTIVE FAULT HAZARDS AND INCORPORATION INTO THE DISTRICT PLAN

5.1 Recurrence Intervals

5.1.1 Existing Data

Existing recurrence interval data for all the named faults in the Taupō District are compiled in Table 5.1 and are briefly summarised below.

Paleoseismic data are currently only available for a small proportion of the total number of faults in the Taupō District, as described in Section 2.4. For most faults, paleoseismic data have been obtained from a trench across one fault trace. These include the Kaiapo Fault (Villamor et al. 2015) and Aratiatia Fault (Berryman et al. 1994), for which recurrence intervals range from 3360 to >10,000 years, but those studies showed that not every fault trace that comprises the whole fault ruptures in every earthquake. That is, ground-rupturing earthquakes occur on these faults more often than is recorded in trenches across a single fault trace.

Recurrence intervals for an entire fault have also been calculated by dividing single-event displacement by slip rate. This has been undertaken using paleoseismic information from natural exposures for the Upper Waikato Stream, Waihi and Poutu fault (zone)s and the recurrence intervals range from 540 ± 100 years to 3500 years (Table 5.1; Gómez-Vasconcelos et al. 2016, 2017). For other faults, recurrence intervals were calculated for the NSHM, which models earthquakes on simplified, major faults for a range of purposes, including the New Zealand Loadings Standards (the Building Code). In the 2010 version of the NSHM (Stirling et al. 2012), recurrence intervals were calculated by dividing single-event displacement by slip rate, whereby single-event displacement was ultimately calculated from the length of earthquake rupture estimated for the specific modelled fault. These values were then evaluated (and validated) against paleoseismic data, where available. The mean calculated recurrence intervals for some of the major faults in the Taupō District range from 530 to 3030 years in the Taupō Rift and 8200 to 13,650 years in the NIDFB (Table 5.1 and Figure 5.1).

Table 5.1 Currently available recurrence interval (RI) data (previous studies) and estimated RIs (this study) for named faults in the Taupō District, arranged in alphabetical order.

Fault Name	Currently Available RI Data			Assigned RI Classes (This Study)		
	RI (Years)	Data Type	Data Source	RI Class	RI Class (Years)	Comments
Aratiatia	1190	Calculated	1, 2, 3	I	≤2000	Conservative min.*
Crater Moon	-	-	-	I	≤2000	Conservative min.*
Hauriki / West Whangamatā	530	Calculated	2, 3	I	≤2000	Possibly a conservative min.*
Kaiapo	3360–5000 major >10,000 minor (one strand only)	Paleoseismic	4	I	≤2000	Conservative min.*
Kaiapo West	-	-	-	I	≤2000	Conservative min.*
Karapiti	-	-	-	I	≤2000	Conservative min.*
Karapiti South	-	-	-	I	≤2000	Conservative min.*
Lake Ohakuri	670	Calculated	2, 3	I	≤2000	Possibly a conservative min.*
Maleme	3500 (one strand only)	Paleoseismic	5, 6	I	≤2000	Conservative min.*
Matangiwaikato	-	-	-	I	≤2000	Conservative min.*
National Park	-	-	-	I	≤2000	Conservative min.*
Ngangautu	-	-	-	I	≤2000	Conservative min.*
Ngangiho	1110	Calculated	2, 3	I	≤2000	Conservative min.*
Orakeikorako	600	Calculated	2, 3	I	≤2000	Possibly a conservative min.*
Orakonui	2000	Calculated	2, 3	I	≤2000	Conservative min.*
Palmer Mill	-	-	-	I	≤2000	Conservative min.*
Poutu	540 ± 100	Paleoseismic	7	I	≤2000	Possibly a conservative min.*
Puketerata	600	Calculated	2, 3	I	≤2000	Possibly a conservative min.*
Rotokawa	-	-	-	I	≤2000	Conservative min.*
Rotopounamu	-	-	-	I	≤2000	Conservative min.*
Taurewa	-	-	-	I	≤2000	Conservative min.*
Te Mihi	-	-	-	I	≤2000	Conservative min.*
Te Whaiti	8200	Calculated	3	IV	>5000–≤10,000	-
The Fairways	-	-	-	I	≤2000	Conservative min.*
Thorpe–Poplar		Paleoseismic	8	I	≤2000	Conservative min.*
Treetrunk	610	Calculated	3	I	≤2000	Possibly a conservative min.*
Tuahu	1140	Calculated	2, 3	I	≤2000	Conservative min.*

Fault Name	Currently Available RI Data			Assigned RI Classes (This Study)		
	RI (Years)	Data Type	Data Source	RI Class	RI Class (Years)	Comments
Tukairangi	-	-	-	I	≤2000	Conservative min.*
Upper Waikato Stream	1600–3500	Paleoseismic	9	I	≤2000	Conservative min.*
Wahianoa	3030	Calculated	3	I	≤2000	Conservative min.*
Waihi	570 ± 100	Paleoseismic	7	I	≤2000	Possibly a conservative min.*
Wairakei	-	-	-	I	≤2000	Conservative min.*
Whakaipo	1060	Calculated	2, 3	I	≤2000	Conservative min.*
Whakaipo West	-	-	-	I	≤2000	Conservative min.*
Whangamatā	630	Calculated	2, 3	I	≤2000	Possibly a conservative min.*
Wheao	13,650	Calculated	3	V	>10,000–≤20,000	-

1: Berryman et al. (1994), 2: McVerry et al. (2005), 3: Stirling et al. (2012), 4: Villamor et al. (2015), 5: McClymont et al. (2009), 6: Villamor et al. (2011), 7: Gómez-Vasconcelos et al. (2017), 8: Villamor et al. (2003), 9: Gómez-Vasconcelos et al. (2016).

* The ≤2000 years recurrence interval applied to all traces of all named Taupō Rift faults are acknowledged to be a conservative minimum (min.) classification because it is possible that not every fault trace that comprises an entire fault ruptures in every earthquake (Figure 5.2). Therefore, the recurrence interval class for individual fault traces could be much longer (larger) than the fault as a whole.

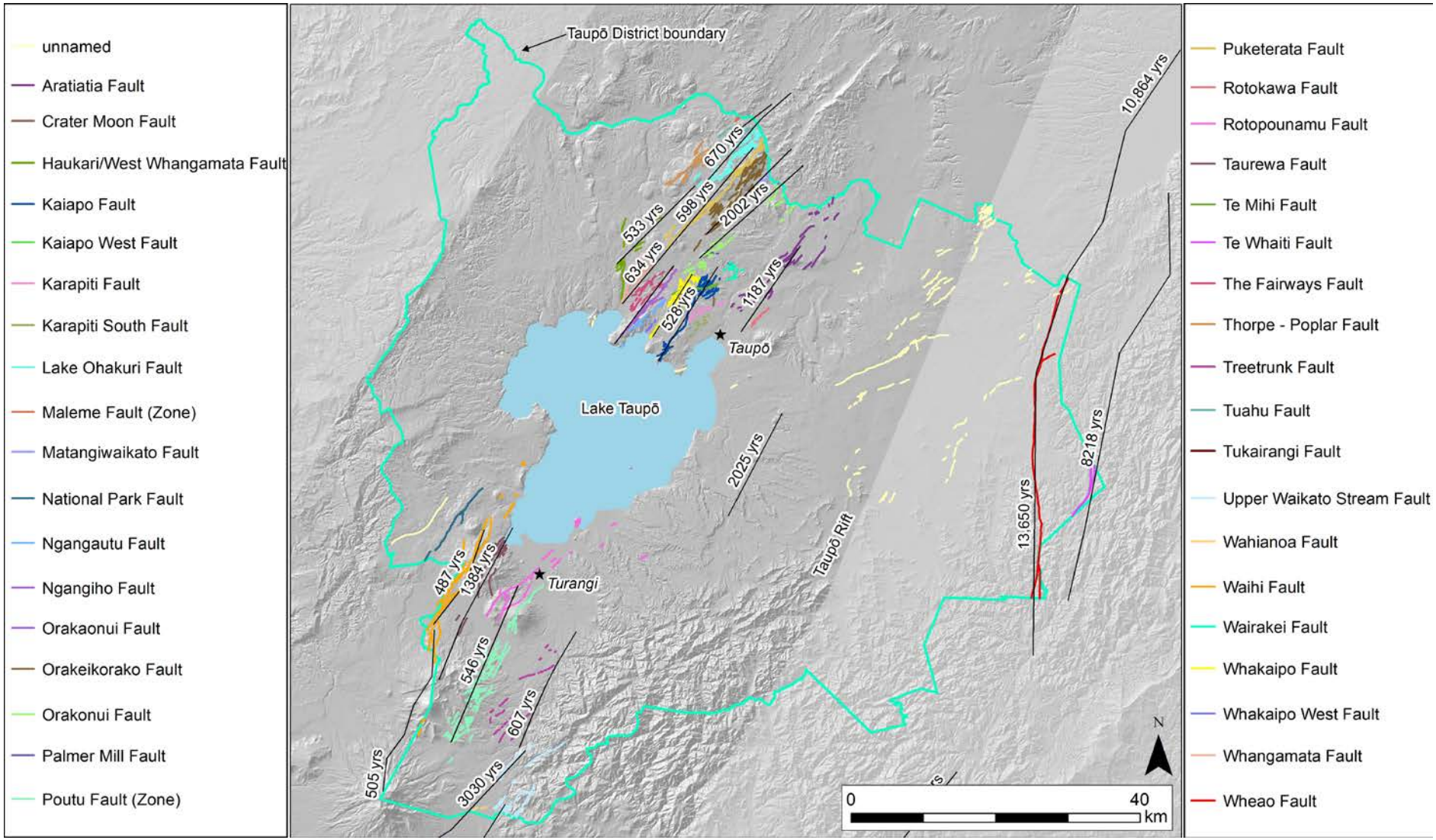

Figure 5.1 Active faults in the Taupō District (colour-coded by name), overlain by summary (generalised) major faults in the 2010 version of the NSHM (black lines). The values in years (yrs) are the calculated recurrence intervals.

5.1.2 Recurrence Interval Classes

There are many challenges to assigning recurrence interval classes to each fault and fault trace in the Taupō District. The largest is a lack of data, with no available paleoseismic data for the NIDFB faults and sparse data for the large number of Taupō Rift faults. Another key issue for the multi-trace Taupō Rift faults is that recurrence intervals vary through both time and space. Spatially, not all traces that comprise an entire fault have the same recurrence intervals because not all traces rupture in each earthquake. This is diagrammatically illustrated in Figure 5.2, whereby earthquakes recorded in a hypothetical trench – where the fault is represented by a single trace – may suggest a recurrence interval of 500 years. However, farther along the fault, where the fault may comprise many traces, each of those may only rupture in some earthquakes and therefore may have longer recurrence intervals.

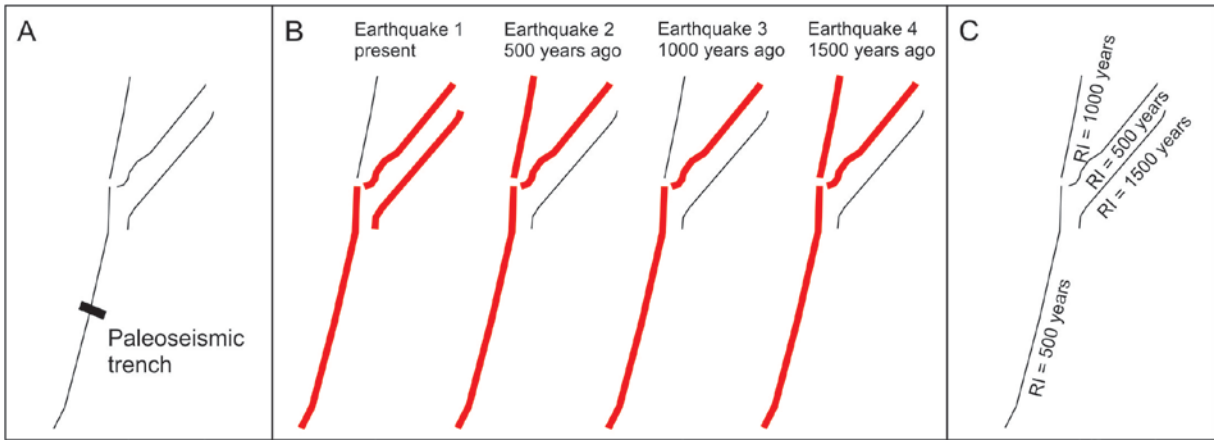

Figure 5.2 Schematic showing how recurrence intervals can vary for different traces on a Taupō Rift fault. (A) Hypothetical paleoseismic trench where past earthquake information is obtained. (B) Specific earthquakes may rupture different combinations of fault traces. (C) Illustrative recurrence intervals (RIs) for individual fault traces. In this hypothetical case – and considering the RI values shown – even though the RI of individual trace may vary considerably (in this case by a factor of 3), all traces would be assigned to RI Class I (≤2000 years).

We have therefore used the following method to assign recurrence interval classes to Taupō District faults (Table 5.1):

1. For the NIDFB, the calculated 2010 NSHM recurrence interval values are used to assign RI Classes V and IV to the Wheao and Te Whaiti faults, respectively. This is considered appropriate because the Wheao and Te Whaiti faults mainly consist of a single fault strand, and therefore a consistent recurrence interval can be assumed along-strike. However, we acknowledge that, because the recurrence interval is calculated from an inferred slip rate and an assumed fault rupture segment length, the recurrence interval is uncertain and the 2010 NSHM only calculated mean values.
2. For named Taupō Rift faults, the sparse paleoseismic and calculated NSHM recurrence interval values are used to assign all faults to RI Class I. For many individual fault traces, it is possible that this could be a minimum (conservative) RI Class assignment (i.e. the RI Class of an individual trace could be greater than Class I), but currently there is no robust method to estimate RI Class for every individual trace, so we assign this based on the fault as a whole.
3. For unnamed faults, for which there are no available data, no RI Class is assigned. These are mainly unnamed, newly mapped ‘Likely’ and ‘Possible’ fault traces west and east of previously identified Taupō Rift faults for which Fault Awareness Areas have been developed.

5.2 Recommendations for Incorporation for Planning Purposes

This section provides recommended planning actions for both the Fault Avoidance Zones and Fault Awareness Areas generated in this report. For Fault Avoidance Zones, these recommendations are based on the MfE Active Fault Guidelines (Kerr et al. 2003). For Fault Awareness Areas, the recommendations are based on the ECan FAA Guidelines (Barrell et al. 2015). This section also considers the inclusion of natural hazard information on Land Information Memorandums and Project Information Memorandums, with specific reference to Saunders and Mathieson (2016).

The recommended planning provisions provide a starting point for community consultation and the final planning provisions may be either more or less restrictive as deemed appropriate by the community and the Council.

5.2.1 Guiding Principles

It is understood that the Taupō District Plan is under a full review, is currently in Phase 1 of 3 of plan preparation and that natural hazards are captured within this phase. While it is recommended that the Fault Avoidance Zones and Fault Awareness Areas are incorporated into the Taupō District Plan, and any other hazard information maps for Taupō District (for example, the Waikato Regional Hazards Portal), it is recognised that the statutory process for incorporating new natural hazard information that has the potential to affect development into the District Plan is not straightforward and also somewhat open to interpretation of the territorial authority as to how it is applied. Therefore, guided by Section 32 and Schedule 1 of the Resource Management Act, when seeking to incorporate natural hazard information into a district plan, the following guidance principles, driven by transparency and information sharing, should be considered:[6]

1. Identify the areas and landowners affected by the imposition of Fault Avoidance Zones and Fault Awareness Areas, including their development potential (whether zoned appropriately or not).
2. Consider the potential planning implications of including the Fault Avoidance Zones and Fault Awareness Areas (as set out in Tables 5.2–5.4) in the Taupō District Plan. For example, are the areas affected by the Fault Avoidance Zones and Fault Awareness Areas potential residential development sites, located within sites protected through other statutory mechanisms or located through areas with minimal development potential.
3. Contemplate the overarching direction of the objectives and policies in relation to the Fault Avoidance Zones and Fault Awareness Areas. For example, seeking to avoid the effects of ground rupture on buildings.
4. Consider the activities that will be managed through active fault overlays. For example, will the MfE Active Fault Guidelines be adopted as drafted or will they be extended to structures over a certain size; how will buildings and/or building use be managed/ differentiated; will earthworks, subdivision, infrastructure and hazardous substances be captured by active fault provisions?

6 It is also noted that the MfE Active Fault Guidelines contain the following four principles:
1. Gather accurate active fault hazard information.
2. Plan to avoid fault rupture hazard before development and subdivision.
3. Take a risk-based approach in areas already developed or subdivided.
4. Communicate risk in built-up areas subject to fault rupture.

5. Consider the development challenges the district faces. For example, are these focused on greenfield areas, infill or infrastructure. This report addresses greenfield and infill development, as the focus of the MfE Active Fault Guidelines is life safety. However, infrastructure providers will likely take an interest in active fault overlays within the District Plan.
6. Undertake analysis (e.g. using GIS) to determine the area of operative versus proposed zonings affected by active fault overlays, identify potential policy conflicts (for example, restrictions put in place by active fault overlays and residential zonings seeking to enable higher-density development) and contemplate the use of multi-tiered provision frameworks (for example, overlay provisions would typically take precedence over zoning provisions, and therefore precincts may be required).
7. Review the engineering options available to the activities managed by the active fault overlays and whether these could feasibly reduce the risk to an acceptable level, and enable the purpose of the active fault overlays to be achieved and land use to occur.
8. Socialise the Fault Avoidance Zones and Fault Awareness Areas, and their implications within a District Plan setting, with internal Council departments (resource consents, building consents, infrastructure controllers, parks and reserves, emergency managers), including gathering their existing processes with regard to development and active faults.
9. Socialise the Fault Avoidance Zones and Fault Awareness Areas, and their implications within a District Plan setting, with the Council's Executive and Councillors. This would likely require the involvement of the authors of this report to present findings and present ground-surface rupture hazard science.
10. Seek affirmation from the Council to proceed with the incorporation of Fault Avoidance Zones and Fault Awareness Areas into the District Plan.
11. Socialise the Fault Avoidance Zones and Fault Awareness Areas, and their implications, with landowners, focusing on land with significant and short- to mid-term development potential.
12. Socialise the Fault Avoidance Zones and Fault Awareness Areas with other groups, including Mana Whenua, Regional Council, ratepayers associations, residents groups, local boards, landowners, development groups and regional planning branches.
13. If timeframes allow, circulate a Draft District Plan for feedback, noting that this needs to occur approximately 12 months ahead of notifying a Proposed Plan.

Regarding the significant amount of engagement sought by these principles, Step 1 of GNS Science's Risk-Based Planning Toolbox contains guidance on the development of an engagement strategy, and internal and external communication.[7]

7 https://www.gns.cri.nz/Home/RBP/Risk-based-planning/A-toolbox/Risk-based-planning-approach-and-steps/Step-1-Know-your-hazard/Building-an-engagement-strategy
https://www.gns.cri.nz/Home/RBP/Risk-based-planning/A-toolbox/Risk-based-planning-approach-and-steps/Step-1-Know-your-hazard/Internal-communication
https://www.gns.cri.nz/Home/RBP/Risk-based-planning/A-toolbox/Risk-based-planning-approach-and-steps/Step-1-Know-your-hazard/External-communication

5.2.2 District Plan Maps

Examples of the incorporation of active fault mapping within District Plans around New Zealand occur in the following district plans:

- Proposed Kāpiti District Plan, which utilises the MfE Active Fault Guidelines methodology.
- Nelson Resource Management Plan, which applies a single Fault Hazard Overlay.
- Selwyn District Plan, which maps faults as a line.

It is recommended that all Fault Avoidance Zones and Fault Awareness Areas should be shown in the Taupō District Plan and any other planning or hazard information maps for Taupō District. Adopting the MfE Active Fault Guidelines and ECan FAA Guidelines, Sections 5.2.3 and 5.2.4 set out the resource consent activity status for buildings within the Fault Avoidance Zones and Fault Awareness Areas.

5.2.3 Fault Avoidance Zones

Based on the MfE Active Fault Guidelines, which takes a risk-based approach formulated around life safety, recommended resource consent categories for activities within the Fault Avoidance Zones are given in Tables 5.2 and 5.3. Building importance categories and the relationships between recurrence interval class and building importance class from the MfE Active Fault Guidelines are contained in Appendix 3.

Table 5.2 Recommended resource consent categories for greenfield sites in relation to fault complexity for the Fault Avoidance Zones generated in this study.

Greenfield Sites						
Building Importance Category (See Appendix 3 for Definitions)		**1**	**2a**	**2b**	**3**	**4**
RI Class	**Fault Complexity**	**Resource Consent Category**				
Aratiatia, Crater Moon, Hauriki / West Whangamatā, Kaiapo, Kaiapo West, Karapiti, Karapiti South, Lake Ohakuri, Maleme, Matangiwaikato, National Park, Ngangautu, Ngangiho, Puketerata, Orakeikorako, Orakonui, Palmer Mill, Poutu, Puketerata, Rotokawa, Rotopounamu, Taurewa, Wairakei, Te Mihi, The Fairways, Thorpe–Poplar, Treetrunk, Tuahu, Tukairangi, Upper Waikato Stream, Wahianoa, Waihi, Wairakei, Whakaipo, Whakaipo West, Whangamatā faults						
I <2000 years	Well-defined Distributed Uncertain	Permitted Permitted Permitted	*Non-complying* *Discretionary* *Discretionary*	*Non-complying* *Non-complying* *Non-complying*	*Non-complying* *Non-complying* *Non-complying*	Prohibited Non-complying Non-complying
Te Whaiti Fault						
IV 5000–10,000 years	Well-defined Distributed Uncertain	Permitted Permitted Permitted	Permitted* Permitted Permitted	Permitted* Permitted Permitted	*Non-complying* *Discretionary* *Discretionary*	Non-complying Non-complying Non-complying
Wheao Fault						
V 10,000–20,000 years	Well-defined Distributed Uncertain	Permitted Permitted Permitted	Permitted* Permitted Permitted	Permitted* Permitted Permitted	Permitted* Permitted Permitted	Non-complying Non-complying Non-complying

* The recommended resource consent category is permitted but could be controlled or discretionary, given that the fault location is well-defined.

Italics show that the activity status is more flexible. For example, where '*Discretionary*' is indicated, controlled activity status may be considered more suitable.

Table 5.3 Recommended resource consent categories for developed and already subdivided sites in relation to fault complexity for the Fault Avoidance Zones generated in this study.

Developed and Already Subdivided Sites						
Building Importance Category (See Appendix 3 for Definitions)		**1**	**2a**	**2b**	**3**	**4**
RI Class	**Fault Complexity**	**Resource Consent Category**				
Aratiatia, Crater Moon, Hauriki / West Whangamatā, Kaiapo, Kaiapo West, Karapiti, Karapiti South, Lake Ohakuri, Maleme, Matangiwaikato, National Park, Ngangautu, Ngangiho, Puketerata, Orakeikorako, Orakonui, Palmer Mill, Poutu, Puketerata, Rotokawa, Rotopounamu, Taurewa, Wairakei, Te Mihi, The Fairways, Thorpe–Poplar, Treetrunk, Tuahu, Tukairangi, Upper Waikato Stream, Wahianoa, Waihi, Wairakei, Whakaipo, Whakaipo West, Whangamatā faults						
I <2000 years	Well-defined Distributed Uncertain	Permitted Permitted Permitted	*Non-complying* *Discretionary* *Discretionary*	*Non-complying* *Non-complying* *Non-complying*	*Non-complying* *Non-complying* *Non-complying*	Non-complying Non-complying Non-complying
Te Whaiti Fault						
IV 5000–10,000 years	Well-defined Distributed Uncertain	Permitted Permitted Permitted	Permitted* Permitted Permitted	Permitted* Permitted Permitted	Permitted* Permitted Permitted	Non-complying Non-complying Non-complying
Wheao Fault						
V 10,000–20,000 years	Well-defined Distributed Uncertain	Permitted Permitted Permitted	Permitted* Permitted Permitted	Permitted* Permitted Permitted	Permitted* Permitted Permitted	Permitted Permitted** Permitted**

* The recommended resource consent category is permitted but could be controlled or discretionary, given that the fault location is well-defined.

** Although the activity status is permitted, care should be taken in locating Building Importance Category (BIC) 4 structures on or near known active faults. Controlled or discretionary activity status may be more suitable.

Italics show that the activity status is more flexible. For example, where '*Discretionary*' is indicated, controlled activity status may be considered more suitable.

5.2.4 Fault Awareness Areas

Taking a risk-based approach using the ECan FAA Guidelines, recommended actions for activities within the Fault Awareness Areas for these faults are given in Table 5.4.

Table 5.4 Recommended actions for the Fault Awareness Areas generated in this study.

Proposed Activity	**Recommended Actions**		
	For FAA categories: 'Definite' (well-expressed), 'Definite' (mod. expressed), 'Likely' (well-expressed), 'Likely' (mod. expressed), with RI Class I, II or III	For FAA categories: 'Definite' (well-expressed), 'Definite' (mod. expressed), 'Likely' (well-expressed), 'Likely' (mod. expressed), with RI Class IV, V or VI	For all other FAA categories: 'Definite' (not expressed), 'Likely' (not expressed), 'Possible'
Single residential dwelling (BIC 2a and 2b, in part)	Permitted activity.		
Normal structures and structures not in other categories (BIC 2b, apart from single dwellings)	Consideration of the surface fault rupture hazard should be a specific assessment matter if resource consent for a new structure is required for some other reason. Site-specific investigation, including detailed fault mapping at 1:35,000 or better and appropriate mitigation measures for the accurately mapped fault (e.g. set-back or engineering measures).		Permitted activity.
Important or critical structures (BIC 3 and 4)	Consideration of the surface fault rupture hazard should be a specific assessment matter if resource consent for a new structure is required for some other reason. Site-specific investigation, including detailed fault mapping at 1:35,000 or better and appropriate mitigation measures determined for the accurately mapped fault (e.g. set-back or engineering measures).		
New subdivision (excluding minor boundary adjustments)	Consideration of the surface fault rupture hazard should be a specific assessment matter. Site-specific investigation, including detailed fault mapping at 1:35,000 or better and appropriate mitigation measures for the accurately mapped fault (e.g. set-back or engineering measures).		New subdivision (excluding minor boundary adjustments).
Plan changes	Consideration of the surface fault rupture hazard should be a specific assessment matter. Site-specific investigation, including detailed fault mapping at 1:35,000 or better and appropriate mitigation measures for the accurately mapped fault (e.g. set-back or engineering measures.		

5.2.5 Land Information Memoranda and Property Information Memoranda

Guidance for including information about Fault Awareness Areas on Land Information Memoranda (LIMs) and Property Information Memoranda (PIMs) is provided in the ECan FAA Guidelines. This guidance, with some minor modifications, can also be used for Fault Avoidance Zones, which are based on more detailed mapping.

An analysis of the role of LIMs in the communication of natural hazard information is provided in Saunders and Mathieson (2016). A key point raised within Saunders and Mathieson (2016) revolves around the interaction between information on a LIM and information within a district plan. A legal opinion was obtained, which considered that:

> *"Information does not need to be included on a LIM if it is apparent from an operative district plan. It follows that until a proposed district plan is operative, the relevant information must still be included on a LIM."*

Local Government New Zealand has also produced a guidance publication on this matter,[8] but note that this area is complex and councils should seek specific legal advice where necessary.

With regard to regional and district level planning, Saunders and Mathieson (2016) make the following recommendations:

- Establish a working group within the region to create consistency of what natural hazards information is included in the LIMs for the region.
- Standardise, at the regional level, what hazard information goes into the LIMs, especially if there has been modelling or research that shows the entire region has the potential to be affected by a natural hazard.
- The express and standard LIM services need to be consistent with each other. The information they contain needs to offer the same advice, in the same format.
- Include real estate agents and property lawyers in any dissemination of information. This could include a seminar to present new information specifically for real estate agents and property lawyers.
- List on the LIM any remedial works done to mitigate hazards.

5.3 Ground-Surface Rupture Hazard

5.3.1 Ground-Surface Rupture Features

Historical ground-surface fault ruptures in the Taupō District are summarised in Section 2.2 and paleoseismic data in Section 2.4. We also provide summaries of the M_W 6.5 1987 Edgecumbe, M_W 7.1 2010 Darfield and M_W 7.8 2016 Kaikōura earthquake ground deformation characteristics in Appendix 2.

For faults in the NIDFB that are predominantly strike-slip (Appendix 1.2), the ground-surface ruptures will likely be dominated by horizontal displacement, but will probably also result in vertical steps, with *en-echelon* (overlapping, curved) cracks, and both vertically and horizontally deform infrastructure such as roads and fence lines. The Darfield and Kaikōura earthquakes provide useful analogues, such as those shown in Figure 5.3.

8 https://www.lgnz.co.nz/assets/Uploads/16edd4fd27/46292-LGNZ-Climate-Change-3-Natural-Hazards.pdf

For faults within the Taupō Rift, fault ruptures in the 1987 Edgecumbe earthquake provide an analogue of future deformation. These are normal faults with predominant relative movement of the blocks across the fault of uplift and subsidence (Appendix 1.2). They are often also associated with gashes or fissures and with folding of the ground. The Taupō Rift normal faults are likely to produce vertical steps accompanied by extensional cracks, similar to the Edgecumbe earthquake examples in Figure 5.4. The Edgecumbe earthquake is also a useful analogue because the soil structures in the Rangitaiki Plains are similar to the Taupō District. The loose, pumice-type soils in much of the Taupō District will mean that multiple centimetre- to decimetre-scale ruptures distributed over a zone several metres wide (Figure 5.3B, C) will be common.

These examples all show that ground-surface ruptures resulting from moderate to large earthquakes on active faults in the Taupō District are likely to range from centimetre to metre scale. This deformation can in places be either relatively concentrated (i.e. discrete) or spread-out (i.e. distributed). Both the amount of displacement, and the manner in which that displacement is either concentrated or distributed, influences the impact that surface rupture may have on structures sited on or across that rupture. For the northern Taupō Rift, Villamor et al. (2001) assign an average co-seismic displacement of ~1–1.5 m, which is also applicable to this area.

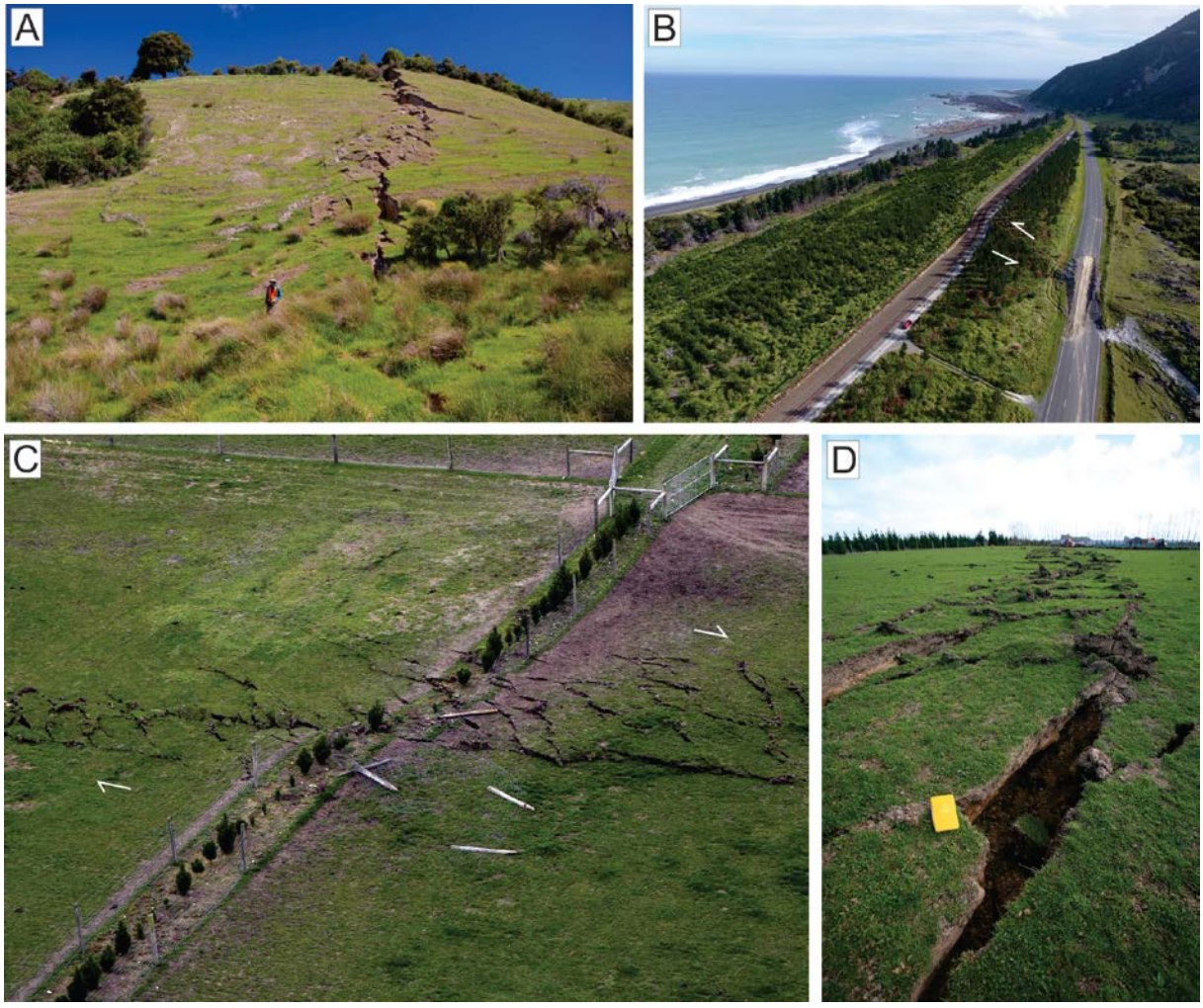

Figure 5.3 Examples of strike-slip ground-surface fault rupture in the 2016 Kaikōura (A, B) and 2010 Darfield (C, D) earthquakes. Photographs taken by Kate Pedley (A), Julian Thompson (B), Nicola Litchfield (C) and unknown (D).

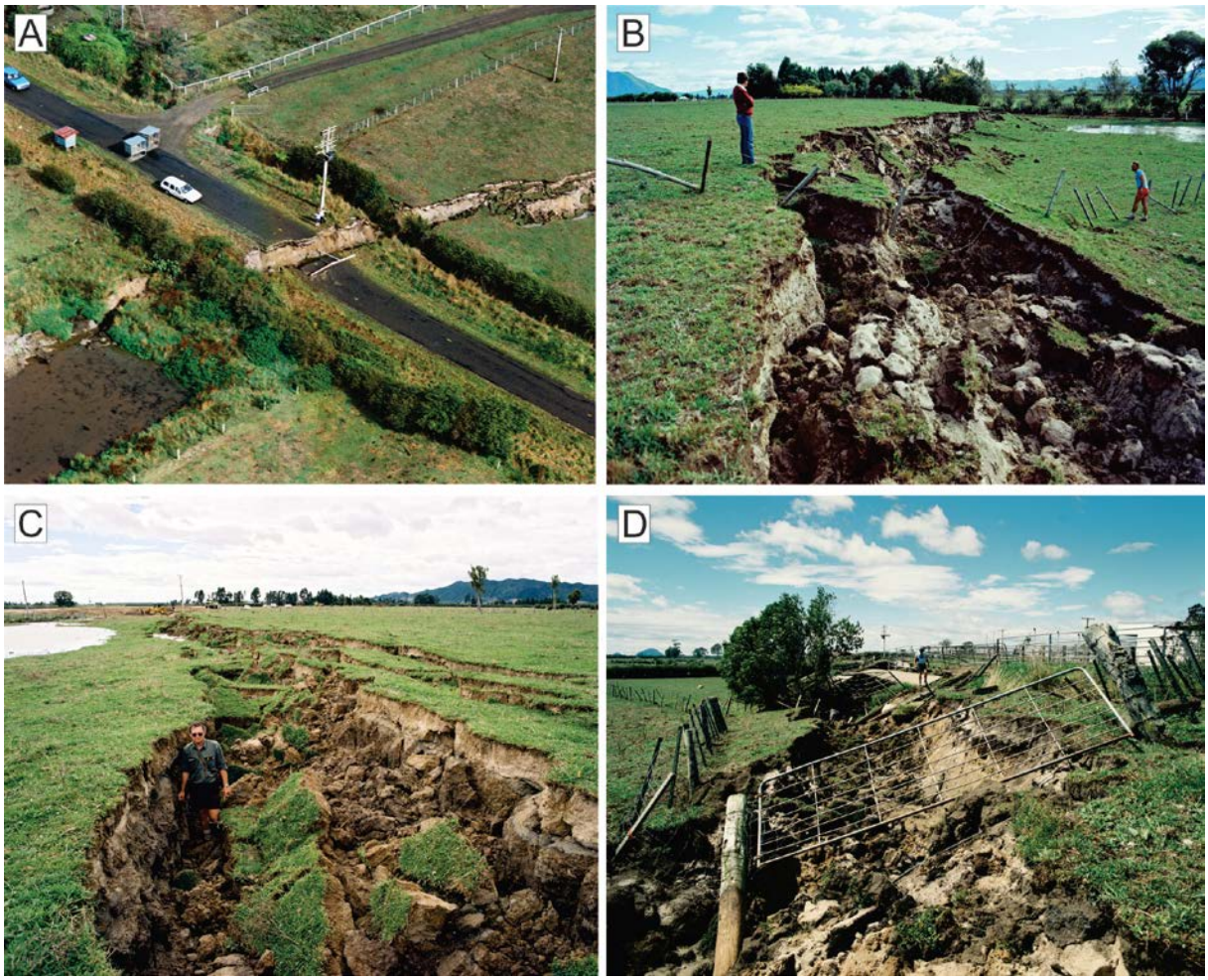

Figure 5.4 Examples of normal ground-surface fault rupture in the 1987 Edgecumbe earthquake. Photographs by Lloyd Homer.

5.3.2 Ground-Surface Rupture Impacts on Small to Medium Timber-Framed Houses

The MfE Active Fault Guidelines is the primary document in New Zealand providing guidance with regards to the mitigation of ground-surface fault rupture hazard. In these guidelines, the recommended mitigation strategy is avoidance; however, engineering mitigation strategies are also permitted in appropriate circumstances, though little, if any, guidance is provided regarding what those engineering strategies and appropriate circumstances might be. This deficiency was largely the consequence of a lack of data. That is, at the time that the guidelines were issued, there were very few New Zealand examples to draw from where New Zealand engineered structures had been impacted by ground-surface fault rupture, and the impacts of that rupture evaluated with regards to: a) the characterisation of the ground strains and displacements generated by that surface rupture, b) the structural damage the surface rupture produced and c) the possible engineering strategies that could be employed to mitigate that damage.

Since the MfE Active Fault Guidelines were published, there have been two large New Zealand earthquakes that have generated ground-surface fault rupture that has directly impacted engineered buildings; the 2010 Darfield earthquake and the 2016 Kaikōura earthquake (Van Dissen et al. 2011, 2019). The amount and style of surface rupture deformation varied considerably, ranging from decimetre-scale distributed folding with estimated shear strains in the order of $\leq 10^{-2}$ to metre-scale discrete rupture with estimated shear strains up to 10^{0}. Collectively, about two dozen buildings were directly damaged by ground-surface fault rupture

resulting from these two earthquakes. These were typically single-storey timber-framed houses, barns and woolsheds with regular-shaped floor plans and lightweight roofing materials. Based on these examples (which are elaborated on in Appendix 2), several pertinent observations can be made regarding the performance of New Zealand residential structures when subjected to surface fault rupture deformation of varying levels of strain and amounts of displacement.

1. Single-storey, regular-shaped, timber-framed residential structures with light roofs and of modest dimensions (floor area of ≤~200 m^2) subjected to low/moderate surface fault rupture deformation (i.e. shear strains ≤10^{-2} and discrete displacements of decimetre-scale or less) do not appear to pose a collapse hazard.
2. At those levels of deformation, the prospects of damage-control and repairability (and therefore post-event functionality) appear to be improved for such residential structures if the cladding contributes to the robustness of the superstructure (e.g. plywood, timber weatherboard) and is not brittle.
3. This favourable behaviour is enhanced if building systems moderate the direct transmission of ground deformation into the superstructure (either by decoupling or by other means) and allow for re-levelling of the structure post-event.
4. For residential structures with the above-mentioned attributes, non-collapse performance can be achieved at even higher levels of strain (~10^0) and larger discrete displacements (metre-scale) in a predominantly horizontal displacement setting (i.e. strike-slip) if the superstructure decouples from (is isolated from) the underlying ground deformation. The New Zealand dataset does not contain examples of the performance of residential structures subjected to such large surface fault rupture strains and displacements in a predominantly vertical displacement setting. In a horizontal displacement setting, the decoupled superstructure still rests on (and is supported by) the ground. This may not be the case in a predominantly vertical displacement setting where there is the possibility that fault rupture will leave a significant portion of the decoupled superstructure un-supported and this may lead, if not to collapse, then at least to significant tilting and angular distortions. In addition, in a reverse/thrust vertical displacement setting there is the potential for a 'bulldozer zone' to develop at the base of the scarp where fault-displacement forces the scarp to thrust horizontally across the ground surface, and this too can severely impact structures.

In Appendix 2, we present case-study examples from the 2010 Darfield and 2016 Kaikōura earthquakes, and the 1987 Edgecumbe earthquake also, showing the impacts surface fault rupture had on residential (or residential-type) structures. These examples provide insight into construction styles that could be employed, in suitable circumstances, to facilitate non-collapse performance resulting from surface fault rupture and, in certain instances, post-event functionality. We also provide comment on how these examples may enable a more nuanced application of the MfE Active Fault Guidelines in, again, appropriate circumstances.

5.4 Active Fault Completeness

There are three important factors to take into account when assessing the completeness of the active fault map presented in this study: 1) uncertainty of the tectonic origin of some mapped faults (i.e. whether they are indeed faults), 2) uncertainty of whether the faults are currently active (i.e. are we sure that the feature is a fault but no longer active) and 3) no surface expression of an active fault (i.e. the potential for missing faults).

1) Of the Taupō District active faults mapped in this study, 76% are classified as ‘Definite’ (40%) or ‘Likely’ (26%). Of the remaining 24% classified as ‘Possible’, we estimate that the majority are probably active faults but cannot rule out other origins for some. Potential other origins include river erosion near some of the rivers and larger streams, landslide scars in the steeper hill country or eroded bedrock landforms in older sedimentary rocks. In addition, we highlighted earlier that the age of the recently mapped, unnamed faults in the Rangitaiki–Wairapukau area is unknown. Further studies including paleoseismic trenches can reveal the origin of the mapped feature.

2) A general indication of whether the mapped Taupō District faults are currently active can be obtained from comparing them with mapped inactive faults. In Figure 5.5, we show ‘Inactive’ and ‘Probably inactive’ faults in the 1:250,000-scale geological map of New Zealand (black lines; Heron 2014 and updated in 2018). This shows that, of the active faults mapped in this study, only two faults correspond to those mapped by Heron (2014) as ‘Inactive’ and ‘Probably inactive’ (A and B on Figure 5.5). It is possible that these three faults are inactive faults as previously mapped, but our interpretation from the currently available datasets (aerial photographs and 2-m- and 8-m-resolution DSMs) suggests they may be active. We also note that we have been finding new active fault traces as LiDAR data becomes available but, conversely, some faults are now considered inactive. It will therefore be important to revisit the potential activity for those faults when LiDAR data are available in those areas.

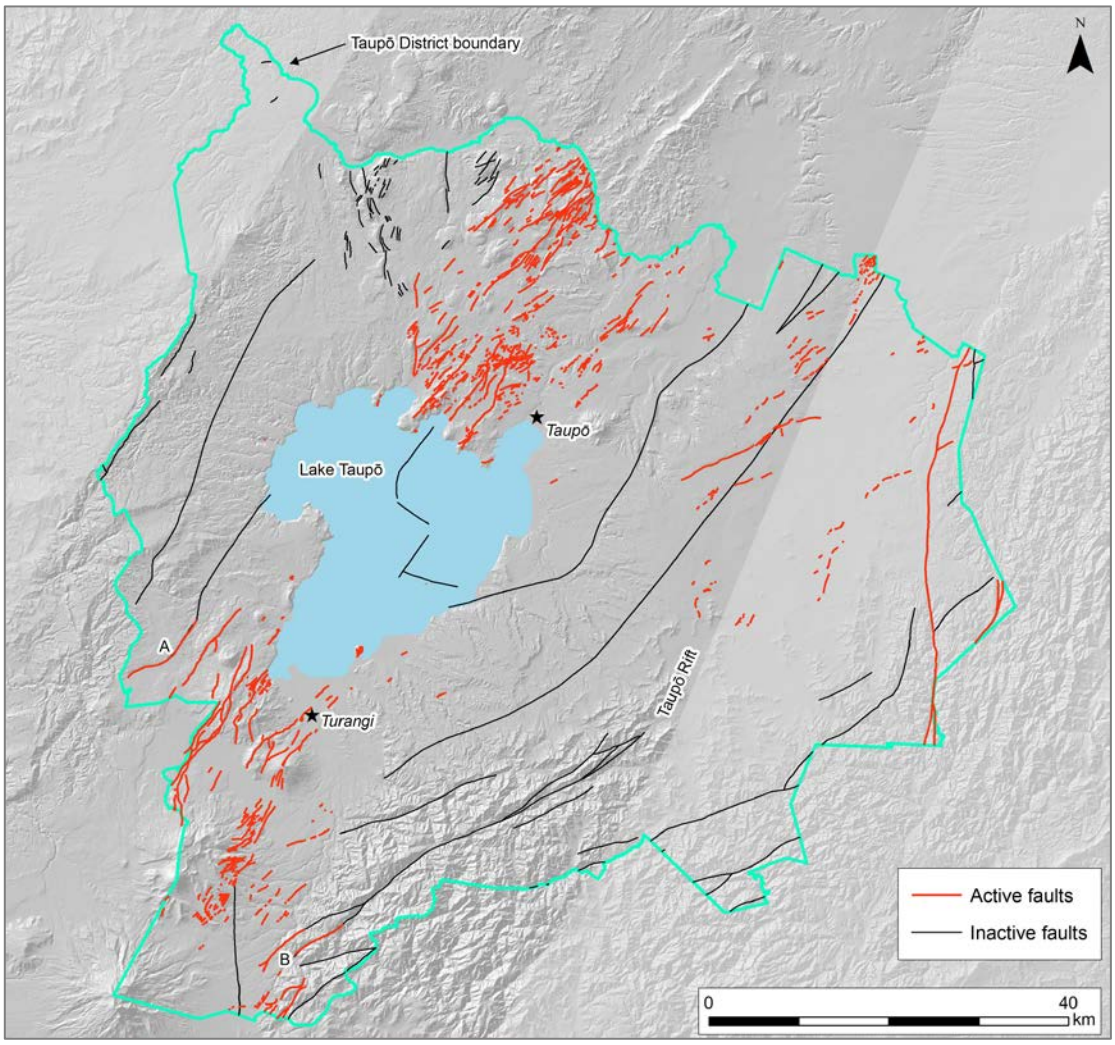

Figure 5.5 Taupō District active faults (this study) superimposed upon ‘Inactive’ and ‘Probably inactive’ faults. The ‘Inactive’ and ‘Probably inactive’ faults are from Heron (2014). A and B are faults discussed in the text.

3) Large volcanic eruptions within the Taupō Rift mantle the landscape with layers of ash and pyroclastic flows that, if thick enough, can cover fault traces/scarps. The fault scarps that we are able to map are those that are either: a) very active and produce scarps high enough that they are not totally buried by the volcanic materials, or were previously covered but have subsequently created new scarps displacing the new materials; or b) faults that are not very active (and thus have been buried by volcanic materials) but have ruptured very recently (e.g. the last 2000 years). These latter faults tend to be associated with small, subtle scarps and are usually only detected using LiDAR data or high-resolution aerial photographs. It is possible that we will locate new fault scarps in areas with no LiDAR data once the data are available, but even in areas with LiDAR data we could be missing some faults that are either not very active or have not ruptured recently. For this latter situation, mitigation for planning purposes may not be possible. This is particularly important for the area around Lake Taupō covered by the ~1700-year-old Taupō Ignimbrite.

5.5 Recommendations for Work Needing to be Undertaken for an Individual Wishing to Build in a Fault Avoidance Zone or Fault Awareness Area

As requested in the project brief, in this section we make some specific recommendations regarding a process for an individual wishing to build within a Fault Avoidance Zone or Fault Awareness Area. More general recommendations from this study are contained in Section 6.

Regarding work needed to be undertaken for *an individual wishing to build in a Fault Awareness Area and to have an expert define a Fault Avoidance Zone*, GNS Science recommends:

- Assess the Building Importance Category of the proposed building and the recurrence interval of the fault to determine the level of work required, based on the recommendations in Table 5.2.
- If the building is not a permitted activity, then consider obtaining a geotechnical assessment to determine if the building could be moved outside the Fault Awareness Area.
- If this is not possible, then:
  - determine the best available dataset to map the fault as accurately as possible (preferably LiDAR, but, if necessary, a Digital Surface Model or aerial photographs).
  - Map the fault in a GIS.
  - Characterise the mapped fault with the attributes shown in Tables 3.1–3.3.
  - Develop the Fault Avoidance Zone based on the methodology in Section 3.3.
- If possible, plan to build outside of the Fault Avoidance Zone. If not, then follow steps such as below.

Regarding work needed to be undertaken *for an individual wishing to build in a Fault Avoidance Zone and to determine specific risks and whether building there is acceptable*, GNS Science recommends:

- Assess the Building Importance Category of the proposed building and the recurrence interval of the fault to determine the level of work required, based on the recommendations in Table 5.3.

- If the building is a non-complying activity, obtain a geotechnical assessment to assess if the building could be moved outside the Fault Avoidance Zone. If this is not possible, then undertake a field investigation to either: 1) assess the proposed tectonic origin of the mapped faults (if it is a 'possible' fault), 2) assess the recurrence interval in case it could be larger than assigned here, and/or 3) locate the likely fault rupture zone more precisely.
  - 1) and 2) will likely require consultation with a paleoseismology expert. Such a study could include techniques such as exposing the fault plane in a trench, logging and surveying the trench and assessing the timing of past earthquakes. This will also help with point 3) (see below).
  - 3) could be approached by excavating a trench to determine the exact location of the faults and the extents of the likely fault rupture zone. A setback of 20 m will have to be applied to the likely fault rupture zone, outside of which the building can be placed. This approach (3) does not involve a complete assessment of the fault (recurrence interval, etc.). Instead, it only aims to better define the Fault Avoidance Zone and usually reduces the Fault Avoidance Zone substantially. Note that this approach will benefit from consulting with an expert in paleoseismology, but, at minimum, it will require that the trench walls are cleaned to remove digger scrape marks, identify faults, photograph and survey the location of the faults to add them to the site plans. This type of excavation differs substantially from geotechnical exploration pits in that the trench has to be excavated in a safe way for the consultants/scientist to be able to assess the trench walls.

The above recommendations are specifically for individual buildings and are not suitable for subdivision development. For subdivisions, we would recommend the following order of options:

- Avoidance of Fault Awareness Areas or Fault Avoidance Zones.
- Development configuration for open space in the Fault Awareness Areas or Fault Avoidance Zones (including ground-truthing geotechnical assessment).
- Development configuration for roading in the Fault Awareness Areas or Fault Avoidance Zones (including ground-truthing geotechnical assessment).

6.0 RECOMMENDATIONS

Based on the findings in this report, GNS Science recommends that Taupō District Council:

- Replace any active fault datasets currently held and being used by Taupō District Council with those from this study.
- Include all Fault Avoidance Zones and Fault Awareness Areas developed in this study in the Taupō District Plan and in any other planning or hazard information maps for Taupō District.
- Develop planning provisions using the information provided in this report, including guiding principles and the risk-based decision-making tools of the MfE Active Fault Guidelines and the ECan FAA Guidelines.
- Consider if engineering mitigation options are allowed for buildings, and under what general circumstances.
- Consider ground-surface rupture hazard for assessing lifeline developments that cross active faults in the District.
- Encourage consultants to follow the recommendations and methodologies presented in this report for assessing active fault ground-surface rupture hazard.
- When LiDAR data are obtained in areas not currently covered, update the fault map and, where possible, replace Fault Awareness Areas with Fault Avoidance Zones.
- Obtain better constraints on recurrence interval class, in particular for faults where future population growth is expected. This could be achieved through a combination of site-specific paleoseismic (trenching) studies and more detailed analysis of fault scarp height and morphology using LiDAR data.

7.0 ACKNOWLEDGEMENTS

Robert Langridge and Kyle Bland (GNS Science) provided peer review of this report.

8.0 REFERENCES

Alloway BV, Lowe DJ, Barrell DJA, Newnham RM, Almond PC, Augustinus PC, Bertler NAN, Carter L, Litchfield NJ, McGlone MS, et al. 2007. Towards a climate event stratigraphy for New Zealand over the past 30 000 years (NZ-INTIMATE project). *Journal of Quaternary Science*. 22(1):9–35. doi:10.1002/jqs.1079.

Barrell DJA. 2013. General distribution and characteristics of active faults and folds in the Selwyn District, North Canterbury. Dunedin (NZ): GNS Science. 53 p. Consultancy Report 2012/325. Prepared for: Environment Canterbury.

Barrell DJA. 2019. General distribution and characteristics of active faults and folds in the Queenstown Lakes and Central Otago districts, Otago. Dunedin (NZ): GNS Science. 99 p. Consultancy Report 2018/207. Prepared for: Otago Regional Council.

Barrell DJA, Jack H, Gadsby M. 2015. Guidelines for using regional-scale earthquake fault information in Canterbury. Dunedin (NZ): GNS Science. 30 p. Consultancy Report 2014/211. Prepared for: Canterbury Regional Council (Environment Canterbury).

Barrell DJA, Townsend DB. 2012. General distribution and characteristics of active faults and folds in the Hurunui District, North Canterbury. Dunedin (NZ): GNS Science. 30 p. + 1 CD. Consultancy Report 2012/113. Prepared for: Environment Canterbury.

Beanland S, Haines J. 1998. The kinematics of active deformation in the North Island, New Zealand, determined from geological strain rates. *New Zealand Journal of Geology and Geophysics*. 41(4):311–323. doi:10.1080/00288306.1998.9514813.

Berryman KR, Beanland S, Wesnousky S. 1998. Paleoseismicity of the Rotoitipakau Fault Zone, a complex normal fault in the Taupo Volcanic Zone, New Zealand. *New Zealand Journal of Geology and Geophysics*. 41(4):449–465. doi:10.1080/00288306.1998.9514822.

Berryman KR, Johnston DM, Otway PM, Wilson CJN. 1994. Analysis of active fault data for seismotectonic hazard assessment of Aratiatia hydro and Taupo control gates. Lower Hutt (NZ): Institute of Geological & Nuclear Sciences. 41 p. Client Report 333905. Prepared for: WORKS Consultancy Services; Electricity Corporation of New Zealand.

Berryman KR, Villamor P, Nairn IA, Van Dissen RJ, Begg JG, Lee JM. 2008. Late Pleistocene surface rupture history of the Paeroa Fault, Taupo Rift, New Zealand. *New Zealand Journal of Geology and Geophysics*. 51(2):135–158. doi:10.1080/00288300809509855.

Bland KJ, Nicol A, Kamp PJJ, Nelson CS. 2019. Stratigraphic constraints on the late Miocene–Pleistocene evolution of the North Island Fault System and axial ranges in the central Hikurangi subduction margin, New Zealand. *New Zealand Journal of Geology and Geophysics*. 62(2):248–272. doi:10.1080/00288306.2018.1545675.

Canora-Catalán C, Villamor P, Berryman KR, Martínez-Diaz JJ, Raen T. 2008. Rupture history of the Whirinaki Fault, an active normal fault in the Taupo Rift. *New Zealand Journal of Geology and Geophysics*. 51(4):277–293. doi:10.1080/00288300809509866.

Gómez-Vasconcelos MG, Villamor P, Cronin SJ, Procter J, Kereszturi G, Palmer A, Townsend DB, Leonard GS, Berryman KR, Ashraf S. 2016. Earthquake history at the eastern boundary of the South Taupo Volcanic Zone, New Zealand. *New Zealand Journal of Geology and Geophysics*. 59(4):522–543. doi:10.1080/00288306.2016.1195757.

Gómez-Vasconcelos MG, Villamor P, Cronin S, Procter J, Palmer A, Townsend DB, Leonard GS. 2017. Crustal extension in the Tongariro graben, New Zealand: insights into volcano-tectonic interactions and active deformation in a young continental rift. *Geological Society of America Bulletin*. 129(9–10):1085–1099. doi:10.1130/b31657.1.

Gómez-Vasconcelos MG, Villamor P, Procter J, Palmer A, Cronin S, Wallace C, Townsend DB, Leonard GS. 2019. Characterisation of faults as earthquake sources from geomorphic data in the Tongariro Volcanic Complex, New Zealand. *New Zealand Journal of Geology and Geophysics*. 62(1):131–142. doi:10.1080/00288306.2018.1548495.

Grange LI. 1932. Taupo earthquakes, 1922: rents and faults formed during earthquake of 1922 in Taupo District. *New Zealand Journal of Science and Technology*. 14(3):139–141.

Grindley GW. 1960. Geological map of New Zealand: sheet 8 Taupo [map]. 1st ed. Wellington (NZ): Department of Scientific and Industrial Research. 1 folded map, scale 1:250,000. (Geological map of New Zealand 1:250,000; 8).

Grindley GW, Hull AG. 1986. Historical Taupo earthquakes and earth deformation. In: *Recent crustal movements of the Pacific region*. Wellington (NZ): Royal Society of New Zealand. p. 173–186. (Royal Society of New Zealand Bulletin; 24).

Heron DW, custodian. 2014. Geological map of New Zealand [map]. 1st ed. Lower Hutt (NZ): GNS Science. 1 CD, scale 1:250,000. (GNS Science geological map 1:250,000; 1).

Kerr J, Nathan S, Van Dissen RJ, Webb P, Brunsdon D, King AB. 2003. Planning for development of land on or close to active faults: a guideline to assist resource management planners in New Zealand. Lower Hutt (NZ): Institute of Geological & Nuclear Sciences. 71 p. Client Report 2002/124. Prepared for: Ministry for the Environment.

Langridge RM, Morgenstern R. 2018. Active fault mapping and fault avoidance zones for Horowhenua District and Palmerston North City. Lower Hutt (NZ): GNS Science. 72 p. Consultancy Report 2018/75. Prepared for: Horizons Regional Council.

Langridge RM, Ries WF, Litchfield NJ, Villamor P, Van Dissen RJ, Barrell DJA, Rattenbury MS, Heron DW, Haubrock S, Townsend DB, et al. 2016. The New Zealand Active Faults Database. *New Zealand Journal of Geology and Geophysics*. 59(1):86–96. doi:10.1080/00288306.2015.1112818.

Lee JM, Bland KJ, Townsend DB, Kamp PJJ, compilers. 2011. Geology of the Hawke's Bay area [map]. Lower Hutt (NZ): GNS Science. 93 p. + 1 folded map, scale 1:250,000. (GNS Science 1:250,000 geological map; 8).

Leonard GS, Begg JG, Wilson CJN, compilers. 2010. Geology of the Rotorua area [map]. Lower Hutt (NZ): GNS Science. 102 p. + 1 folded map, scale 1:250,000. (GNS Science 1:250,000 geological map; 5).

Litchfield NJ, Morgenstern R, Van Dissen RJ, Langridge RM, Pettinga JR, Jack H, Barrell DJA, Villamor P. 2019. Updated assessment of active faults in the Kaikōura District. Lower Hutt (NZ): GNS Science. 71 p. Consultancy Report 2018/141. Prepared for: Canterbury Regional Council (Environment Canterbury).

Litchfield NJ, Van Dissen R, Sutherland R, Barnes PM, Cox SC, Norris R, Beavan RJ, Langridge R, Villamor P, Berryman K, et al. 2014. A model of active faulting in New Zealand. *New Zealand Journal of Geology and Geophysics*. 57(1):32–56. doi:10.1080/00288306.2013.854256.

McClymont AF, Villamor P, Green AG. 2009. Fault displacement accumulation and slip rate variability within the Taupo Rift (New Zealand) based on trench and 3-D ground-penetrating radar data. *Tectonics*. 28:TC4005. doi:10.1029/2008tc002334.

McNamara DD, Milicich SD, Massiot C, Villamor P, McLean K, Sépulveda F, Ries WF. 2019. Tectonic controls on Taupo Volcanic Zone geothermal expression: insights from Te Mihi, Wairakei Geothermal Field. *Tectonics*. 38(8):3011–3033. doi:10.1029/2018tc005296.

McVerry GH, Stirling MW, Villamor P. 2005. Estimation of spectra for Waikato River bridge, east Taupo bypass. Lower Hutt (NZ): Institute of Geological & Nuclear Sciences. 39 p. Client Report 2005/124. Prepared for: Opus International Consultants.

Mouslopoulou V, Nicol A, Little TA, Walsh JJ. 2007. Displacement transfer between intersecting regional strike-slip and extensional fault systems. *Journal of Structural Geology*. 29(1):100–116. doi:10.1016/j.jsg.2006.08.002.

Nicol A, Walsh J, Berryman K, Villamor P. 2006. Interdependence of fault displacement rates and paleoearthquakes in an active rift. *Geology*. 34(10):865–868. doi:10.1130/g22335.1.

Otway PM, Grindley GW, Hull AG. 1984. Earthquakes, active fault displacement and associated vertical deformation near Lake Taupo, Taupo Volcanic Zone. Lower Hutt (NZ): New Zealand Geological Survey. 73 p. Report NZGS 110.

Rowland JV, Sibson RH. 2001. Extensional fault kinematics within the Taupo Volcanic Zone, New Zealand: soft-linked segmentation of a continental rift system. *New Zealand Journal of Geology and Geophysics*. 44(2):271–283. doi:10.1080/00288306.2001.9514938.

Saunders WSA, Mathieson JE. 2016. Out on a LIM: the role of Land Information Memorandum in natural hazard management. Lower Hutt (NZ): GNS Science. 97 p. (GNS Science miscellaneous series; 95).

Stirling M, McVerry G, Gerstenberger M, Litchfield N, Dissen R, Berryman K, Barnes P, Wallace L, Villamor P, Langridge R, et al. 2012. National Seismic Hazard Model for New Zealand: 2010 update. *Bulletin of the Seismological Society of America*. 102(4):1514–1542. doi:10.1785/0120110170.

Townsend DB, Leonard GS, Conway CE, Eaves SR, Wilson CJN, compilers. 2017. Geology of the Tongariro National Park area [map]. Lower Hutt (NZ): GNS Science. 109 p. + 1 sheet, scale 1:60,000. (GNS Science geological map; 4).

Villamor P, Berryman KR. 2001. A late Quaternary extension rate in the Taupo Volcanic Zone, New Zealand, derived from fault slip data. *New Zealand Journal of Geology and Geophysics*. 44(2):243–269. doi:10.1080/00288306.2001.9514937.

Villamor P, Berryman KR. 2006. Evolution of the southern termination of the Taupo Rift, New Zealand. *New Zealand Journal of Geology and Geophysics*. 49(1):23–37. doi:10.1080/00288306.2006.9515145.

Villamor P, Berryman KR, Nairn IA, Wilson KJ, Litchfield NJ, Ries W. 2011. Associations between volcanic eruptions from Okataina Volcanic Center and surface rupture of nearby active faults, Taupo rift, New Zealand: insights into the nature of volcano-tectonic interactions. *Geological Society of America Bulletin*. 123(7–8):1383–1405. doi:10.1130/b30184.1.

Villamor P, Berryman KR, Webb TH, Stirling MW, McGinty PJ, Downes GL, Harris JS, Litchfield NJ. 2001. Waikato seismic loads – Task 2.1 revision of seismic source characterisation. Lower Hutt (NZ): Institute of Geological & Nuclear Sciences. 109 p. Client Report 2001/59. Prepared for: URS & Mighty River Power.

Villamor P, Clark KJ, Watson M, Rosenberg MD, Lukovic B, Ries W, Gonzalez A, Milicich SD, McNamara DD, Pummer B, et al. 2015. New Zealand geothermal power plants as critical facilities: an active fault avoidance study in the Wairakei Geothermal Field, New Zealand. In: Horne R, Boyd T, editors. *Proceedings, World Geothermal Congress 19–24 April 2015, Australia-New Zealand*. Bochum (DE): International Geothermal Association. 12 p.

Villamor P, Nicol A, Seebeck HF, Rowland J, Townsend DB, Massiot C, McNamara DD, Milicich SD, Ries WF, Alcaraz SA. 2017. Tectonic structure and permeability in the Taupō Rift: new insights from analysis of LiDAR derived DEMs. In: *Proceedings 39th New Zealand Geothermal Workshop, 22–24 November 2017, Rotorua, New Zealand*. Auckland (NZ): University of Auckland. Paper 25.

Villamor P, Van Dissen RJ, Alloway BV, Palmer AS, Litchfield NJ. 2007. The Rangipo Fault, Taupo rift, New Zealand: an example of temporal slip-rate and single-event displacement variability in a volcanic environment. *Geological Society of America Bulletin*. 119(5–6):529–547. doi:10.1130/b26000.1.

Villamor P, Wilson KJ. 2007. Active fault mapping at Mapara Valley, Taupo district. Lower Hutt (NZ): GNS Science. 5 p. Consultancy Report 2007/289LR. Prepared for: Taupō District Council.

Wilson CJN, Rowland JV. 2016. The volcanic, magmatic and tectonic setting of the Taupo Volcanic Zone, New Zealand, reviewed from a geothermal perspective. *Geothermics*. 59(B):168–187. doi:10.1016/j.geothermics.2015.06.013.

This page left intentionally blank.

APPENDICES

This page left intentionally blank.

APPENDIX 1 ACTIVE FAULT DEFINITIONS

A1.1 What is an Active Fault?

Active faults are those faults considered capable of generating strong earthquake shaking and ground-surface fault rupture, causing significant damage. Ground-surface-rupturing earthquakes are typically of magnitude M_W >6.5, although, in the Taupō Rift, centimetre- to metre-scale ground deformation has occurred in swarms of smaller earthquakes.

An active fault in New Zealand is generally defined as one that has deformed the ground surface within the past 125,000 years (Langridge et al. 2016). This is defined in part, for practical reasons, as those faults that deform marine terraces and alluvial surfaces that formed during the 'Peak Last Interglacial period' or Marine Isotope Stage (MIS) 5e or younger (MIS 1–4; e.g. Alloway et al. 2007). The exception to this definition is the Taupō Rift, which is considered to be evolving so quickly that an active fault is defined as one that has deformed the ground surface within the past 25,000 years (Villamor and Berryman 2001; Langridge et al. 2016). In practise, these are faults that cut the widespread Oruanui volcanic and fluvial deposits that are 25,000 years or younger. For the Taupō District, we therefore define active faults in the Taupō Rift as those with evidence of activity in the last 25,000 years, and for those in the North Island Dextral Fault Belt (NIDFB) as those with evidence of activity in the last 125,000 years.

The purpose of this Appendix is to introduce how active faults express themselves, i.e. their behaviour, styles of deformation, activity and geomorphic expression. Active faults are typically expressed in the landscape as linear traces displacing surficial geologic features, which may include hillslopes, alluvial terraces and fans. The age of these displaced features can be used to define how active a fault is.

Active faults are often defined by a fault scarp or trace. A fault scarp is formed when a fault displaces or deforms the land surface or seafloor and produces an abrupt linear step, which smooths out with time to form a scarp (Figure A1.1). In some cases, where a fault moves horizontally, only a linear trace or furrow may be observed.

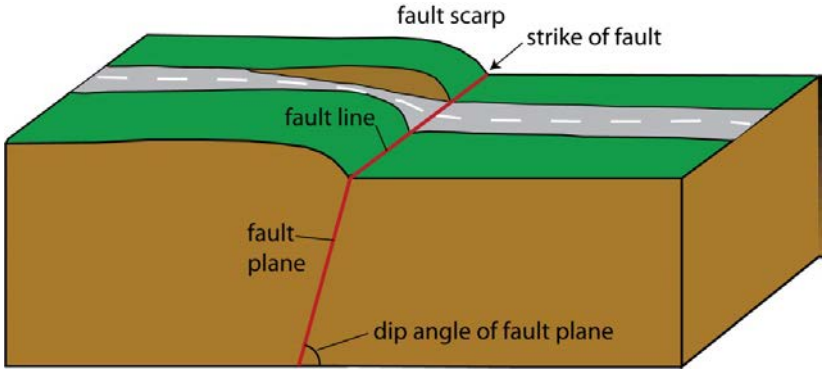

Figure A1.1 Block model of a generic active fault. Fault displacement produces a scarp along the projection of the fault plane at the Earth's surface (fault line or trace).

A1.2 Styles of Fault Movement

Faults can be categorised as: strike-slip faults, where the dominant style (sense) of motion is horizontal (movement in the strike direction of the fault), and dip-slip faults, where the dominant sense of motion is vertical (defined by movement in the dip direction of the fault).

Strike-slip faults are defined as either right-lateral (dextral), where the motion on the opposite side of the fault is to the right (Figure A1.2), or left-lateral (sinistral), where the opposite side of the fault moves to the left. The Wheao and Te Whaiti faults in the eastern Taupō District are predominantly dextral strike-slip faults.

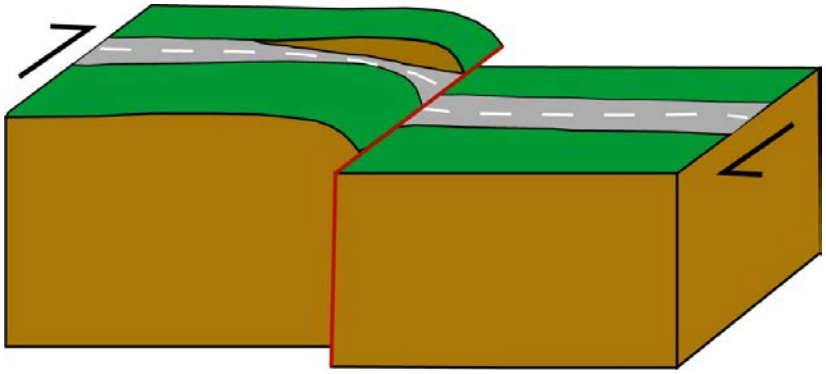

Figure A1.2 Block model of a strike-slip fault (red line). The fault is a right-lateral (dextral) fault, as shown by the black arrows and the sense of movement across the two blocks and a right separation across the road.

Dip-slip faults can be divided into reverse faults, formed mainly under contraction (where the hanging-wall block of the fault is pushed up; Figure A1.3) and normal faults, formed under extension (where the hanging-wall block of the fault drops down; Figure A1.4). The majority of faults in the Taupō District are normal faults, formed in association with extension and volcanism in the Taupō Rift and Taupō Volcanic Zone.

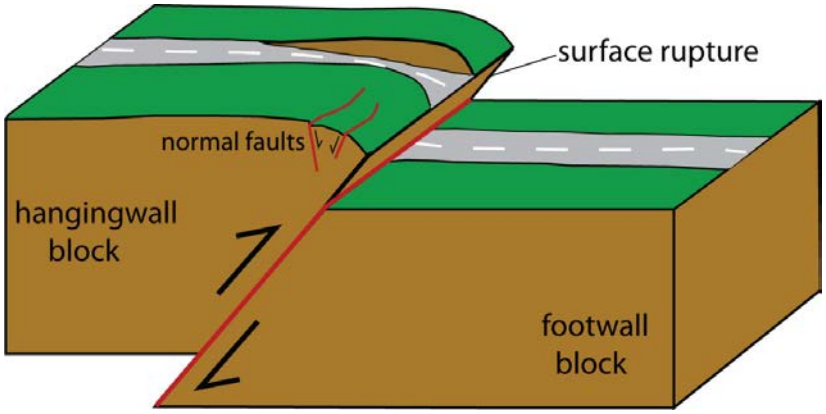

Figure A1.3 Block model of a reverse dip-slip fault that has recently ruptured. Movement of the blocks is vertical and in the dip direction of the fault plane. In this case, the hanging-wall block has been pushed up over the footwall block. Folding and normal faulting are common features of deformation in the hanging-wall block of reverse faults.

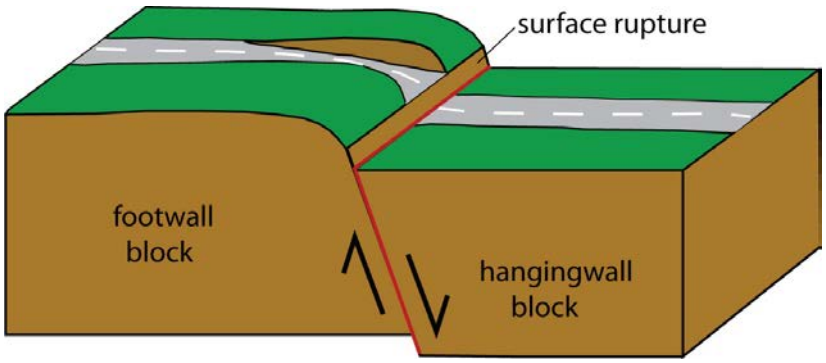

Figure A1.4 Block model of a normal dip-slip fault. The relative movement of the blocks is vertical and in the dip direction of the fault plane. The hanging-wall block has dropped down, enhancing the height of the fault scarp.

APPENDIX 2 IMPACTS OF SURFACE FAULT RUPTURE ON RESIDENTIAL STRUCTURES IN RECENT NEW ZEALAND EARTHQUAKES AND IMPLICATION FOR THE MITIGATION OF SURFACE FAULT RUPTURE HAZARD

A2.1 Introduction

The New Zealand Ministry for the Environment's active fault guidelines titled 'Planning for development of land on or close to active faults: A guideline to assist resource management planners in New Zealand' (Kerr et al. 2003) is the primary document providing guidance with regard to the mitigation of ground-surface fault rupture hazard. In these guidelines (hereafter referred to as the MfE Active Fault Guidelines), the recommended mitigation strategy is avoidance; however, engineering mitigation strategies are also permitted in appropriate circumstances, though little, if any, guidance is provided regarding what those engineering strategies and appropriate circumstances might be. This deficiency was largely the consequence of a lack of data. That is, at the time that the guidelines were issued, there were very few New Zealand examples to draw from where New Zealand engineered structures had been impacted by ground-surface fault rupture and the impacts of that rupture evaluated with regards to: a) the characterisation of the ground strains and displacements generated by that surface rupture, b) the structural damage the surface rupture produced and c) possible engineering strategies that could be employed to mitigate that damage.

Since the MfE Active Fault Guidelines were published, there have been two large earthquakes in New Zealand that have generated ground-surface fault rupture that has directly impacted engineered buildings; the 2010 Darfield earthquake and the 2016 Kaikōura earthquake (Figure A2.1). Collectively, about two dozen buildings or residential-type structures were directly damaged by ground-surface fault rupture resulting from these two earthquakes. In this Appendix, we present approximately a dozen case-study examples from these two earthquakes, and the 1987 Edgecumbe earthquake also, illustrating the impacts surface fault rupture had on residential (or residential-type) structures. These examples provide insight into construction styles that could be employed, in suitable circumstances, to facilitate non-collapse performance resulting from surface fault rupture and, in certain instances, post-event functionality. We also provide comment on how these examples may enable a more nuanced application of the MfE Active Fault Guidelines in, again, appropriate circumstances.

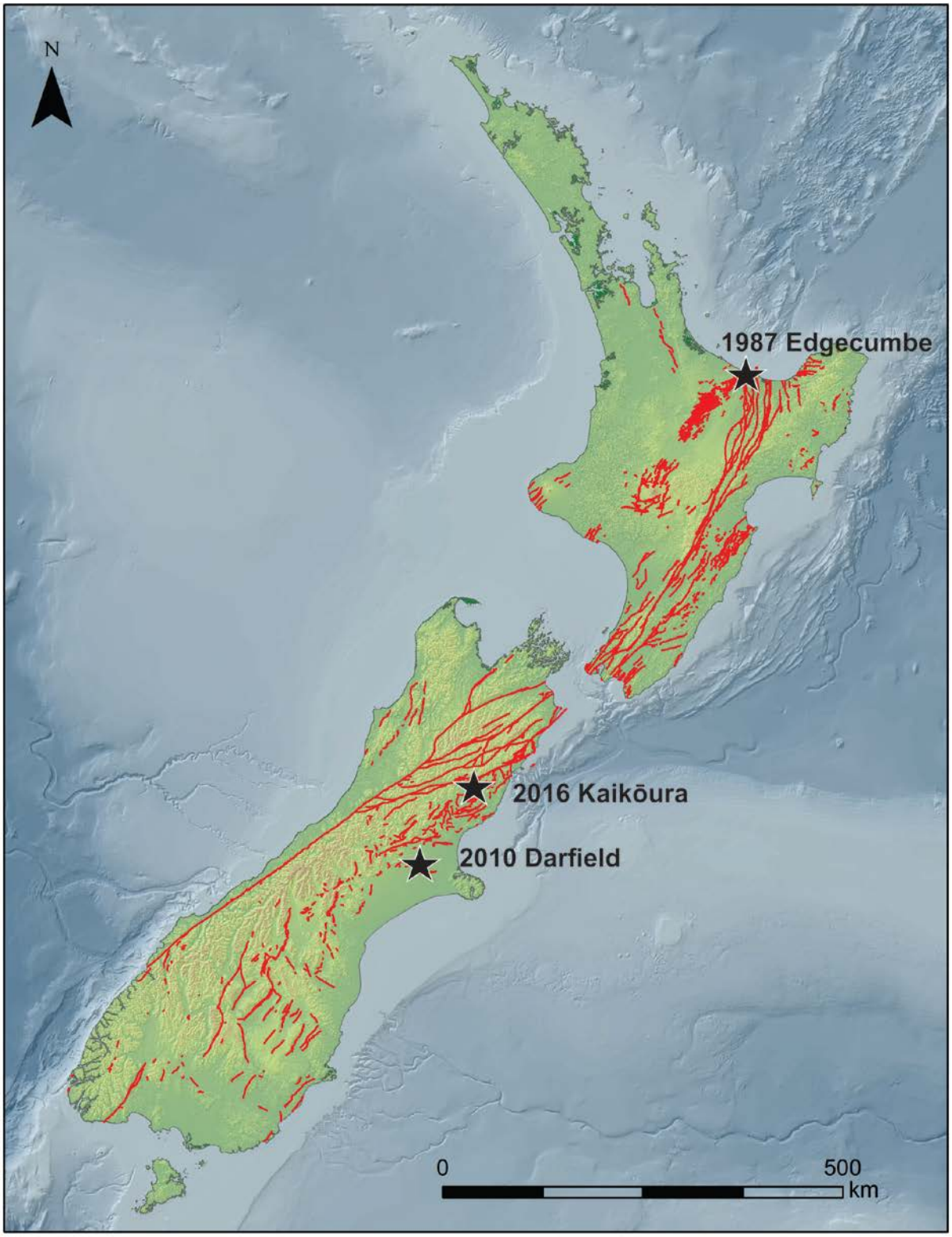

Figure A2.1 On-land known active faults of New Zealand (red lines) and epicentres of New Zealand's three most recent ground-surface-rupturing earthquakes (black stars): 1987 M_W 6.5 Edgecumbe earthquake, 2010 M_W 7.1 Darfield earthquake and 2016 M_W 7.8 Kaikōura earthquake. Active faults from Langridge et al. (2016).

A2.2 1987 Edgecumbe Earthquake

The Edgecumbe earthquake struck the Rangitaiki Plains, eastern Bay of Plenty, on 2 March 1987 (Figure A2.2). The earthquake had a magnitude of M_L 6.3, and generated metre-scale ground-surface fault rupture along the Edgecumbe Fault (maximum displacement, 2.5 m vertical and 1.8 m extension) (Figures A2.3 and A2.4) and decimetre- to centimetre-scale surface rupture displacement on several other nearby faults (Anderson and Webb 1989, Beanland et al. 1989, Nairn and Beanland 1989). The predominant sense of displacement on all these faults was normal.

Damage to residential structures caused by the Edgecumbe earthquake was primarily the result of strong ground shaking and, subordinately, liquefaction (e.g. Pender and Robertson 1987). However, ground-surface fault rupture along the Edgecumbe Fault did extend through and severely damage the concrete yards of two milking sheds in the McCracken Road area (Figures A2.5 and A2.6). The impact that Edgecumbe Fault ground-surface rupture had on these yards provides an informative illustration of the severe structural damage that could be expected to result from metre-scale normal fault rupture extending though a lightly reinforced concrete slab foundation of a residential structure.

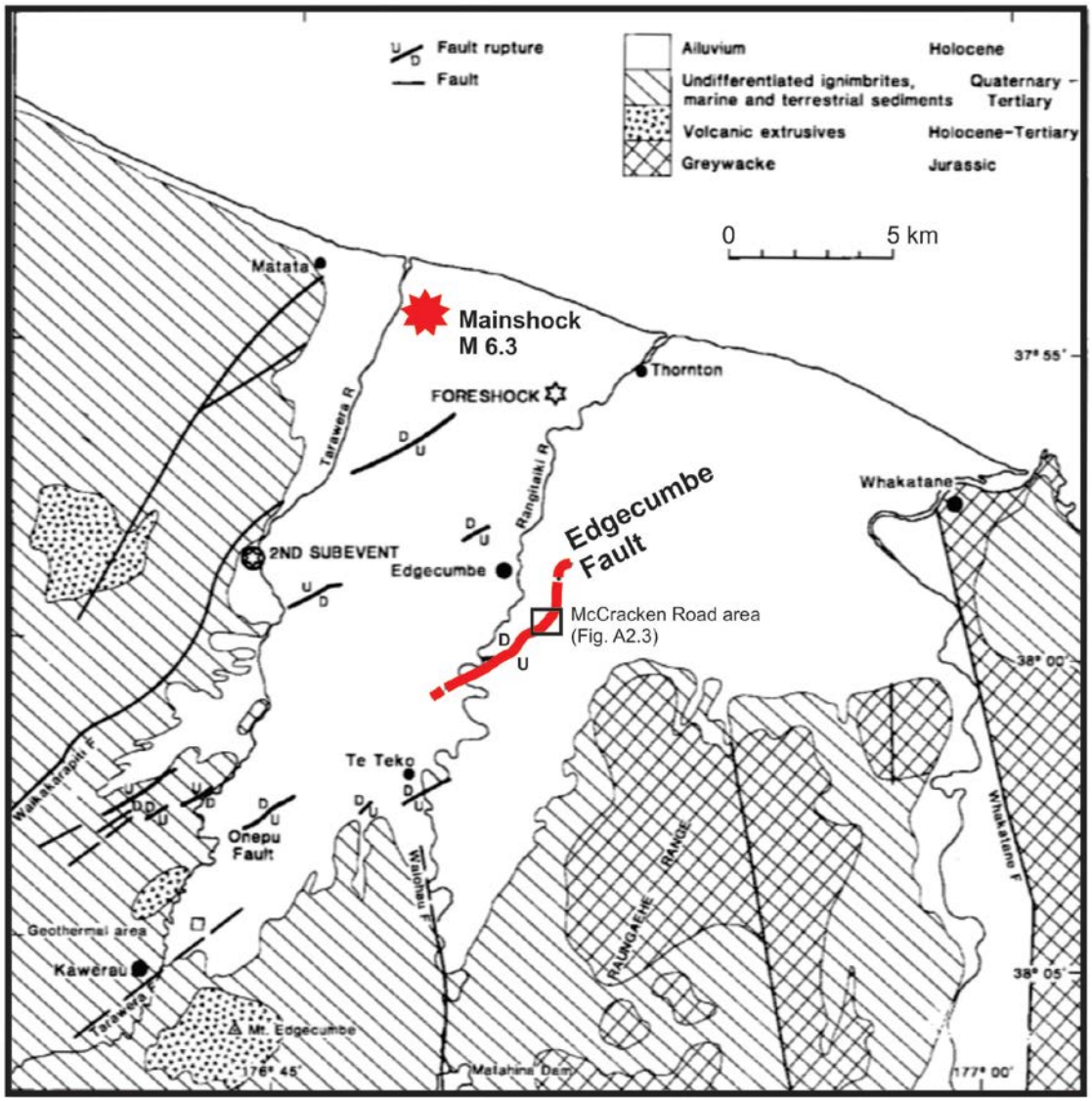

Figure A2.2 Edgecumbe earthquake: 2 March 1987, M_W 6.5 (M_L 6.3). Map shows location of mainshock epicentre (red star) and Edgecumbe Fault rupture (red line). Also shown is the location of the McCracken Road area depicted in Figure A2.3. After Figure 1 of Anderson and Webb (1989).

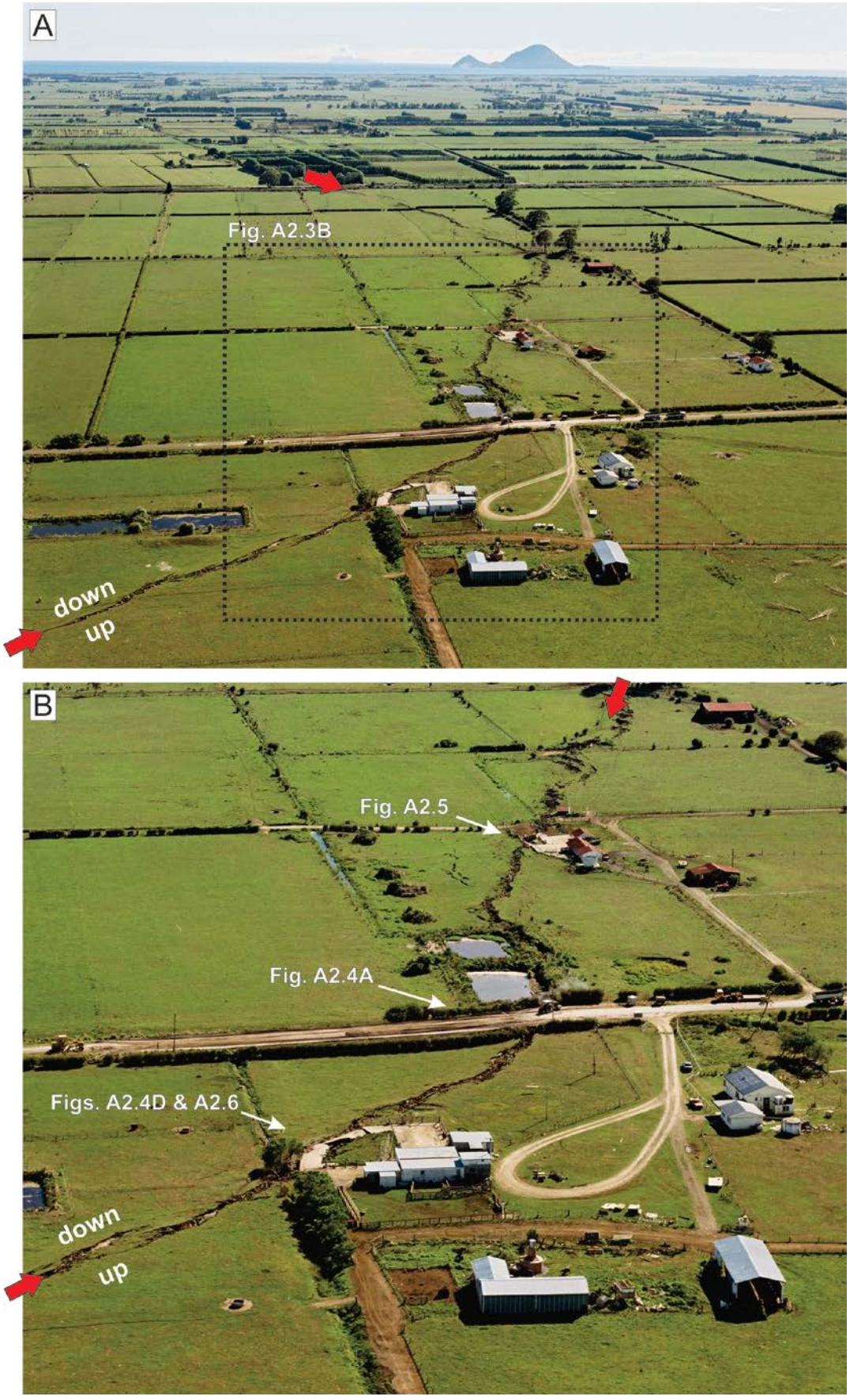

Figure A2.3 Edgecumbe Fault ground-surface rupture (red arrows) in the McCracken Road area, 1987 Edgecumbe earthquake. (A) Oblique aerial view looking northeast. (B) Enlarged portion of (A), showing locations of Figures A2.4A, D; A2.5; and A2.6. Photos by Lloyd Homer.

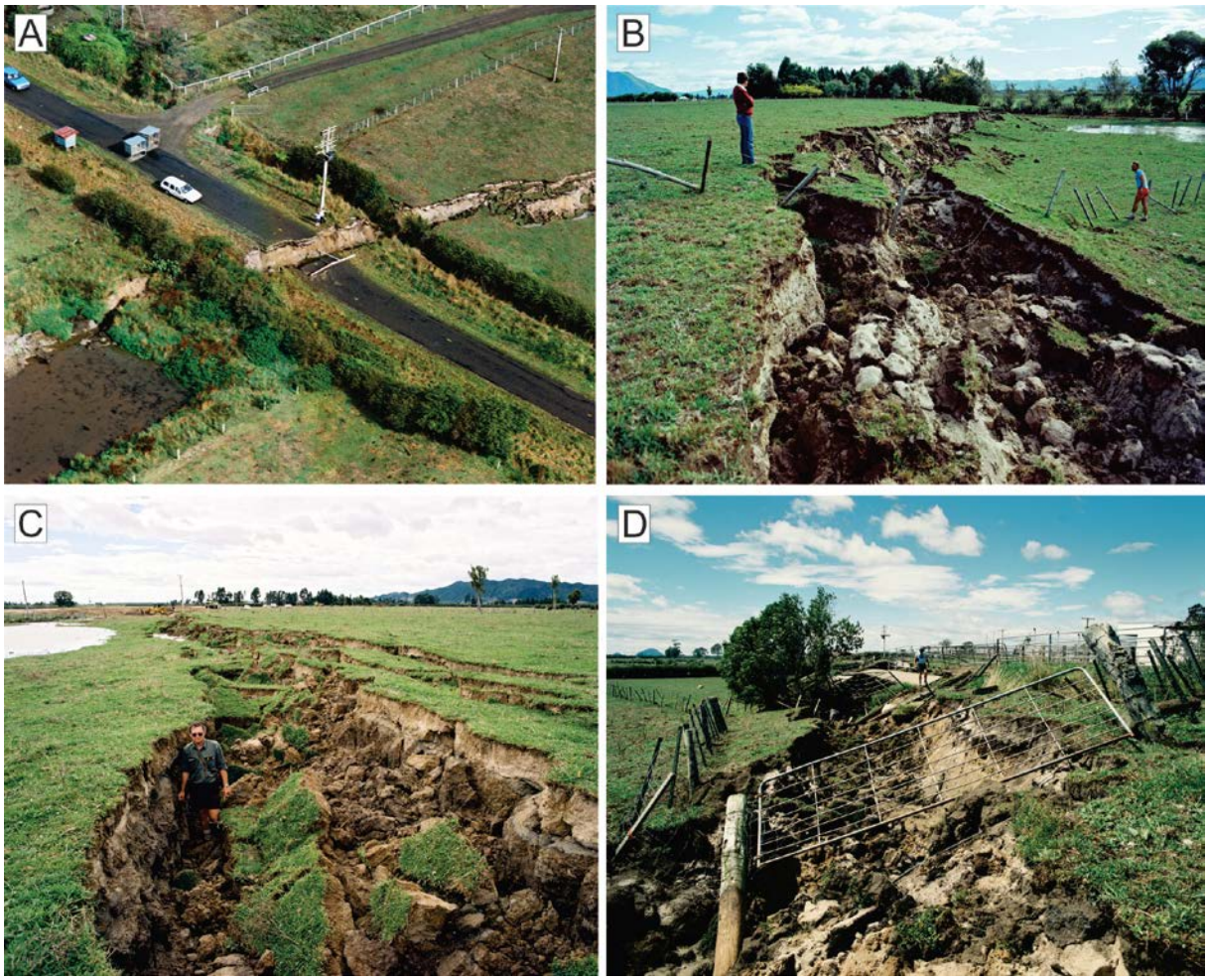

Figure A2.4 Examples of metre-scale normal ground-surface fault rupture along the Edgecumbe Fault, 1987 Edgecumbe earthquake. Photos by Lloyd Homer.

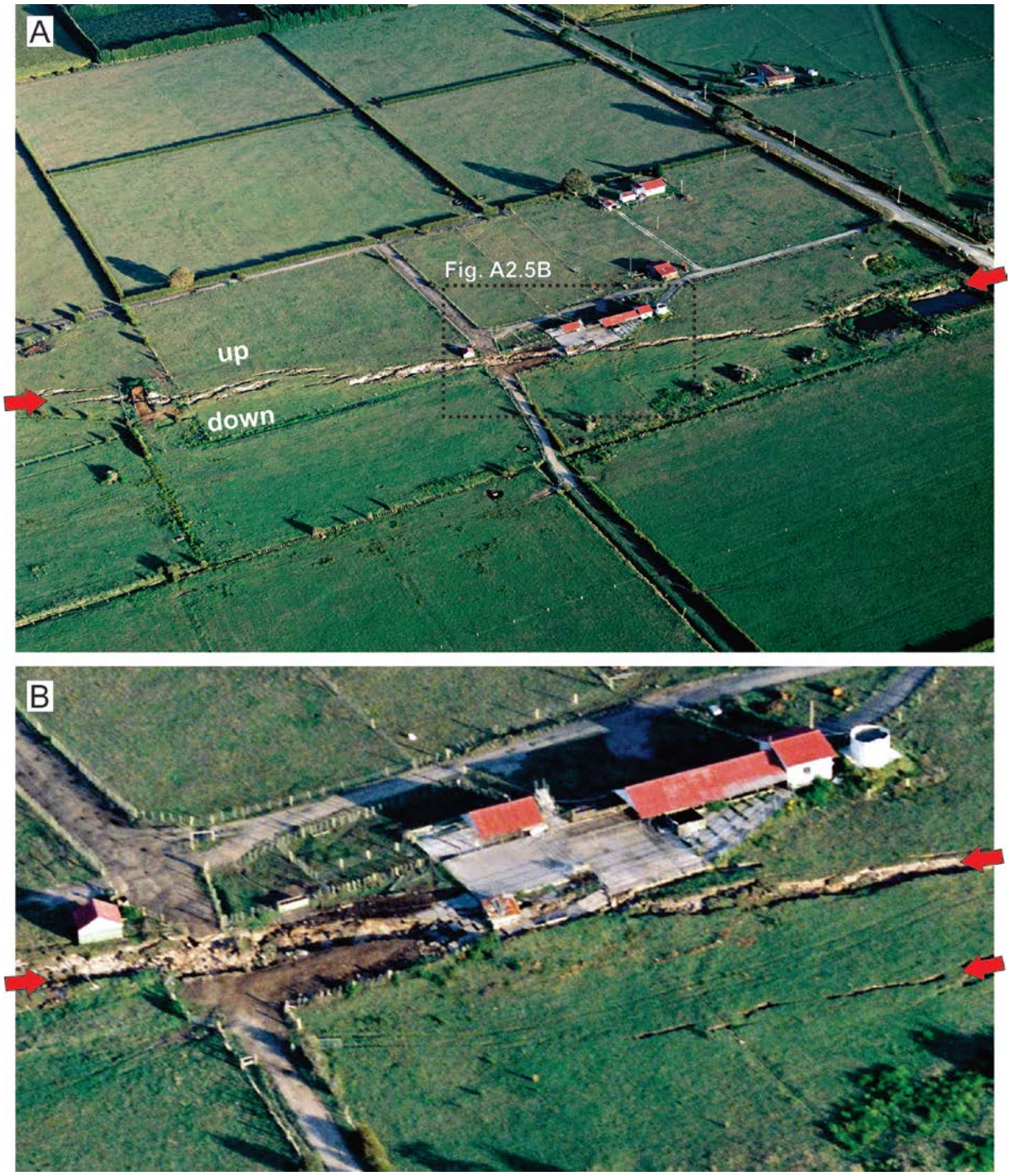

Figure A2.5 Edgecumbe Fault ground-surface rupture (red arrows) and damage to concrete yard of milking shed north of McCracken Road, 1987 Edgecumbe earthquake. (A) Oblique aerial view looking east-southeast. (B) Enlarged portion of (A). See Figure A2.3B for location. Photos by Lloyd Homer.

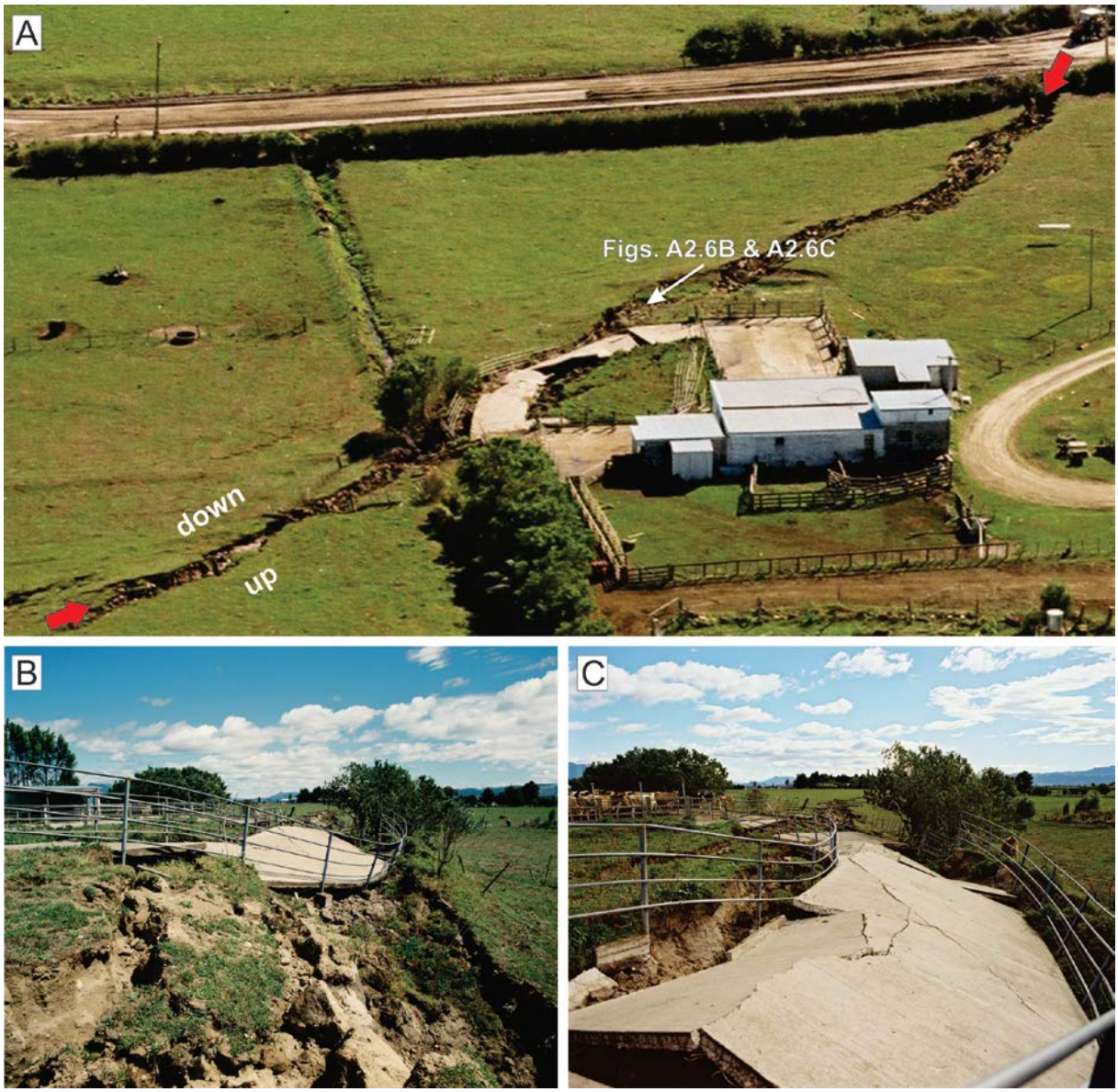

Figure A2.6 Edgecumbe Fault ground-surface rupture (red arrows) and damage to concrete race of milking shed south of McCracken Road, 1987 Edgecumbe earthquake. (A) Oblique aerial view looking northeast. See Figure A2.3B for location. (B, C) Details of reinforced concrete milking shed race damaged by metre-scale normal fault rupture. Views looking west-southwest. Photos by Lloyd Homer.

A2.3 2010 Darfield Earthquake

Much of the material presented in this section comes from Van Dissen et al. (2011).

A2.3.1 Introduction

The M_W 7.1 Darfield earthquake of 4 September 2010 had a shallow focus (~11 km deep) and an epicentre located within ~40 km west of Christchurch (Figure A2.7). It was a complex event, involving rupture of multiple fault planes with most of the earthquake's moment release resulting from slip on the previously unknown Greendale Fault (Beavan et al. 2010, Gledhill et al. 2010, Holden et al. 2011). Greendale Fault rupture propagated to the ground surface and extended east–west for ~30 km (Quigley et al. 2010, 2012). Surface rupture was mainly dextral strike-slip (Figures A2.7–2.9).

About a dozen buildings, mainly single-storey houses and farm sheds, were affected by Greendale Fault ground-surface rupture but none collapsed, largely because most of the buildings were relatively flexible and resilient timber-framed structures and also because deformation was distributed over a relatively wide zone. In this section of the Appendix, we present a summary of the characteristics of Greendale Fault surface rupture deformation and the impacts this deformation had on residential (or residential-type) structures.

A2.3.2 Greendale Fault Surface Rupture Displacement and Expression

A variety of methods were used to map and characterise the Greendale Fault surface rupture, including tape and compass, GPS surveys, aerial photography, airborne LiDAR and shallow excavations (Quigley et al. 2010, 2012; Duffy et al. 2013; Hornblow et al. 2014). The zone of Greendale Fault ground-surface rupture deformation extends for about 30 km from ~4 km west of the hamlet of Greendale (from which the fault gets its name) to an eastern tip ~2 km north of the town of Rolleston (Figure A2.7). The gross morphology of the surface rupture is that of an *en-echelon* series of east–west-striking, left-stepping surface traces (Figures A2.7 and A2.8). The largest step-over is ~1 km wide, and there is a multitude of smaller ones. Push-up 'bulges' formed at most of these restraining left-steps, with amplitudes up to ~1 m but typically less than 0.5 m (Figure A2.8B, C).

Displacement along the full length of surface rupture averages ~2.5 m (predominantly dextral) with maximum of ~5 m along the central section of fault trace. Perpendicular to the strike of the Greendale Fault, surface rupture displacement is distributed across a ~30–300-m-wide deformation zone, largely as horizontal flexure. The width of the surface rupture deformation zone is greatest at step-overs and damaging ground strains developed within these. On average, 50% of the horizontal displacement occurs over 40% of the total width of the deformation zone, with offset on discrete shears, where present, typically accounting for less than about 30% of the total displacement. Across the paddocks deformed by fault rupture, there is a threshold of surface rupture displacement of ~1–1.5 m; greater than this discrete ground cracks and shears occur and form part of the surface rupture deformation zone and less than this they are rarely present. The distributed nature of Greendale Fault surface rupture displacement undoubtedly reflects a considerable thickness of poorly consolidated alluvial gravel deposits underlying the Canterbury Plains at this location.

A2.3.3 Engineered Structures Impacted by Surface Fault Rupture

About a dozen buildings, typically single-storey timber-framed houses and farm sheds with lightweight roofs, lay either wholly, or partially, within the Greendale Fault's surface rupture deformation zone (Figures A2.7, A2.8, A2.10–13). None of these buildings collapsed, but all were more damaged than comparable structures immediately outside the zone of surface rupture deformation. From a life-safety standpoint, all these buildings performed satisfactorily, but, with regard to post-event functionality, there are notable differences. Houses with only lightly reinforced concrete slab foundations suffered moderate to severe structural and non-structural damage. Three other buildings performed more favourably: one had a robust concrete slab foundation, another had a shallow-seated pile foundation that isolated ground deformation from the superstructure, and the third had a structural system that enabled the house to tilt and rotate as a rigid body. Below, we present four informative case-study examples.

A2.3.3.1 Telegraph Road House – Greendale Fault

The Telegraph Road house (Figure A2.10) was a timber-framed, brick-clad residential structure with a concrete slab foundation (at most, only lightly reinforced) and lightweight roof. It was located within the Greendale Fault's ground-surface fault rupture deformation zone (~150 m wide at this site) that accommodated a total of 4–5 m of dextral displacement. The house was badly damaged by distributed deformation, and ~0.5 m of discrete strike-slip rupture that entered the house through the front door (Figure A2.10B) passed through the house's foundation (including living room) and exited through the back door (Figure A2.10D).

Not long after the earthquake, this house was demolished and a new one constructed nearby.

A2.3.3.2 Kivers Road Woolshed – Greendale Fault

The Kivers Road woolshed was a timber-framed structure located within a 25–50-m-wide ground-surface fault rupture deformation zone of the Greendale Fault. At this site, surface fault rupture deformation comprised both discrete shears and distributed deformation and accommodated ~2.7 m of net slip (predominantly strike-slip) (Figure A2.11). The woolshed was made up of two parts, a larger metal-clad structure with a timber floor founded on shallow-seated ~700-mm-high concrete piles (Figure A2.11D) and a smaller lean-to structure attached to the side (Figure A2.11A, C). The lean-to was a pole building (part metal-clad and part wood-clad) with an unreinforced concrete floor. The response of the two different construction styles to surface fault rupture was noticeably different. The support poles of the lean-to were set into the ground; dextral fault rupture under the lean-to led to lateral displacement of the support poles on either side of the rupture and significant distortion of the walls and roof (Figure A2.11C). In contrast, surface rupture deformation under the larger piled structure was, in large measure, isolated from the superstructure by rotation of the shallow-seated piles. The timber flooring and framing and metal cladding proved a resilient structural system that limited internal distortion.

This woolshed has subsequently been demolished.

A2.3.3.3 Greendale Substation – Greendale Fault

The Greendale substation (Figure A2.12) is a light-industrial building with a reportedly well-reinforced concrete slab foundation. During the Darfield earthquake, the building was tilted and rotated, but relatively undamaged by ~1.7 m dextral and < 1 m vertical displacement (south-side up) distributed across a ~100-m-wide surface rupture deformation zone of the Greendale Fault. The long axis of the building is oriented ~55° counter-clockwise to the general strike of the fault rupture. Distributed displacement imposed tensile ground strains across the site with an orientation roughly sub-parallel to the building's long axis. The foundation of the building was robust enough to resist these strains (i.e. no cracking of the foundation was evident) and, instead, the soil pulled away from either end of the building's foundation (yellow 't' in Figure A2.12C, D).

The Greendale substation is still in service today, ten years after the Darfield earthquake and the Greendale Fault's ground-surface rupture.

A2.3.3.4 Gillanders Road House – Greendale Fault

The Gillanders Road house (Figure A2.13) is a light-gauge steel-framed, plywood- and weatherboard-clad residential structure with a steel pile foundation, steel I-beam bearers, steel joists and plywood flooring. As a result of Greendale Fault ground-surface rupture, the house was tilted and rotated, but only slightly damaged, by ~1 m of distributed vertical and dextral fault rupture spread over several tens of metres width. Despite this house being essentially 'locked' into the ground (piles are concreted to ~1 m depth into the ground), it suffered only slight damage because surface rupture deformation was distributed and relatively evenly spread across the site, and because the structural system was strong and stiff enough to tilt and rotate as a rigid body. Given this structure's resilient, and somewhat uncommon, construction style, it proved a relatively straightforward process to reinstate.

This building was subjected to both ground-surface fault rupture and strong ground shaking and performed in a fashion that not only greatly exceeded life-safety objectives, but also greatly facilitated post-event reinstatement. However, if the building had been subjected to greater amounts of deformation, especially discrete displacement, the pile foundation may have been able to transfer enough deformation into the superstructure to damage it. Design modifications to potentially mitigate this, yet still retain the building's noteworthy resilience, could be to: 1) use piles specifically designed to yield during surface fault rupture; and/or 2) use two sets of bearers, with one set attached to the piles and oriented parallel to the strike of the fault and another orthogonal set on top, onto which the floor joists are attached. With due geological and engineering consideration, both of these options (and conceivably others) could potentially be employed to successfully isolate ground rupture from the superstructure and still retain the advantageous ease of re-levelling qualities of this type of construction.

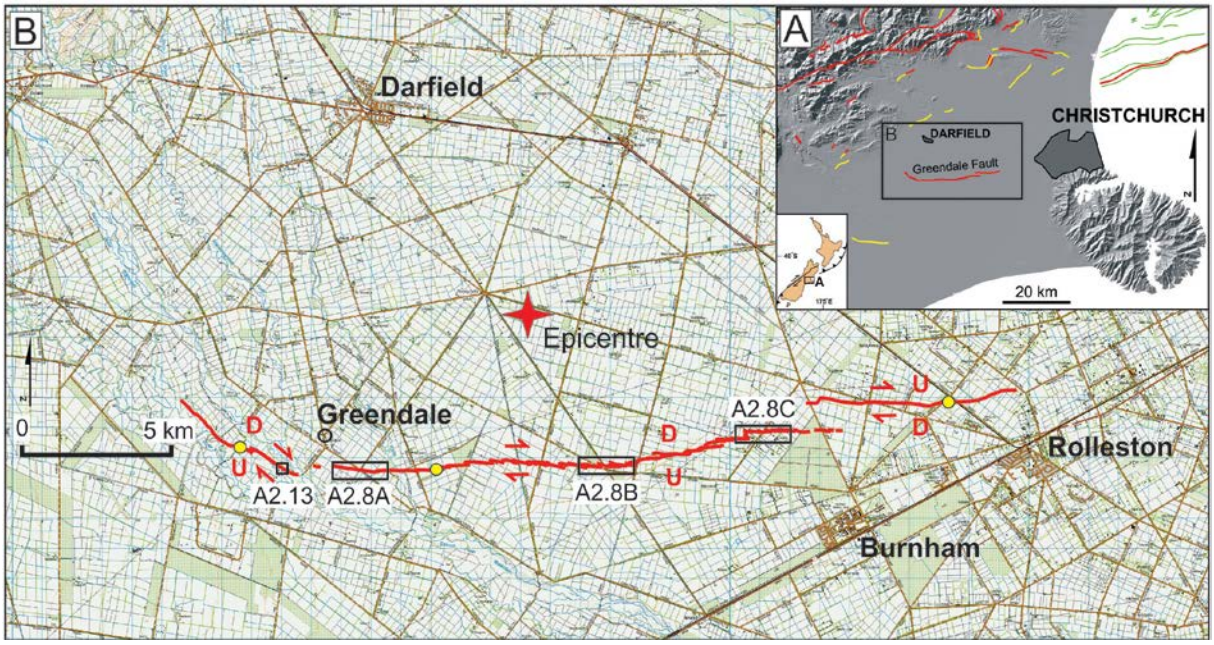

Figure A2.7 (A) Digital Elevation Model (DEM) of the Christchurch area of the Canterbury region showing locations of the Greendale Fault and other known tectonically active structures. Red lines are active faults, and yellow and green lines are, respectively, on-land and offshore active folds (combined data from Forsyth et al. [2008] and GNS Active Faults Database, http://data.gns.cri.nz/af/). (B) Mapped surface trace of the Greendale Fault (Quigley et al. 2010). Red arrows indicate relative sense of lateral displacement, while vertical displacement is denoted by red U = up and D = down. Also shown are locations of Figures A2.8A–C and A2.13, Darfield earthquake epicentre (red star; Gledhill et al. 2010) and buildings damaged by surface fault rupture (yellow dots) that are neither encompassed by Figure A2.8 nor depicted elsewhere in this Appendix.

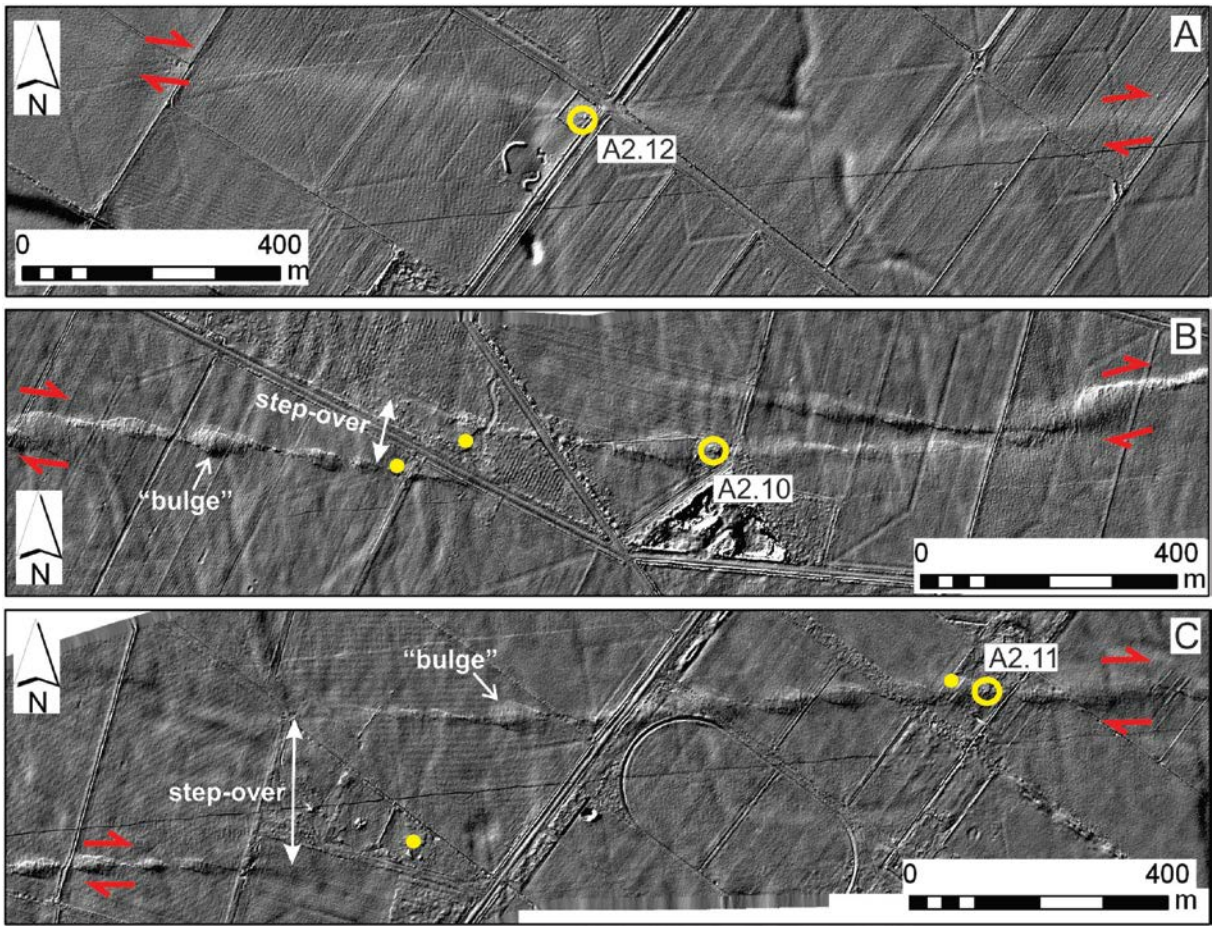

Figure A2.8 LiDAR hillshade DEMs (illuminated from the northwest) of three ~1.8-km-long sections of the Greendale Fault (see Figure A2.7 for locations), showing characteristic left-stepping *en-echelon* rupture pattern (especially evident in B and C) and dextral offset of roads, fences, irrigation channels, hedges and crop rows. Red arrows straddle the surface fault rupture and show the sense of lateral displacement. Representative examples of fault step-overs and push-up 'bulges' are identified in B and C. Open yellow circles show the locations of buildings damaged by surface fault rupture that are depicted in Figures A2.10–12. Small yellow dots show the locations of other buildings damaged by surface rupture deformation that are not discussed in this appendix. The general amount of net surface rupture displacement in A, B and C is, respectively, 1.5–2.5 m (horizontal to vertical ratio ~3:1, south-side up), 4–5 m (predominantly dextral) and 2.5–4 m (predominantly dextral).

Figure A2.9 Examples of metre-scale dextral strike-slip ground-surface fault rupture along the Greendale Fault, 2010 Darfield earthquake.

Figure A2.10 Telegraph Road house and Greendale Fault surface rupture; see Figures A2.7 and A2.8 for location. Red arrows denote location of discrete surface fault rupture. (A) Aerial view looking south. Photo by Richard Cosgrove. (B) View looking west-northwest. Photo by Hayden Mackenzie. (C) View looking south-southwest. Photo by Hayden Mackenzie. (D) View looking east-southeast. Photo by Dougal Townsend.

Figure A2.11 Kivers Road woolshed and Greendale Fault surface rupture; see Figures A2.7 and A2.8 for location. Red arrows denote location of discrete surface fault rupture. (A) Aerial view looking northeast – note dextral offset of irrigation channel in right-hand side of photograph. Photo by Richard Cosgrove. (B) View looking west. Photo by Dougal Townsend. (C) View looking east. Photo by Dougal Townsend. (D) View looking southwest showing detail of shallow-seated concrete piles. Photo by Russ Van Dissen.

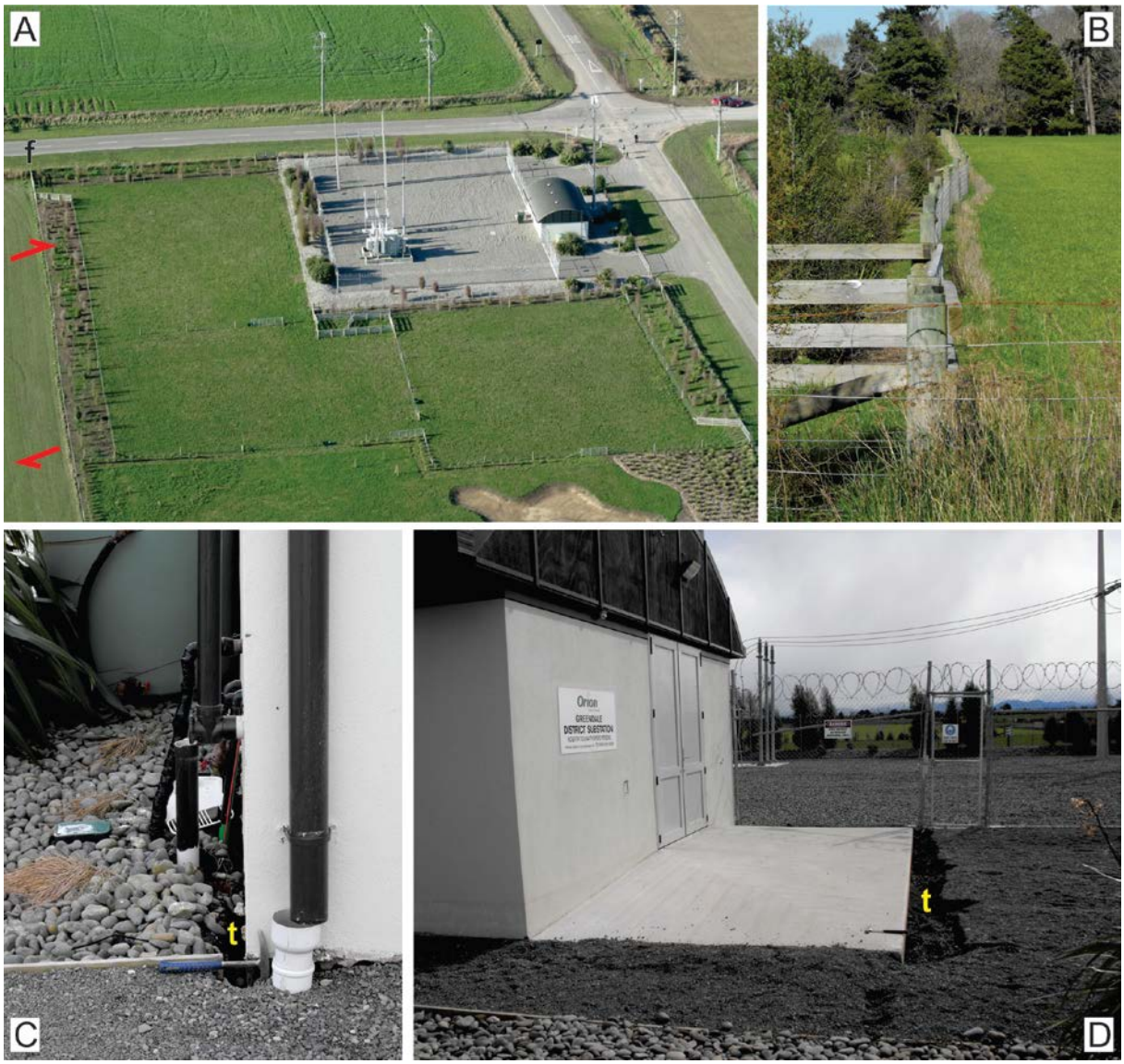

Figure A2.12 Greendale substation and Greendale Fault surface rupture; see Figures A2.7 and A2.8 for location. (A) Aerial view looking northeast. Red arrows denote location, strike and sense of lateral displacement of the surface rupture deformation zone. Photo by Richard Jongens. (B) View looking southwest along fence line adjacent to the substation that crosses the surface rupture deformation zone and records the amount, width and distributed style of fault displacement here (camera location for B is shown by black 'f' in (A). Photo by Russ Van Dissen. (C, D) Views looking northwest. 't' is where soil has pulled away from the building's foundation. See text for details. Photos by Russ Van Dissen.

Figure A2.13 Gillanders Road house and Greendale Fault surface rupture; see Figure A2.7 for location. (A) View looking east. (B) View looking northwest. (C) Close-up of detached down-pipe on east-southeast side of the house. View looking west-northwest. (D) Close-up of pile, bearer and deformed bolted connection. View looking west-northwest. Photos by Russ Van Dissen.

A2.4 2016 Kaikōura Earthquake

Much of the material presented in this section comes from Van Dissen et al. (2019).

A2.4.1 Introduction

The Kaikōura earthquake struck at two minutes past midnight on 14 November 2016. Its epicentre was located near the South Island township of Waiau (Figure A2.14) and, with a magnitude of M_W 7.8, it was the largest on-land earthquake to hit New Zealand in more than a century (Downes and Dowrick 2014). The Kaikōura earthquake generated damaging levels of ground shaking throughout much of north Canterbury, eastern Marlborough and beyond (Bradley et al. 2017; Kaiser et al. 2017). It triggered thousands of landslides (Dellow et al. 2017; Massey et al. 2018) and locally significant liquefaction (Cubrinovski et al. 2017; Stringer et al. 2017; Bastin et al. 2018). The earthquake caused vertical deformation, primarily uplift, along more than 100 km of coastline between Cape Campbell and the Hundalee Fault south of Kaikōura (Clark et al. 2017) (Figure A2.14) and spawned a tsunami with up to ~7 m run-up height – the impacts of which were lessened by the fact that the earthquake occurred at low tide and much of the potentially affected coastline had been uplifted (Power et al. 2017).

In a global context, the Kaikōura earthquake was also one of the most complex earthquakes yet documented, with about two dozen major and minor faults rupturing the ground surface (Figure A2.14) (Hamling et al. 2017; Stirling et al. 2017; Litchfield et al. 2018). Collectively, over 220 km of surface fault rupture was generated by the Kaikōura earthquake (Figure A2.14). This rupture directly impacted several residential (or residential-type) structures. In this section of the Appendix, we document several examples of the impacts this surface fault rupture had on these buildings.

A2.4.2 Residential Structures Impacted by Surface Fault Rupture

About a dozen buildings, mostly single-storey timber-framed houses, barns and woolsheds, were directly impacted by surface fault rupture in the Kaikōura earthquake. Here we present seven instructive case-study examples.

A2.4.2.1 Bluff Cottage – Kekerengu Fault

Of the residential structures impacted by surface fault rupture during the Kaikōura earthquake, Bluff Cottage (Figures A2.15 and A2.16) deserves special mention because of its noteworthy life-safety (non-collapse) performance when subjected to extreme surface fault rupture deformation. Bluff Cottage – which has since been demolished – was a timber-framed single-storey residential structure (house) with a corrugated metal roof and a combination of timber weatherboard and concrete brick cladding. It had a roughly rectangular floor plan (area of ~90 m^2), a timber floor comprising a combination of particle board sheets and tongue and groove hardwood strips/planks and a pre-cast concrete chimney and fireplace (with some steel-rod reinforcing) encased by concrete brick. It had a concrete perimeter foundation with shallow-seated concrete piles. The timber floor joists were skew-nailed to the timber wall plates, which were in turn bolted to the perimeter foundation, and the timber floor bearers were attached to the piles via wire ties.

The age of construction of Bluff Cottage is composite, and not known in detail. The original hut that formed the core of the cottage was constructed prior to the late 1940s (the oldest set of aerial photographs for this part of the country date from 1947 and show that the hut was already in existence). Later, in the late 1970s / early 1980s, a kitchen and sitting room were

added, along with the concrete perimeter foundation. Bluff Cottage was sited on a relatively thin layer (<1–2 m thick) of Holocene loosely packed gravel-dominated Kekerengu River alluvium overlying weak, fault-damaged, bedrock.

Approximately 10 m of discrete (i.e. concentrated, as opposed to distributed) horizontal and 1–2 m vertical surface fault rupture displacement extended through the footprint of Bluff Cottage on the Kekerengu Fault (Figure A2.16) (Kearse et al. 2018). Offset fence lines within ~450 m either side of the cottage also document lateral displacements of ~10–11 m and narrow fault deformation zone widths (Figures A2.15 and A2.17). The foundation of Bluff Cottage was cut in half and displaced by fault rupture. The superstructure of the house was low mass, flexible, regular in shape, timber-floored and relatively weakly attached to the foundation. These properties allowed the superstructure to detach from the mainly laterally displacing foundation and isolate it from the extreme ground deformation taking place beneath. The house suffered severe structural damage, but it did not collapse. From a life-safety perspective, and considering the large displacement and small fault zone width at this site (i.e. metre-scale strike-slip displacements and shear strains in the order of 10^0), this house performed admirably.

A2.4.2.2 Harkaway Villa – Papatea Fault

Harkaway Villa is a timber-framed single-storey house with timber weatherboard cladding and a corrugated metal roof on framed rafters, with internal load-bearing walls (Figures A2.14, A2.18–20). It has a roughly square floor plan (area of ~130 m^2), timber strip (plank) flooring and a timber pile foundation (~60 cm above ground), with joists attached to piles via wire ties and skew nails.

The age of construction of Harkaway Villa is composite. It was built around 1910. About a hundred years later, in 2009, it was moved onto the site (in three pieces) and, at this time, significant renovations were undertaken. The villa is sited on several metres of late Holocene fan alluvium (comprising interbedded silt, sand and loosely packed gravel) which, in turn, likely overlies gravel-dominated Clarence River alluvium.

Harkaway Villa is located within the surface rupture deformation zone of the Papatea Fault which, at this site, is ~90 m wide, comprising both discrete fault rupture and distributed deformation and accommodating ~5 m of vertical deformation (reverse, southwest-side up) and a comparable (or lesser) amount of left-lateral horizontal slip (Figures A2.18–20) (Langridge et al. 2018). The villa is situated ~200 m west from the true-right bank of the Clarence River on the hanging-wall side (southwest side) of the Papatea Fault in the hinge zone between the higher vertical displacement gradient fold/fault scarp to the northeast and the lower vertical displacement gradient ‘back limb’ to the southwest (Figure A2.20). The ground encompassed by the footprint of the structure experienced decimetre-scale folding, horizontal sinistral flexure (i.e. fault drag) and up to ~80 cm of distributed N–S-oriented extension (Figures A2.19 and A2.20). The villa was also tilted ~5° in a down-to-the-NE sense. Fortunately, the superstructure of the house is low mass, flexible, regular in shape, timber-floored and relatively weakly attached to the pile foundation, all of which allowed the superstructure to detach from the foundation and thus isolate much of the ground extension from the superstructure. Despite this house suffering damage significant enough to be ‘red-tagged’, it performed commendably, from a life-safety perspective. It experienced very strong ground shaking, local decimetre-scale surface fault rupture deformation and is located within the hinge zone of a reverse fault scarp that has been classified in other earthquakes as a zone of ‘severe building damage’ (Kelson et al. 2001), yet the villa did not collapse. Not only

did it not collapse, it appears that it could potentially be re-piled and re-levelled, suggesting the possibility of post-event reinstatement (as opposed to demolition and reconstruction).

As stated above, and illustrated in Figure A2.20, Harkaway Villa is located in the transition zone between the higher strain fold/fault scarp to the northeast and the lower strain 'back limb' to the southwest. Utilising a combination of field observations, a differential LiDAR digital elevation model (DEM; 2013 LiDAR subtracted from post-earthquake 2016 LiDAR) at the site (Figure A2.20B, C) and assuming simple shear, ground strains at the villa site can be approximated.

At the steepest portion of the fold/fault scarp region to the northeast of the villa, dip-slip shear strains of ~0.2–0.4 can be derived based on ~1.5 m of elevation gain over 7 m of fault-perpendicular horizontal distance (Figure A2.20C), an estimated/observed fault dip of 45˚–90˚ (Langridge et al. 2018) and assuming simple shear. Strike-slip shear strains of ≤0.2 can be estimated based on an observed horizontal-to-vertical ratio of displacement of ≤1 (Langridge et al. 2018), ~1.5 m of elevation gain over 7 m of fault-perpendicular horizontal distance and assuming simple shear. Based on the above dip-slip and strike-slip shear strain considerations, net shear strains oriented parallel to the plane of the fault of ~0.2–0.4 (rounded to 10^{-1}) are approximated in the region of the fold/fault scarp.

In the 'back limb' area, dip-slip shear strains of ~0.02–0.04 can be estimated based on ~1 m of elevation gain over 50 m of fault-perpendicular horizontal distance (Figure A2.20C), an estimated/observed fault dip of 45˚–90˚ (Langridge et al. 2018) and assuming simple shear. Strike-slip shear strains of ≤0.02 can be estimated based on an observed horizontal-to-vertical ratio of displacement of ≤1 (Langridge et al. 2018), ~1 m of elevation gain over 50 m of fault-perpendicular horizontal distance and assuming simple shear. In the 'back limb' area, and based on the above dip-slip and strike-slip shear strain considerations, net shear strains oriented parallel to the fault plane of approximately 0.02–0.04 (rounded to 10^{-2}) are estimated.

Because Harkaway Villa is located between the fold/fault scarp and 'back limb' regions, we estimate that the ground-surface beneath Harkaway Villa experienced fault-parallel net shear strains in the order of 10^{-2}–10^{-1}, comprising a combination of reverse dip-slip and left-lateral shear strain.

In addition, at the villa site, N–S-oriented horizontal tensile strains of ~0.06 (rounded to 10^{-2}) are estimated based on the observation that the N–S extent of the villa's foundation piles was about 0.8 m greater than the ~13 m N–S length of the superstructure (Figure A2.19D).

A2.4.2.3 Grey House – Papatea Fault

Grey House is a timber-framed single-storey residential structure with a corrugated metal roof and timber weatherboard cladding (Figures A2.18 and A2.21). It has a concrete slab foundation that the owner reports as having been poured 'double thick'. It has a roughly square floor plan with an approximate area of 140 m^2.

Grey House was moved onto its present site in 1933. In 2004, the owner had the house placed on a concrete slab and renovated the house 'from top to bottom'. The only original components of the house are the roof and some weatherboards, windows and interior doors. The site conditions at Grey House are similar to those at Harkaway Villa (i.e. several metres of late Holocene fan alluvium that most likely overlie gravel-dominated Clarence River alluvium).

Grey House is located about 100 m west of Harkaway Villa within the surface rupture deformation zone of the Papatea Fault. At this locality, the Papatea Fault accommodates approximately 6 m of vertical deformation (reverse, southwest-side up), a comparable (or lesser) amount of left-lateral horizontal slip (Langridge et al. 2018) and defines a ~100+-m-wide surface fault rupture deformation zone comprising both discrete fault rupture and distributed deformation (Figure A2.21). The house is located on the hanging-wall side (southwest side) of the Papatea Fault, with metre-scale surface fault rupture passing within ~45 m northeast of the house, metre- to decimetre-scale surface fault rupture passing within ~10 m southwest of the house and centimetre-scale surface fault rupture intersecting the footprint of the house (Figure A2.21A, B). Nevertheless, the house came through the earthquake in good shape. It did not suffer significant structural damage and, following the earthquake, it was judged suitable for habitation and is currently occupied (as at 2020). In addition, the house is located within a portion of the surface rupture deformation zone that experienced minimal tilt; this, too, no doubt facilitated post-event occupation.

Utilising a combination of field observations, a differential LiDAR DEM at the site (Figure A2.21D, E) and assuming simple shear, ground strains at the Grey House site can be approximated. At the location of the house, dip-slip shear strains of ~0.02–0.03 can be estimated based on ~0.5 m of elevation gain over 25 m of fault-perpendicular horizontal distance (Figure A2.21E), an estimated/observed fault dip of 45˚–90˚ (Langridge et al. 2018) and assuming simple shear. Strike-slip shear strains of ≤0.02 can be estimated based on an observed horizontal to vertical ratio of displacement of ≤1 (Langridge et al. 2018), ~0.5 m of elevation gain over 25 m of fault-perpendicular horizontal distance and assuming simple shear. Based on the above dip-slip and strike-slip shear strain considerations, net shear strains oriented parallel to the fault plane of ~0.03–0.04 (rounded to 10^{-2}) are approximated at the Grey House site.

A2.4.2.4 Middle Hill Cottage – Papatea Fault

Middle Hill cottage was a timber-framed single-storey residential structure with a corrugated metal roof, timber weatherboard cladding and timber pile foundation (Figures A2.14, A2.22 and A2.23). It had a roughly rectangular floor plan with an approximate area of 75 m^2.

Middle Hill Cottage was probably constructed in the mid-1900s (the oldest aerial photographs we have access to for this part of the country date from 1961 and show that the cottage was already in existence). It was sited on several metres of Holocene gravel-dominated fan alluvium that likely overlies gravel-dominated Clarence River alluvium.

Middle Hill Cottage was located within the surface rupture deformation zone of the Papatea Fault which, at this site, is ~100 m wide, comprising both discrete fault rupture and distributed deformation and accommodating ~7.5 m of vertical deformation (reverse, west-side up) and a comparable (or lesser) amount of left-lateral horizontal slip (Figures A2.22 and A2.23) (Langridge et al. 2018). The cottage was located on the hanging-wall side of the Papatea Fault, close to the crest of the broad fold/fault scarp that is cut by extensional fissures (Figure A2.22C). The ground encompassed by the footprint of the structure experienced decimetre-scale folding, horizontal sinistral flexure (i.e. fault drag), tilting and distributed E–W-oriented extension. As a result of the Kaikōura earthquake, this house suffered damage significant enough to be ‘red-tagged’, and it has since been demolished. However, from a life-safety perspective, this house performed creditably – it experienced very strong ground shaking, tilting and decimetre-scale surface fault rupture deformation, but it did not collapse.

Utilising a combination of field observations, a differential LiDAR DEM at the site (Figure A2.23B, C), assuming simple shear and adopting a fault dip of 45°–90° and a horizontal to vertical ratio of displacement of ≤1 (Langridge et al. 2018), we estimate that the ground-surface beneath Middle Hill Cottage experienced fault parallel net shear strains in the order of 10^{-2}–10^{-1}, comprising a combination of left-lateral and reverse dip-slip shear strain.

A2.4.2.5 Paradise Cottage – Papatea Fault

Paradise Cottage is a timber-framed single-storey house with corrugated metal roof and cladding (Figures A2.24 and A2.25). It has a roughly square floor plan (area of ~85 m^2). Most of the structure is founded on timber piles, but the laundry room at the back (west side) of the cottage has a concrete slab foundation. About 13 m to the south of the cottage, there is a timber-framed and timber-clad shed.

Paradise Cottage was constructed prior to the early 1960s (aerial photographs from 1961 show that the cottage was already in existence). Paradise Cottage is sited on several metres of Holocene gravel-dominated colluvium and alluvium, and beach sand and gravel, overlying moderately strong bedrock.

At the coast, where Paradise Cottage is located, the Papatea Fault comprises several main strands; the cottage is located across and immediately adjacent to the westernmost of these (Langridge et al. 2018). Here, the western strand of the Papatea Fault accommodates approximately 3.5 m of vertical deformation (east-side up) (Figure A2.24D), a subordinate amount of left-lateral horizontal slip (Langridge et al. 2018) and defines an 8–10-m-wide surface fault rupture deformation zone primarily comprising discrete fault rupture. The cottage is located on the up-thrown side of the fault, at the eastern edge of the surface rupture deformation zone and has had its back-side ripped out by surface fault rupture. The nearby timber shed is located entirely within the fault scarp and has been severely tiled and deformed. Neither the house nor the shed collapsed.

Employing a combination of field observations and a differential LiDAR DEM at the site (Figure A2.24C, D), assuming simple shear and adopting a sub-vertical fault dip and a horizontal to vertical ratio of displacement of <1 (Langridge et al. 2018), we estimate that the ground-surface beneath the shed and the southwest corner of the cottage experienced fault-parallel net shear strains in the order of 10^{-1}.

A2.4.2.6 Glenbourne Woolshed – The Humps Fault

The Glenbourne woolshed is a single-storey, timber-framed structure with corrugated metal roof and cladding (Figures A2.26 and A2.27) and a rectangular floor plan (area of ~300 m^2). The structure stands on concrete piles and has timber flooring overlying timber joists.

The Glenbourne woolshed was constructed in 1980. It is sited on a 2–4 m thickness of late Pleistocene–Holocene loosely packed fluvial gravel above moderately strong bedrock.

Glenbourne Farm is located near the north-east margin of the Culverden Basin, where the low relief topography of the Emu Plains transitions into the steeper slopes of the Mt Stewart Range (Figure A2.14). Here, surface rupture of The Humps Fault comprises three to four main traces mapped over a 3.5 km width perpendicular to fault strike (Figure A2.27) (Nicol et al. 2018). Net dextral displacement across these traces is a factor of 2 larger compared to the average dextral displacement on the western ~20 km of the fault (Nicol et al. 2018). Along the fault, vertical displacements are variably north- or south-side up. At the Glenbourne woolshed, surface rupture displacement was measured using RTK-GPS with the primary trace, located

only ~5 m from the woolshed (Figures A2.26A, C and A2.27A), having ~1–2 m of dextral and ~1.2 m of north-side-up vertical displacement. The woolshed is situated on the down-thrown side of the primary discrete trace in a 10–20-m-wide zone of decimetre-scale ground subsidence that encompasses minor fracturing and small faults with vertical displacements of up to 10 cm (Figure A2.26A). This zone of ground subsidence extends from the stockyard adjacent to, and southwest of, the woolshed to the northeast for over 50 m. Fault-rupture-induced damage to the Glenbourne woolshed appears to be limited to rotation of some of the shallow-seated concrete piles (Figure A2.26B). The superstructure itself is relatively undamaged and intact. We suspect that rotation of the piles isolated the superstructure from the decimetre-scale fault rupture ground deformation underneath. It is pertinent to note that a similarly constructed and piled woolshed sited across the 2010 surface rupture of the Greendale Fault displayed similar performance, with rotation of shallow-seated piles isolating, to a large extent, the superstructure from the underlying fault rupture ground deformation (Figure A2.11) (Van Dissen et al. 2011).

At this location, and elsewhere along The Humps and Leader faults, we have access to pre- and post-earthquake photogrammetric point clouds. Iterative closest point (ICP) differencing of pre- and post-earthquake point clouds (e.g. Nissen et al. 2012) yields gridded values of displacements in the vertical, northing and easting directions at 50 m grid spacings. These gridded values were interpolated into three separate 10 m grid-size rasters (one for each component/direction), and we construct fault-perpendicular transects on these rasters, crossing the structures, to estimate the fault-parallel net shear strains at the location of the structures that incorporate both horizontal and vertical displacements (Figure A2.27). Given the decametre-scale resolution of the ICP method, our shear strain estimations need to be augmented by field observations to accommodate the location, and amount, of discrete displacements that would otherwise be smoothed by the ICP method. Nevertheless, the ICP method provides the opportunity to document the amount and style of broad-scale net displacement across the surface rupture deformation zone, and distributed deformation within the deformation zone, that may otherwise not be readily apparent, or well-characterised, by field measurements of discrete displacement alone. While the ICP method is used here to estimate 3D displacements that should be internally consistent across fault profiles, there is some uncertainty introduced in both gridding processes, and this yields uncertainty regarding the exact amount and distribution of deformation along the profiles at the specific location of the structures. This, in turn, yields uncertainty in our strain estimations. However, we expect that this effect is small, given the order of magnitude strain estimates reported in this Appendix, and acknowledging that field observations of discrete displacement are taken into account. Using these data, and assuming simple shear and a sub-vertical fault dip (80–90°) at the woolshed site, we estimate net shear strains of ~10^{-2}.

A2.4.2.7 Hillview Cottage – The Humps Fault

Hillview Cottage is a timber-framed, single-storey residential structure with a corrugated metal roof and Fibrolite cladding. It has a concrete slab foundation and a rectangular floor plan with an area of ~50 m^2 (Figures A2.28 and A2.29).

Hillview Cottage was constructed prior to the early 1950s (aerial photographs from 1950 show that the cottage was already in existence). It is sited on late Pleistocene loosely to tightly packed fan-gravel and stiff loess >15 m thick.

Hillview Cottage is located on a zone of concentrated deformation in the central section of The Humps Fault. Just west of the cottage, there is a prominent, ~25-m-wide pull-apart depression that transitions to the east into a narrow zone of Riedel shears and tension fractures

(Figures A2.28 and A2.29A). In the field, an adjacent fault-offset fence yielded RTK-derived offset measurements of 0.9 m dextral and 0.5 m vertical (Nicol et al. 2018). The cottage experienced a chimney collapse (Figure A2.28B) and multiple fractures to the concrete foundation (Figure A2.28C, D). Timber supports for the roof/veranda at the front of the cottage experienced minor amounts of shear and were deformed out-of-plumb (Figure A2.28C, D). Several cladding planks at the base of the exterior of the cottage were broken (Figure A2.28D). Although surface rupture caused structural damage to the cottage, it appears to be far from collapse. Using a combination of the ICP-based analysis (see Glenbourne section) and field observations, we estimate centimetre-scale vertical and decimetre-scale dextral displacement at the site of the cottage. Assuming simple shear and a sub-vertical fault plane, we estimate a net shear strain across the foot print of the structure of ~10^{-2}.

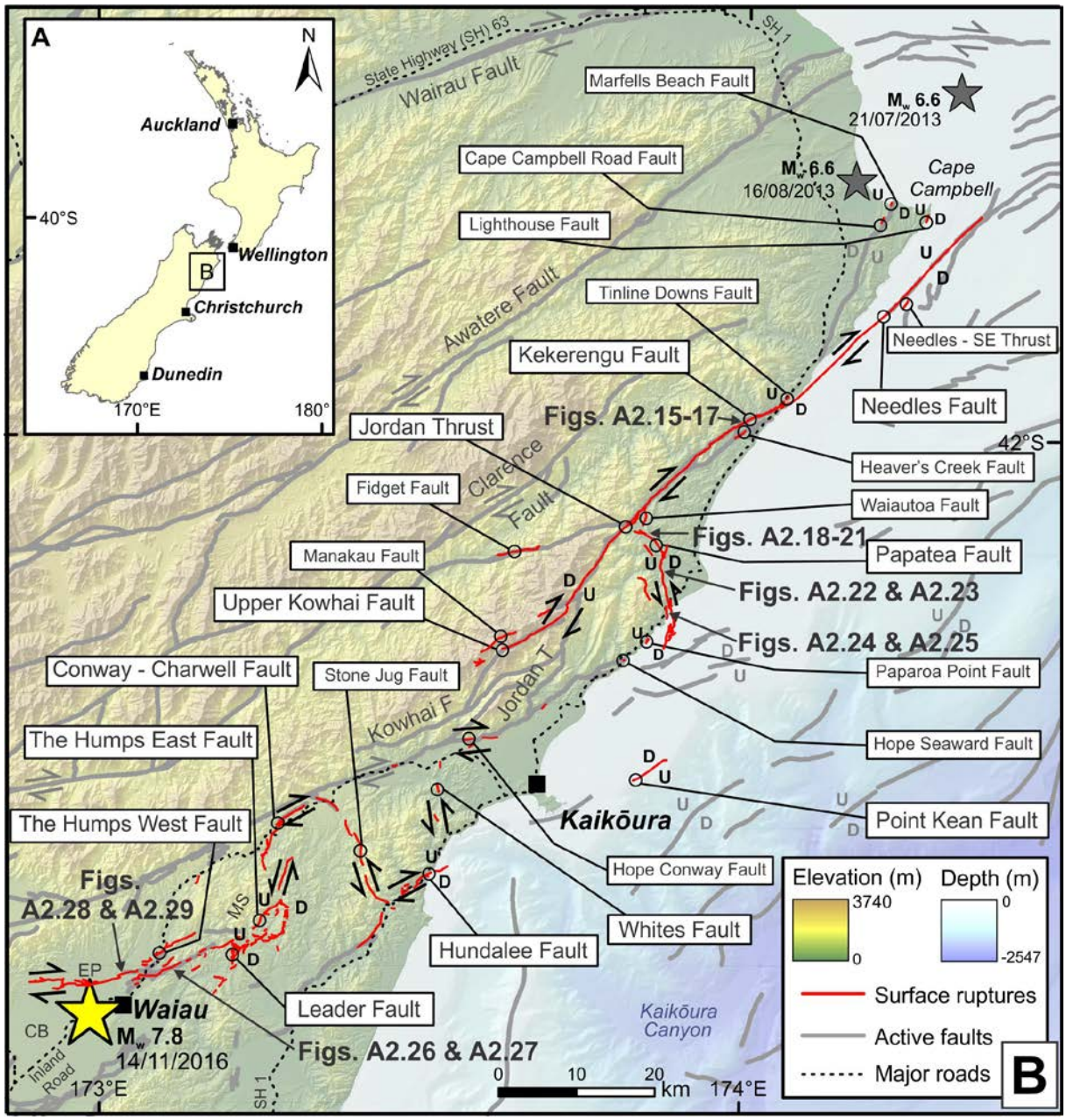

Figure A2.14 Kaikōura earthquake surface fault ruptures (red lines) from Litchfield et al. (2018). Also shown are the locations of Figures A2.15–29, the epicentre of the 2016 Kaikōura earthquake (large yellow star) from Nicol et al. (2018) and the epicentres for the two 2013 Cook Strait earthquakes (small grey stars) from Holden et al. (2013). Abbreviations: CB = Culverden Basin, EP = Emu Plains, F = fault, MS = Mt Stewart Range, T = thrust. A 1:250,000-scale digital version of 2016 surface ruptures is available for download at https://data.gns.cri.nz/af/ (choose 'Download data – Kaikōura'; Langridge et al. 2016).

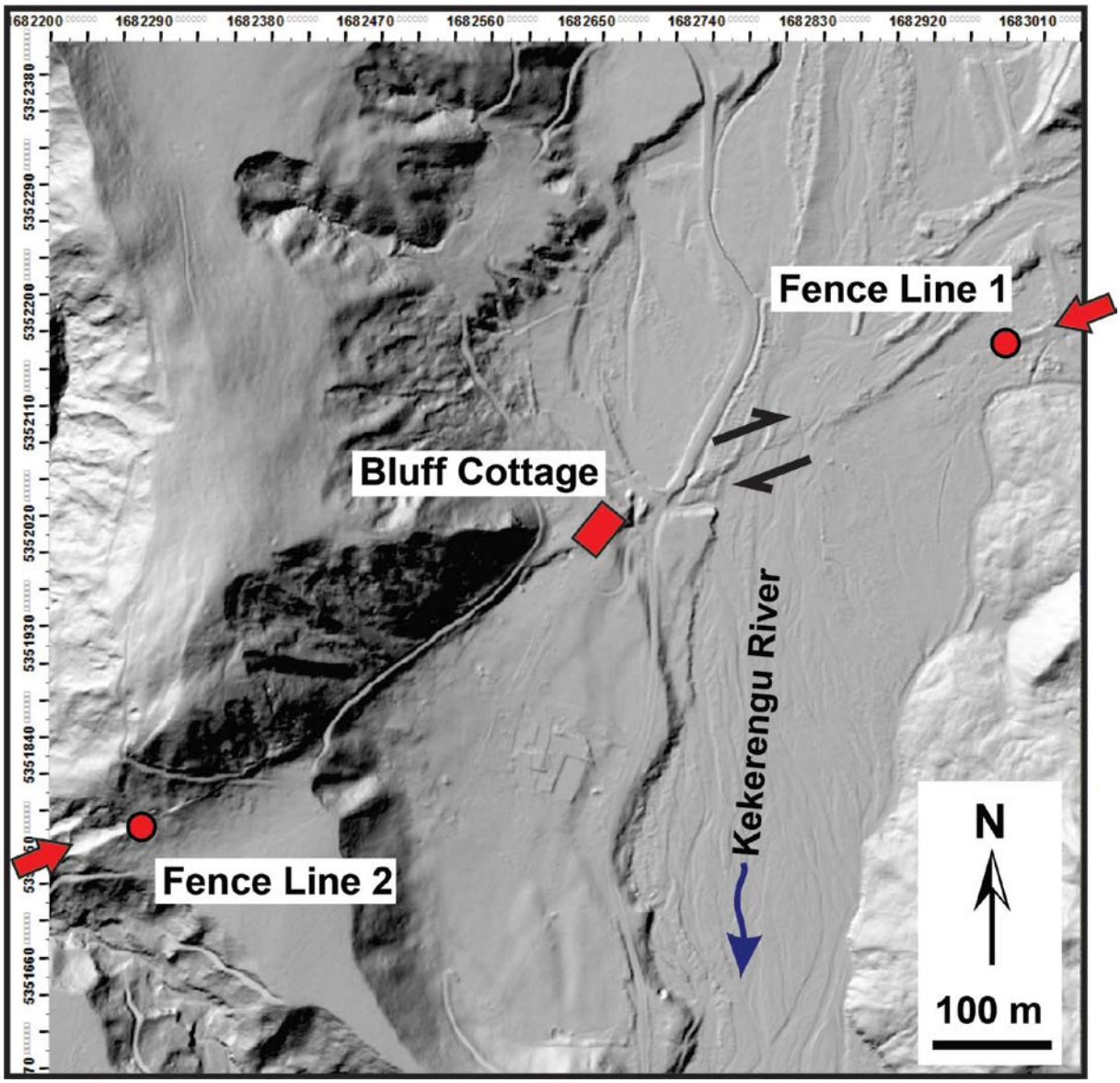

Figure A2.15 2016 post-earthquake LiDAR hill shade DEM, illuminated from the northwest showing location of surface rupture trace of the Kekerengu Fault (red arrows), Bluff Cottage (Figure A2.16), the two offset fence lines depicted in Figure A2.17 and the sense of strike-slip on the Kekerengu Fault (black arrows). Though the size of Bluff Cottage portrayed in this figure is significantly exaggerated, its orientation is accurate. Coordinates are New Zealand Transverse Mercator 2000.

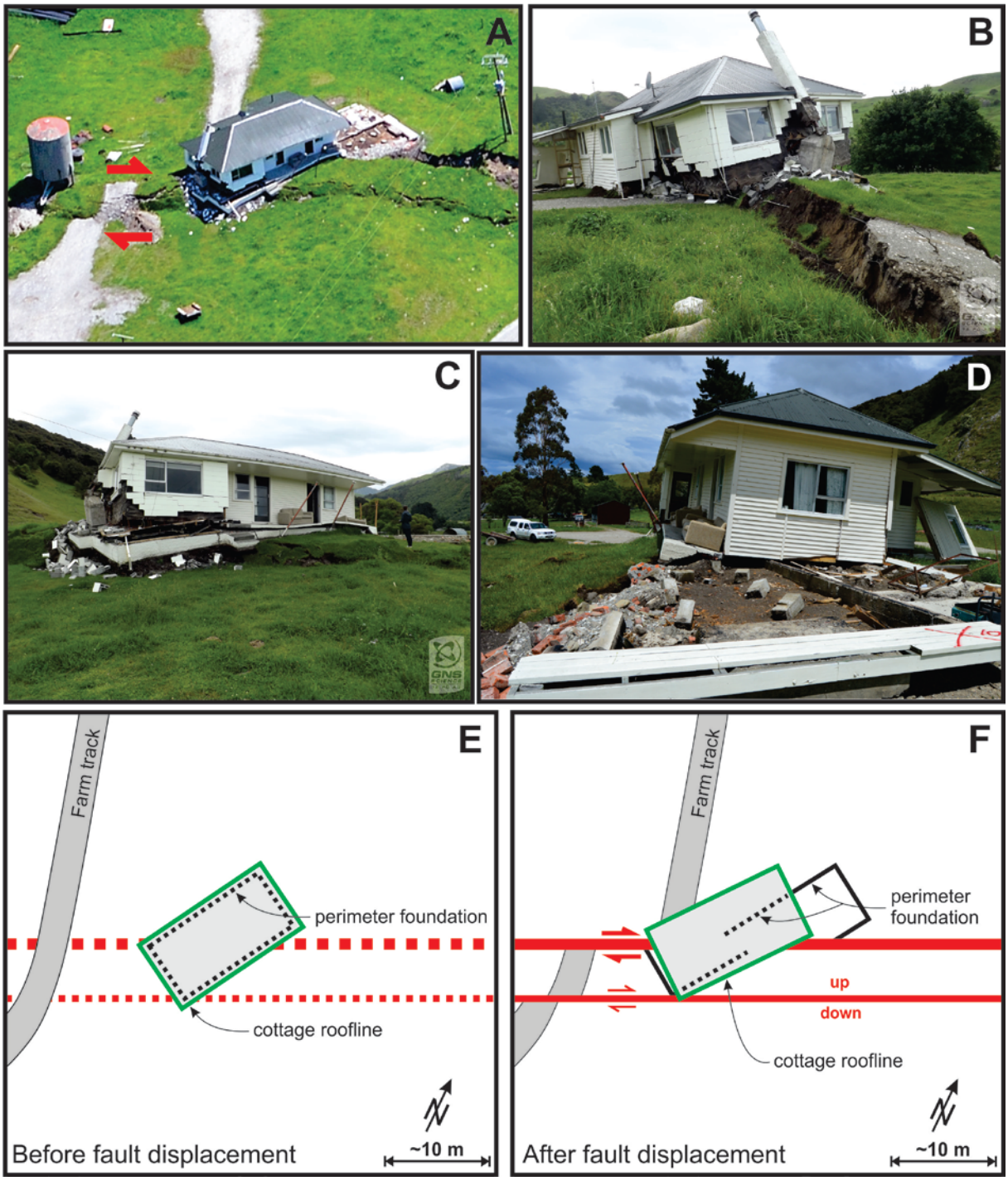

Figure A2.16 Bluff Cottage and Kekerengu Fault surface rupture; see Figures A2.14 and A2.15 for location (Lat: -41.9796, Long: 173.9976). (A) Oblique aerial view looking northwest. Red arrows show the sense of slip of the Kekerengu Fault that generated ~10 m of right-lateral surface rupture displacement at this locality. Photo by Dougal Townsend, taken in November 2016. (B) View of Bluff Cottage looking northeast along the strike of the surface rupture of the Kekerengu Fault. Right-laterally offset farm track to left of cottage in Figure A2.16A is the same farm track visible in lower right and middle left of Figure A2.16B. Photo by Nicola Litchfield, taken in November 2016. (C) View looking northwest. Photo by Nicola Litchfield, taken in November 2016. (D) View looking southwest. Note that the concrete perimeter foundation and piles that were once under the cottage have now been torn from the superstructure of the cottage and laterally displaced toward the viewer, relative to the cottage. Photo by Robert Zinke, taken in November 2016. (E) Schematic map of Bluff Cottage and farm track prior to surface rupture of the Kekerengu Fault. (F) Schematic map of Bluff Cottage and farm track after fault displacement.

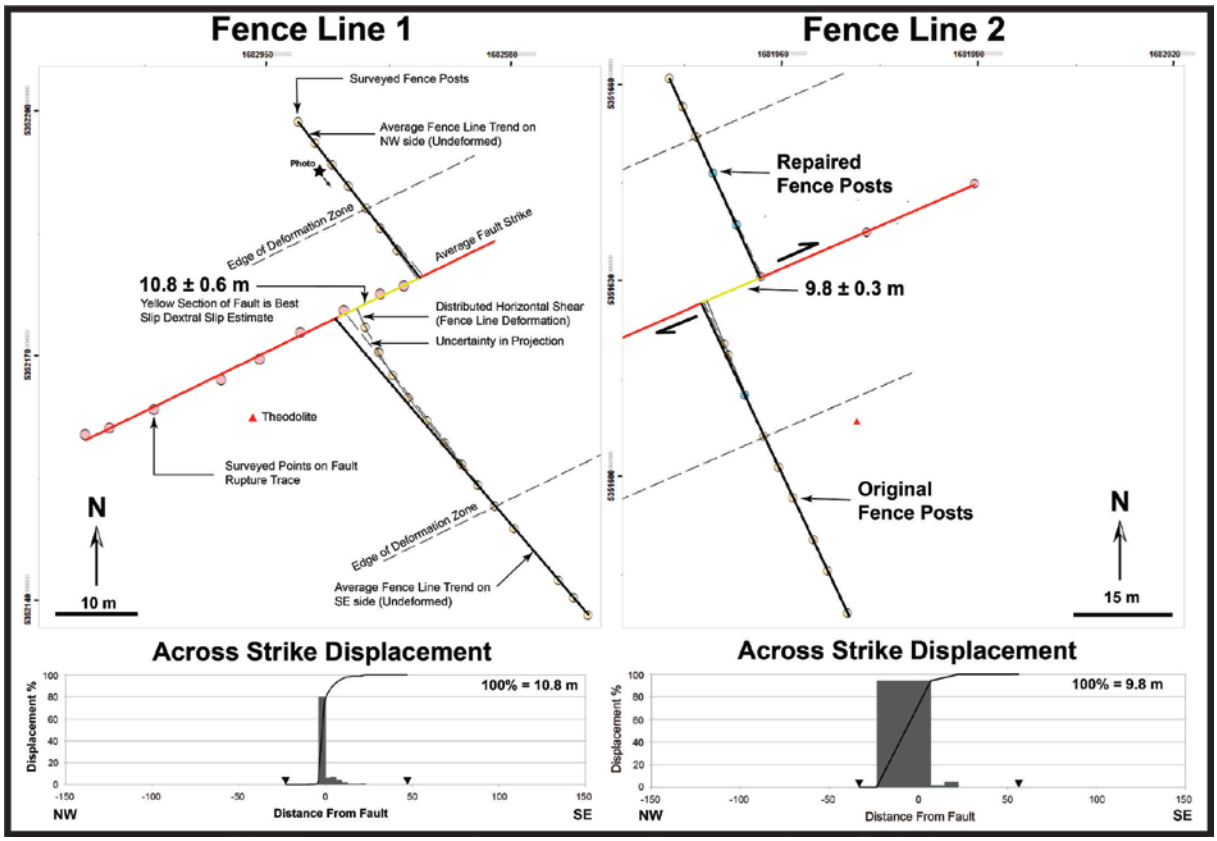

Figure A2.17 Examples of fence line displacements along the Kekerengu Fault near Bluff Cottage that document both the amount of right-lateral displacement and how that displacement is distributed as a function of distance perpendicular to fault strike (see Kearse et al. [2018] for more detail). See Figure A2.15 for locations. Coordinates are New Zealand Transverse Mercator 2000.

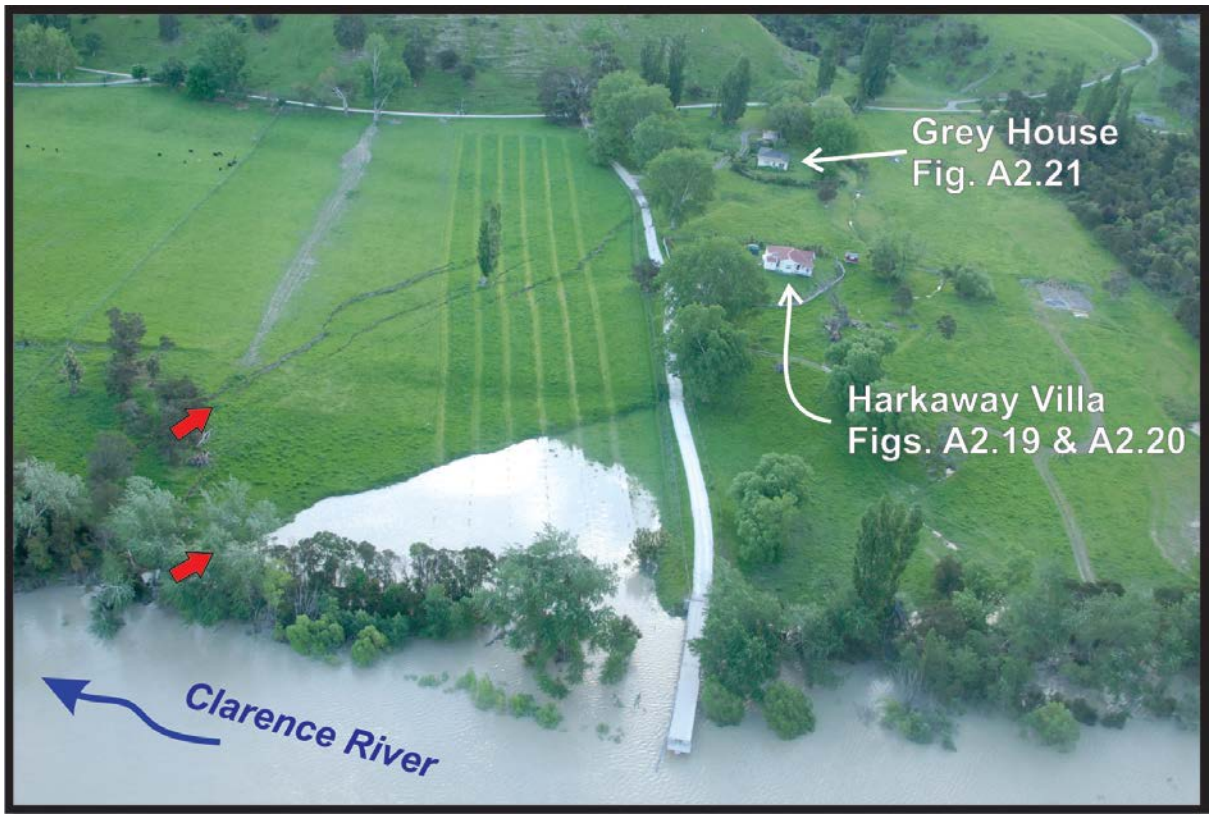

Figure A2.18 Harkaway Villa (Lat: -42.1105, Long: 173.8384), Grey House (Lat: -42.1105, Long: 173.8372) and the Papatea Fault surface rupture; see Figure A2.14 for location. Oblique aerial view looking west, with red arrows denoting position of prominent discrete ruptures in the surface rupture deformation zone of the Papatea Fault. Photo by Will Ries, taken in November 2016.

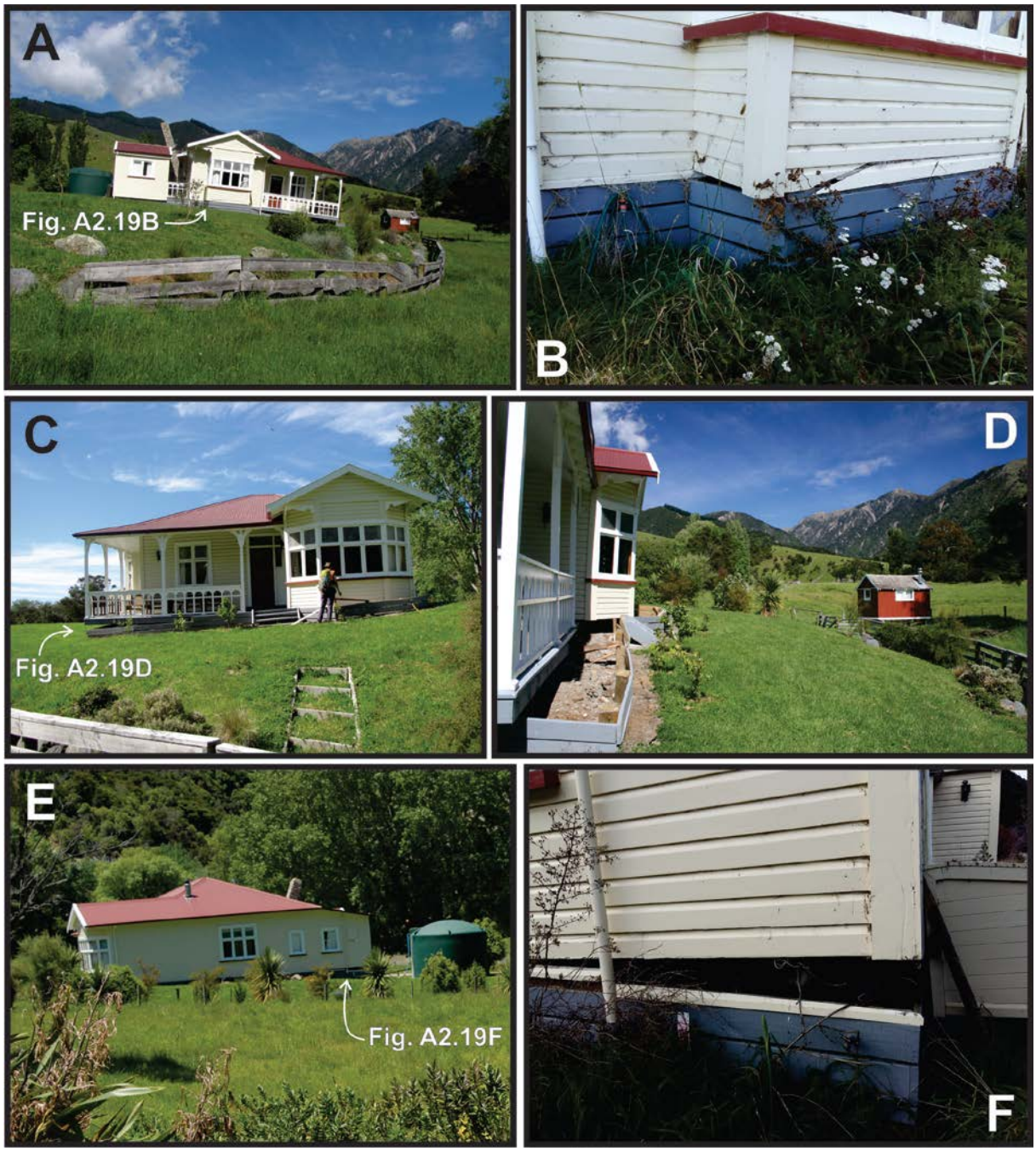

Figure A2.19 Harkaway Villa and Papatea Fault surface rupture. (A) View looking west showing northeast-ward tilt of the villa on the up-thrown (hanging-wall) side of the Papatea Fault. Photo by Julie Rowland, taken in November 2016. (B) View looking northwest showing detail of damage to the east side of the villa. Photo by Julian Garcia-Mayordomo, taken about 18 months after the 2016 Kaikōura earthquake. (C) View looking south of the north side of the villa. Photo by Rob Langridge, taken in November 2016. (D) View looking west of the north side of the villa, showing offset of the foundation piles from the superstructure. Photo by Julie Rowland, taken in November 2016. (E) View looking east of the west side of Harkaway Villa. Photo by Rob Langridge, taken in November 2016. (F) View looking east, showing detail of damage to the west side of the villa. Photo by Julian Garcia-Mayordomo, taken in May 2018.

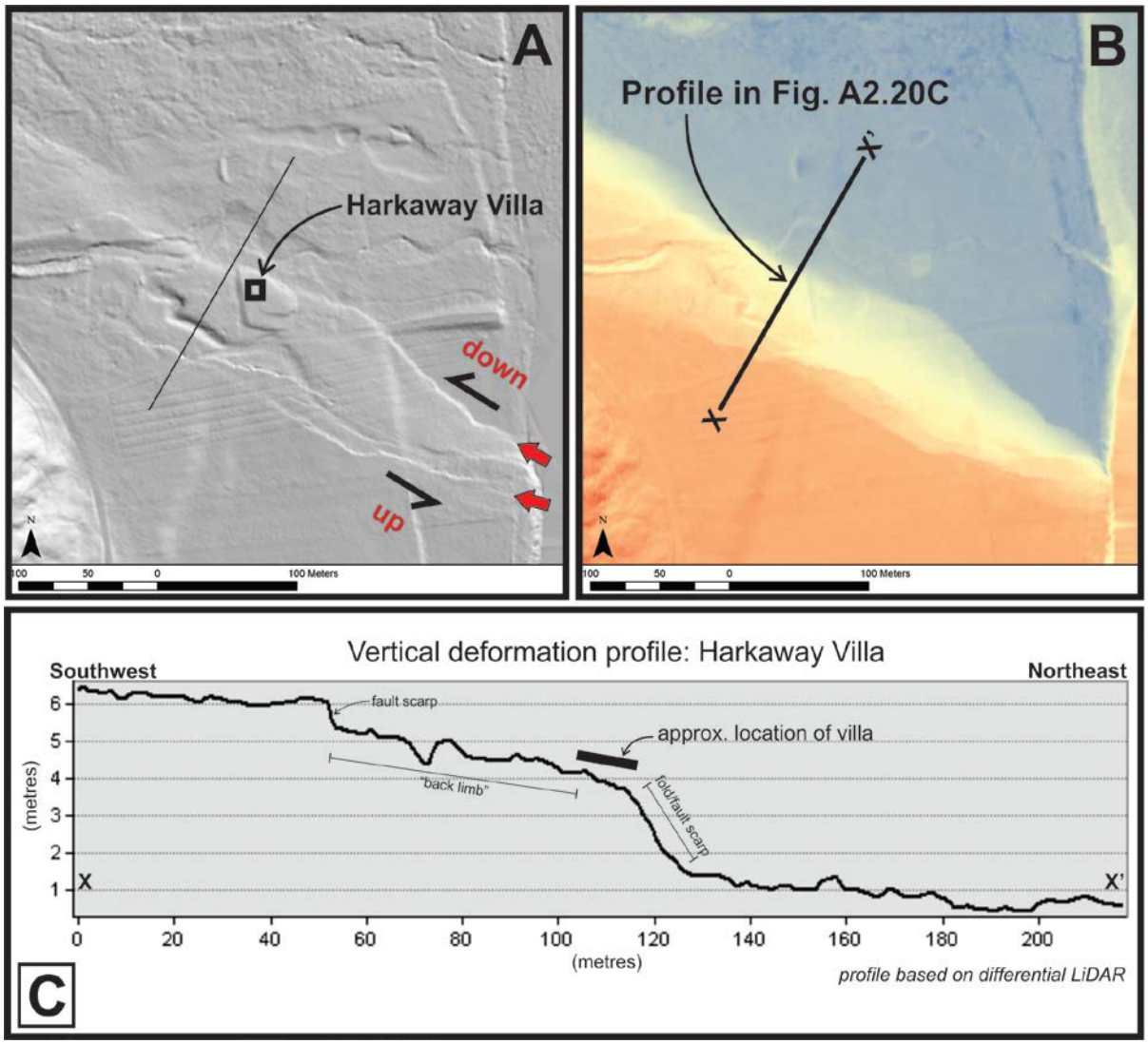

Figure A2.20 Harkaway Villa and Papatea Fault surface rupture. (A) 2016 post-earthquake LiDAR hill shade DEM with black square denoting villa's location and red arrows showing location of prominent discrete ground-surface ruptures. (B) Differential LiDAR DEM with blue colours denoting little vertical change and red colours denoting significant positive vertical change (see C for more detail regarding scale). (C) Vertical deformation profile derived from the differential LiDAR DEM. Vertical exaggeration = 7.5.

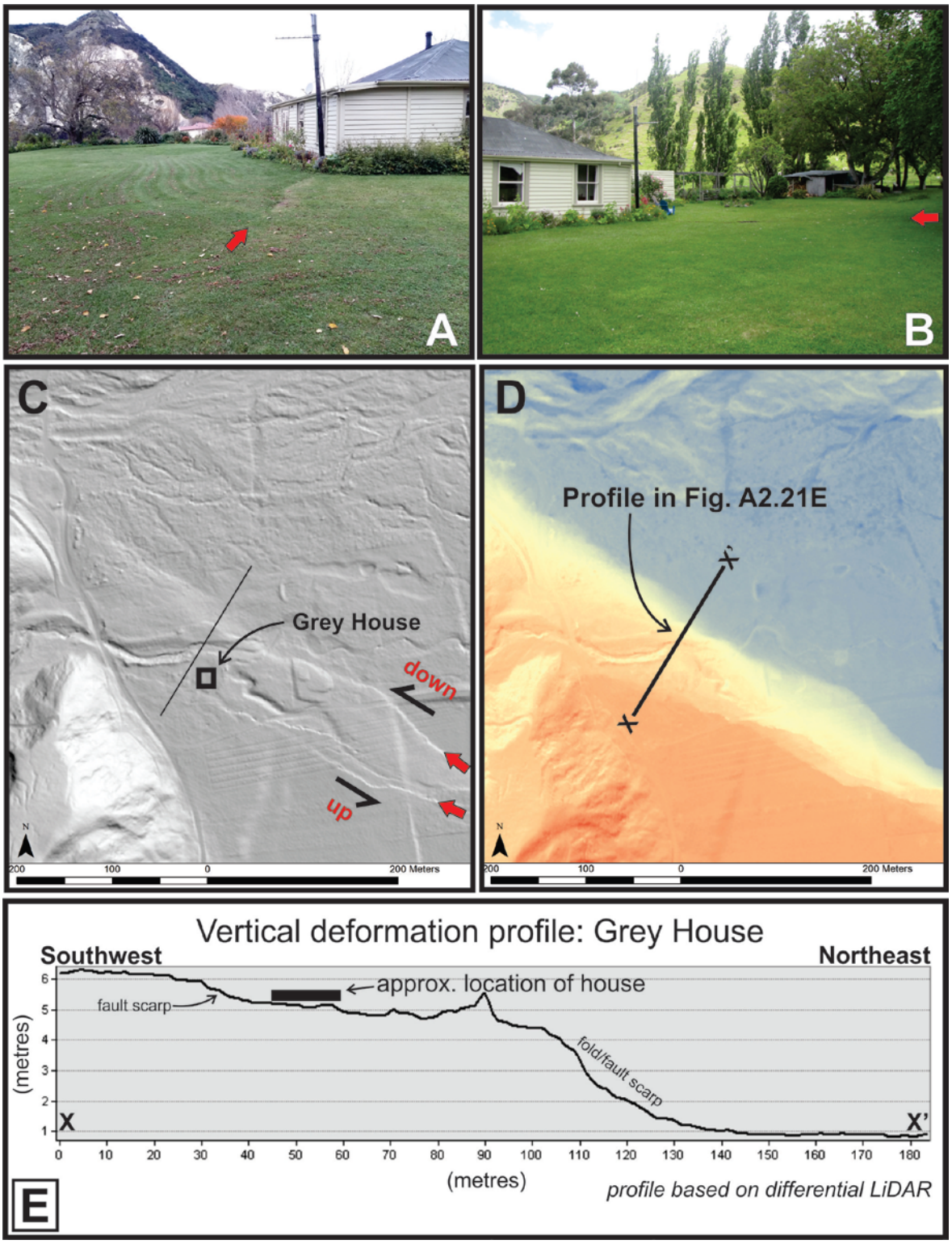

Figure A2.21 Grey House and Papatea Fault surface rupture. (A) View looking east-southeast with red arrow showing location of centimetre-scale discrete rupture that intersects northwest corner of the house. Harkaway Villa (Figures A2.18 and A2.19) is visible in the middle distance. Photo by Julian Garcia-Mayordomo, taken about 18 months after the 2016 Kaikōura earthquake. (B) View looking southwest. Red arrow denotes the location of centimetre-scale discrete rupture that intersects the northwest corner of the house. (C) 2016 post-earthquake LiDAR hill shade DEM with the black square denoting the house's location and red arrows showing the location of prominent discrete ground-surface ruptures. (D) Differential LiDAR DEM with blue colours denoting little vertical change and red colours denoting significant positive vertical change (see E for more detail regarding scale). (E) Vertical deformation profile derived from the differential LiDAR DEM. Vertical exaggeration = 6.4.

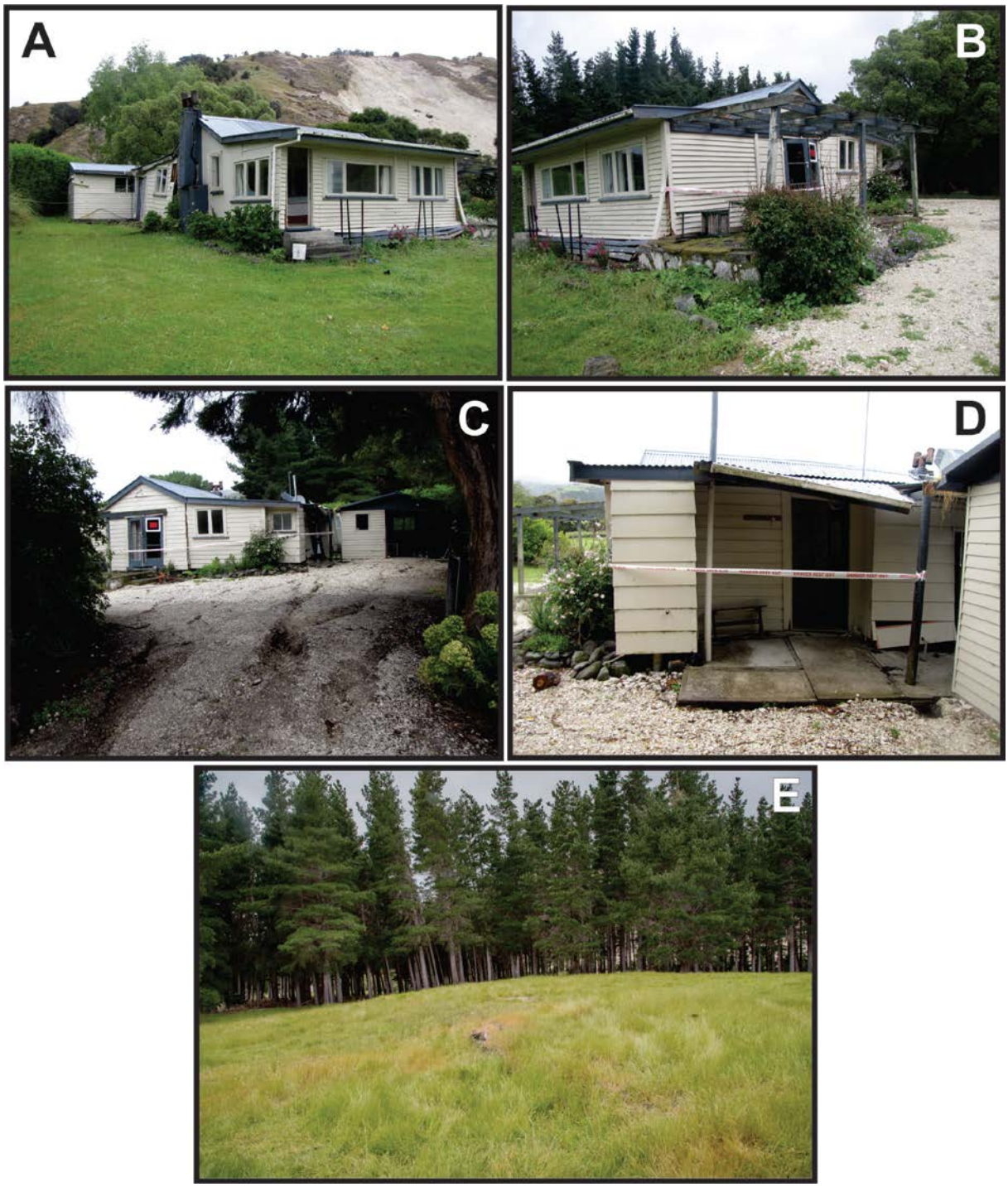

Figure A2.22 Middle Hill Cottage and Papatea Fault surface rupture; see Figure A2.14 for location (Lat: -42.1536, Long: 173.8667). (A) View looking west. Photo by Rob Langridge, taken in December 2016. (B) View looking south-southwest. Photo by Rob Langridge, taken in December 2016. (C) View looking southeast along the strike of extensional fissures located in the crestal region of the primary fold/fault scarp that extend toward, and intersect, the cottage. Photo by Rob Langridge, taken in December 2016. (D) View looking northeast. Photo by Rob Langridge, taken in December 2016. (E) View from the cottage looking south-southeast along-strike of the Papatea Fault's surface rupture deformation zone. Prior to the 2016 rupture of the Papatea Fault, the ground surface in this photograph was approximately flat and horizontal, and the trunks of the pine trees were all sub-vertical. Photo by Stefano Pucci, taken about a year after the earthquake.

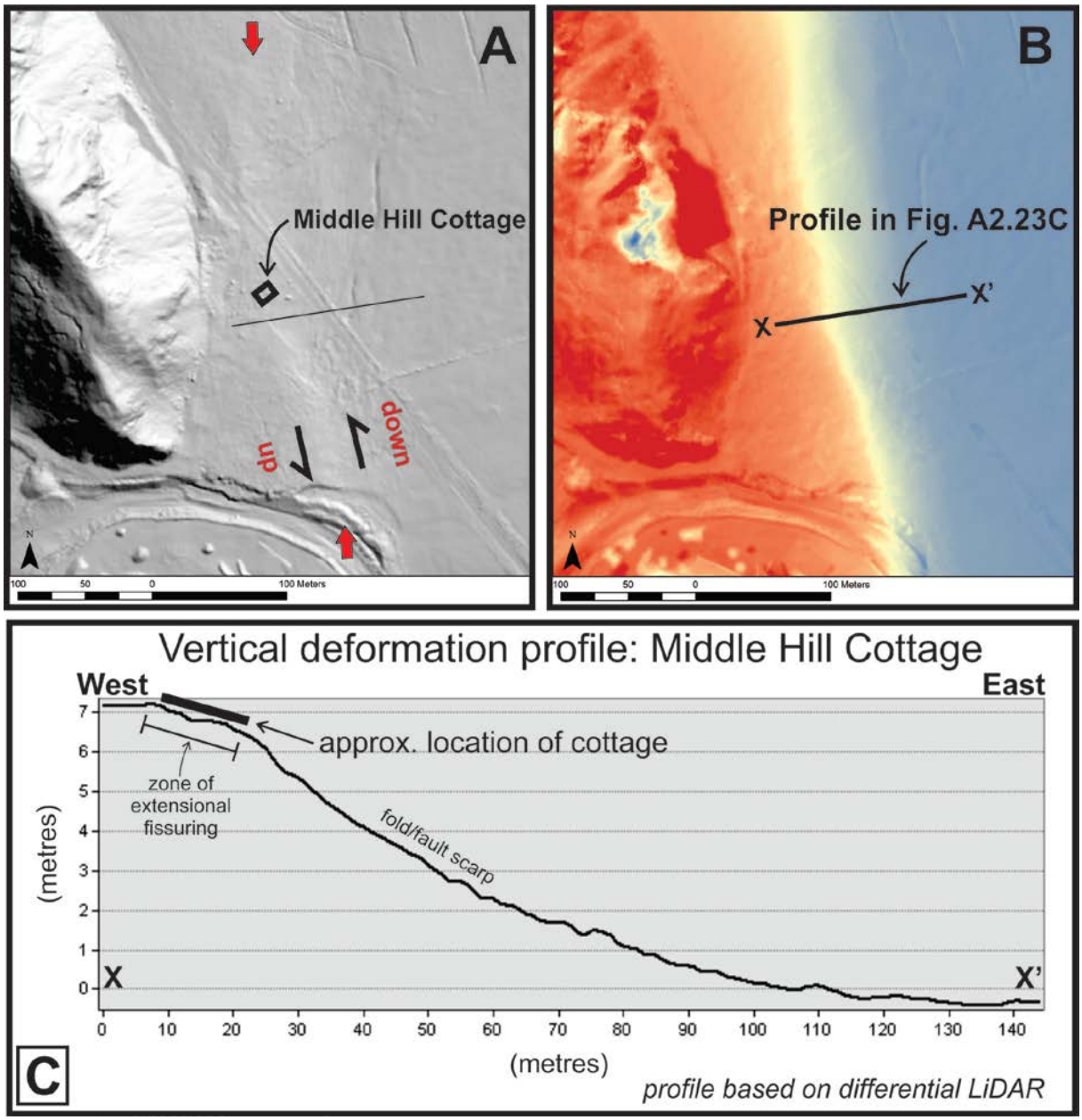

Figure A2.23 Middle Hill Cottage and Papatea Fault surface rupture. (A) 2016 post-earthquake LiDAR hill shade DEM with the black square denoting cottage's location and red arrows showing the location the surface fault rupture scarp. (B) Differential LiDAR DEM with blue colours denoting little vertical change and red colours denoting significant positive vertical change (see C for more detail regarding scale). (C) Vertical deformation profile derived from the differential LiDAR DEM. Vertical exaggeration = 6.1.

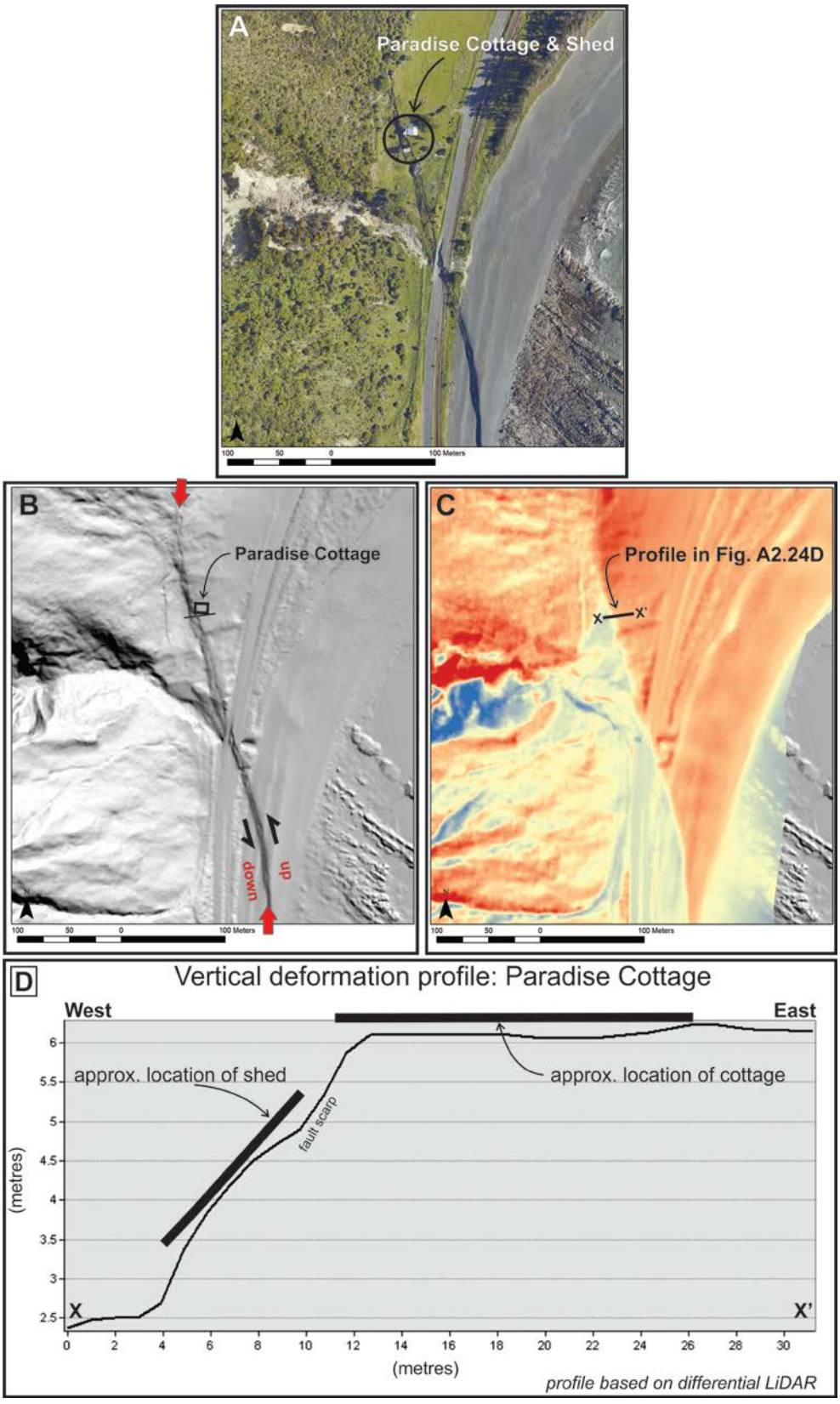

Figure A2.24 Paradise Cottage and Papatea Fault surface rupture; see Figure A2.14 for location (Lat: -42.2010, Long: 173.8753). (A) 2016 post-earthquake vertical aerial orthophotograph. Black circle denotes location of cottage and shed to the south. (B) 2016 post-earthquake LiDAR hill shade DEM showing location of cottage (black square) and prominent discrete ground-surface ruptures (red arrows). (C) Differential LiDAR DEM with blue colours denoting little vertical change and red colours denoting significant positive vertical change (see D for more detail regarding scale). (D) Vertical deformation profile derived from differential LiDAR DEM located half-way between the cottage and the shed. Vertical exaggeration = 3.3.

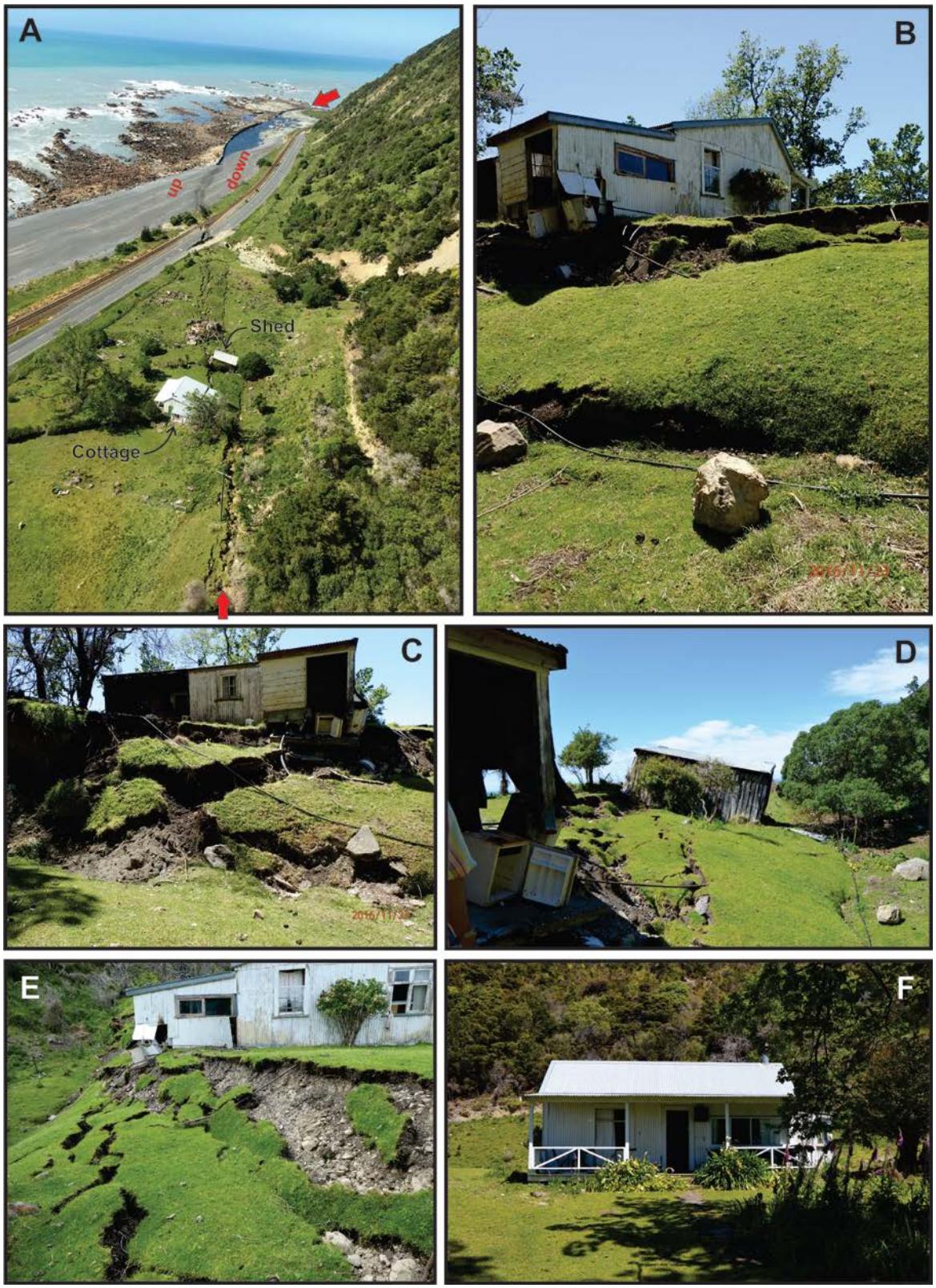

Figure A2.25 Paradise Cottage and Papatea Fault surface rupture; see Figure A2.14 for location. (A) Oblique aerial view looking south-southeast along the strike of the western strand of the Papatea Fault. Red arrows denote the position of prominent discrete rupture. Photo by Will Ries, taken in November 2016. (B) View looking northeast. Photo by Alex Hatem, taken in November 2016. (C) View looking east. Photo by Alex Hatem, taken in November 2016. (D) View looking south-southeast towards the shed. Photo by Robert Zinke, taken in November 2016. (E) View looking north-northwest along-strike of the surface fault rupture. Photo by Tim Little, taken in November 2016. (F) View looking east towards the front side of the cottage. The front of the cottage appears to be little damaged compared with the significant damage behind it. Photo by Robert Zinke, taken in November 2016.

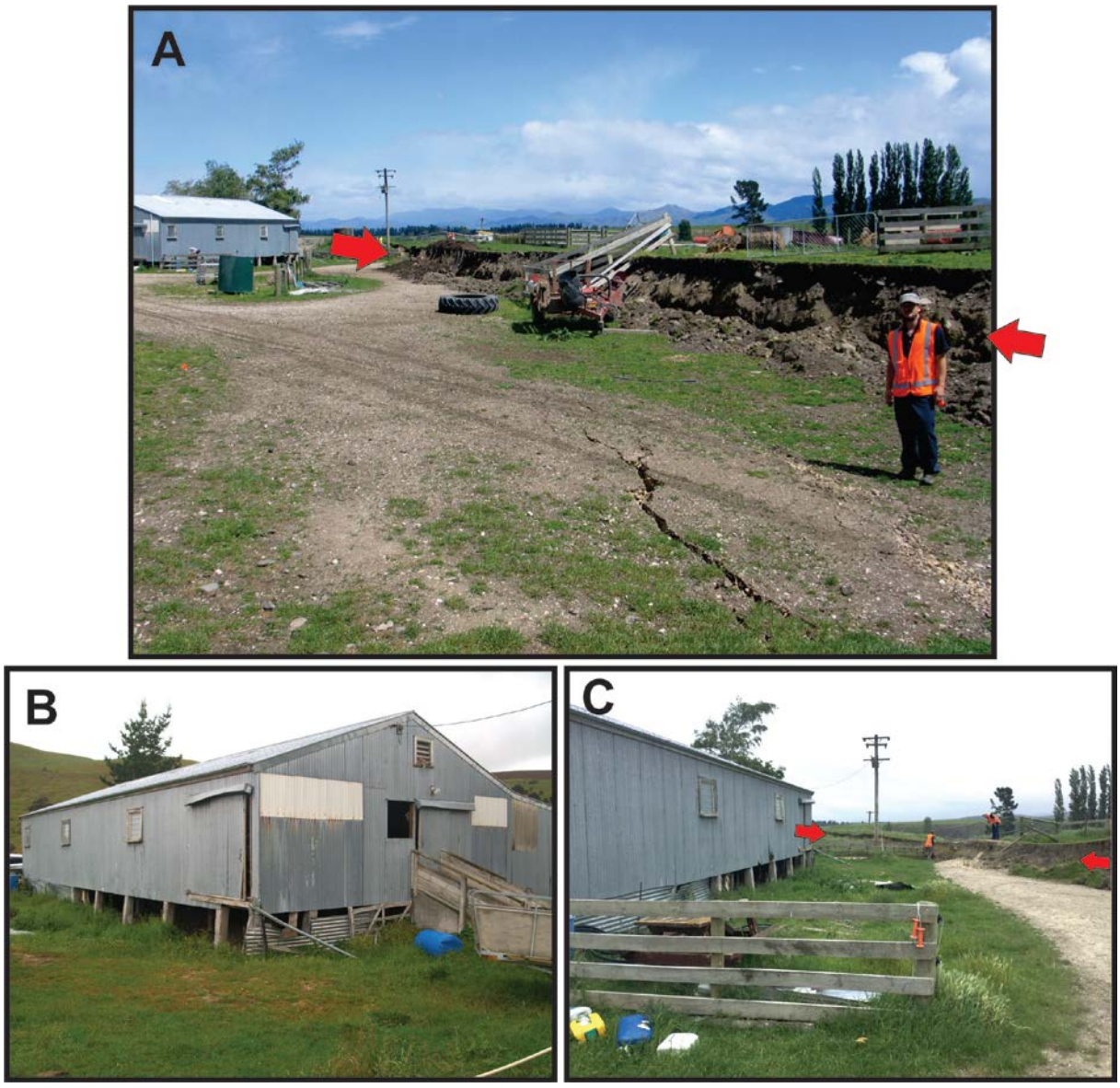

Figure A2.26 Glenbourne Woolshed and The Humps Fault surface rupture; see Figures A2.14 and A2.27 for location (Lat: -42.6152, Long: 173.1058). (A) View looking southwest along the fault rupture towards the woolshed. Note distributed centimetre-scale cracking in the foreground (in front of the high-vis geologist), adjacent to the main trace (red arrow, and behind the high-vis geologist). The distributed centimetre-scale cracking persists along-strike for many tens of metres. Photo by Jarg Pettinga, taken in November 2016. (B) View looking south at the woolshed (main fault scarp is behind the camera). Tilt and rotation of the shallow-seated concrete piles is the only recognisable damage. Photo by Clark Fenton, taken in December 2016. (C) View looking southwest along the side of the woolshed and towards the main fault scarp at this site. Photo by Tim Stahl, taken in November 2016.

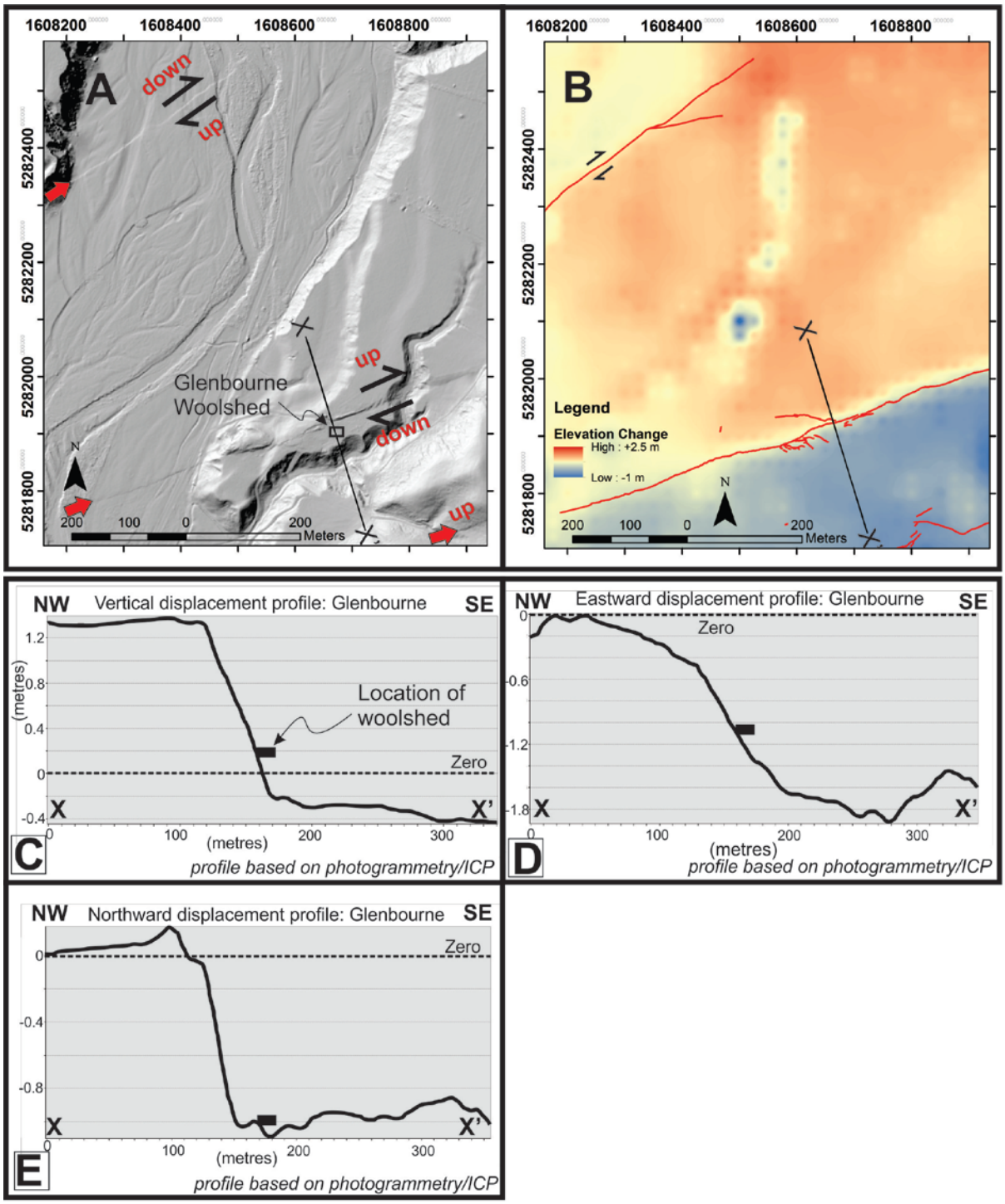

Figure A2.27 Glenbourne Woolshed and The Humps Fault surface rupture. (A) LiDAR hill shade DEM showing location of the woolshed and two prominent discrete fault traces (red arrows), one of which is within ~5 m of the woolshed (see Figure A2.26A, C). (B) Raster of vertical displacements in the same area as (A), using ICP method outlined in the text. (C), (D) and (E) are the vertical, eastward and northward displacement profiles from X to X' on the top two images. The location of the woolshed is shown on each profile. Note that, while relative motions were mapped in the field, the absolute sense of displacement is more complex, with the down-thrown side of the fault moving southwest-ward and the up-thrown side of the fault remaining relatively stable, except in the vertical direction. Y-axis exaggeration in (C) and (D) = 85. Y-axis exaggeration in (E) = 130.

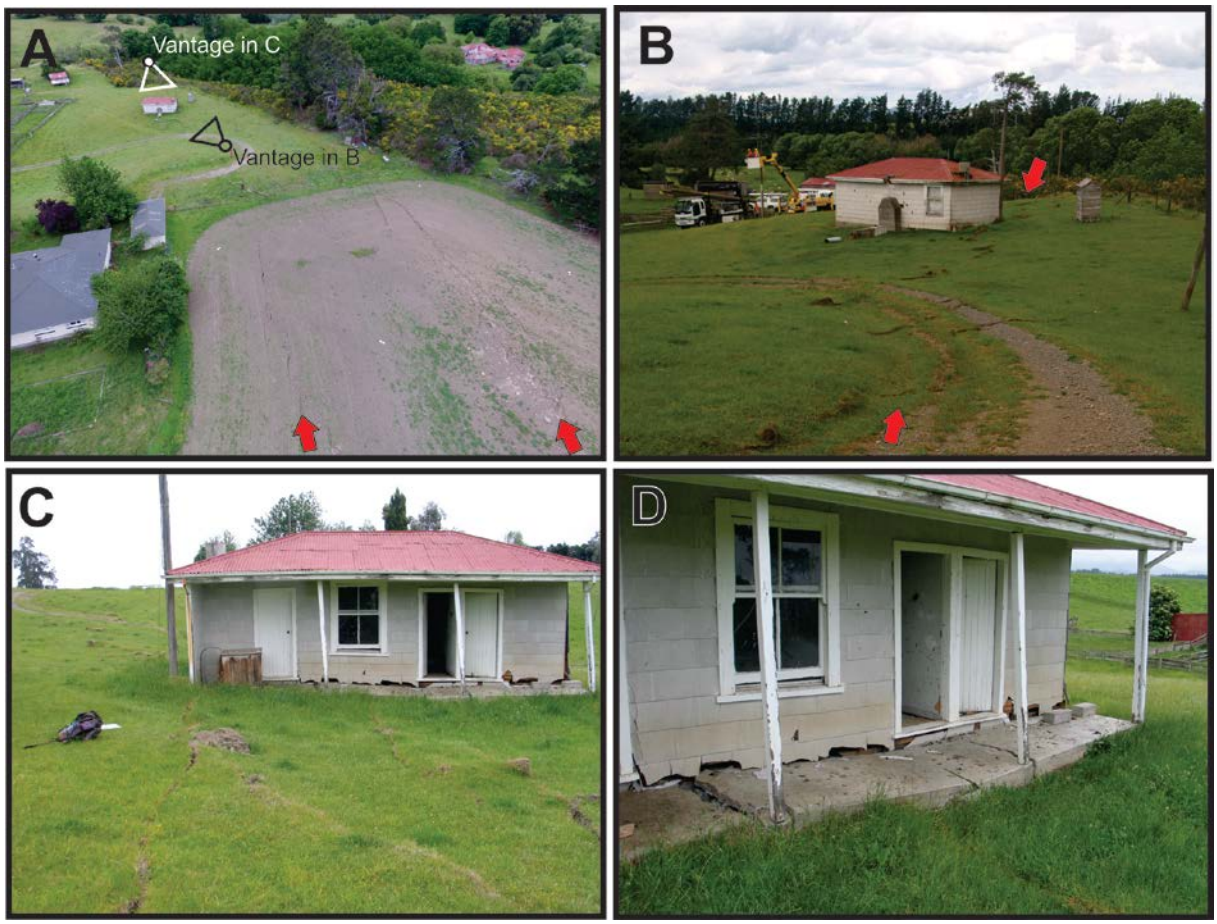

Figure A2.28 Hillview Cottage and The Humps Fault surface rupture; see Figures A2.14 and A2.29 for location (Lat: -42.6287, Long: 173.0154). (A) Oblique aerial view looking east toward the cottage along discrete dextral-normal surface fault ruptures (red arrows). Photo courtesy of Sam McColl, taken from a drone in November 2016. (B) View looking northeast. At this location, the cottage is impacted by decimetre-scale discrete fault rupture (in this case Riedel shears) and centimetres to decimetres of distributed deformation between the shears. Note the collapsed chimney. Photo by Clark Fenton, taken in November 2016. (C, D) Details of damage to the cottage caused by decimetre-scale surface fault rupture. Photos by Jarg Pettinga, taken in November 2016.

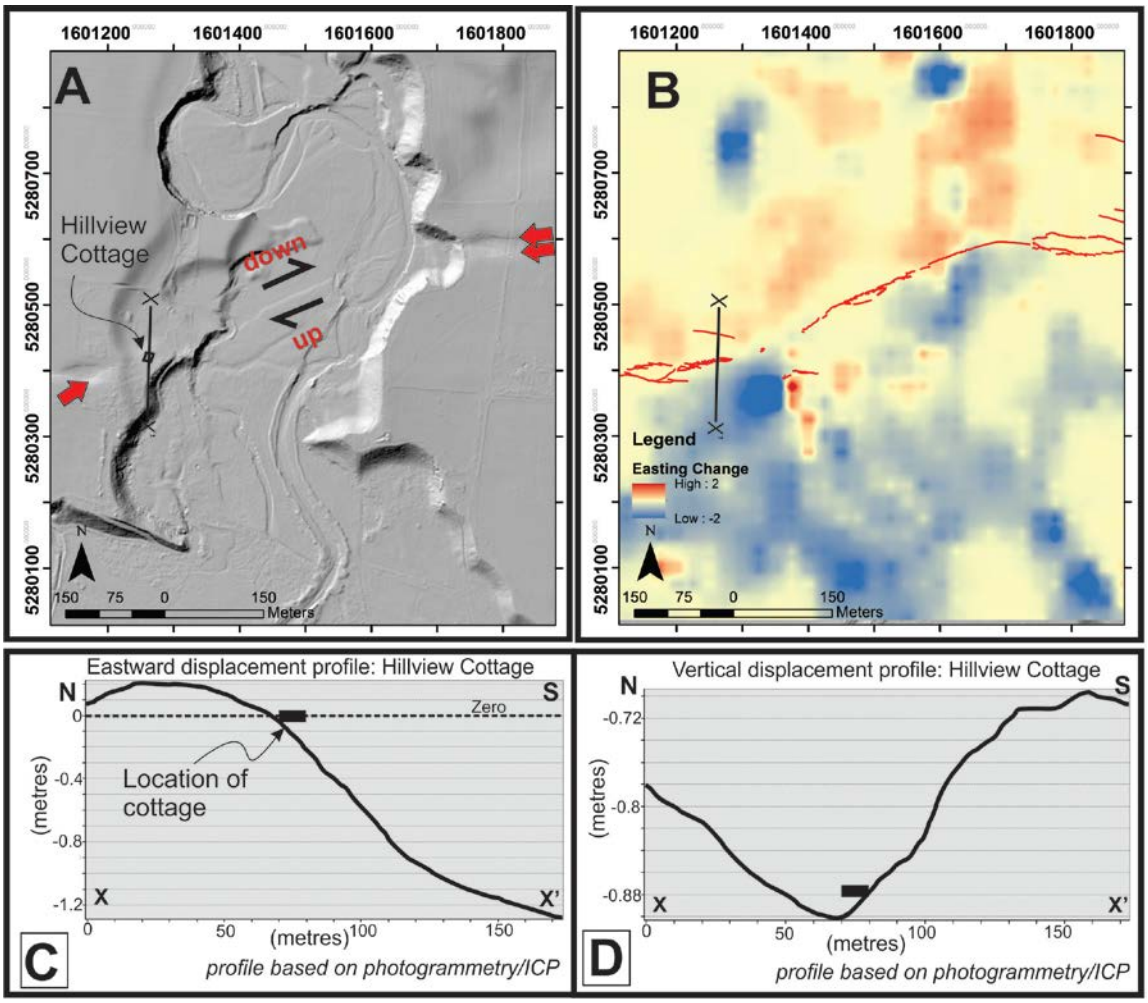

Figure A2.29 Hillview Cottage and The Humps Fault surface rupture. (A) LiDAR hill shade DEM showing location of the cottage within a relatively narrow fault rupture deformation zone (red arrows). (B) Raster of displacement in the east direction (positive is east, negative is west) calculated using ICP method described in text. Some anomalies and artefacts of the grid exist within the dataset, but the overall pattern is one of predominantly dextral displacement. West of the cottage is a small pull-apart, while the 100-m-scale fault geometry is that of a restraining bend. (C, D) The eastward and vertical deformation profiles from X to X', respectively. Y-axis exaggeration in (C) = 60. Y-axis exaggeration in (D) = 385.

A2.5 Discussion

Characterising the hazards associated with surface fault rupture and developing design strategies to mitigate those hazards have been the focus of several publications by JD Bray (e.g. Bray 2001, 2009; Bray and Kelson 2006). In these, he consistently highlights four principal means for mitigating the hazard posed by ground-surface fault rupture:

- land-use planning
- engineering geology
- geotechnical engineering, and
- structural engineering.

Depending on fault rupture characteristics and site conditions, he advocates several potentially effective design measures that include: establishing non-arbitrary setback distances; constructing earth fills to partially absorb and distribute underlying rupture; isolating foundations from underlying ground movement (e.g. through the use of slip layers); and designing strong, ductile foundations that resist imposed earth pressures.

Observations of building response in recent New Zealand ground-surface fault rupture earthquake are supportive of Bray's recommendations. Those houses with lightly reinforced concrete slab foundations would have benefited from having foundations that were stronger and more ductile and/or able to isolate underlying fault rupture from the overlying house. Buildings less damaged by surface rupture deformation were those that had foundations that were strong enough to resist imposed strains or isolated ground deformation (wholly or partly) from the superstructure. From the perspective of post-event reinstatement, buildings that performed best also had the capacity to tilt and rotate as a rigid body, thereby limiting the amount of internal deformation/damage. For buildings that could be subjected to tilting due to surface rupture deformation, design measures that not only limit damage, but also facilitate re-levelling are advantageous.

In a large earthquake, surface fault rupture deformation places additional demands on structures, compared to similar structures exposed only to strong ground shaking. Based on the building damage examples presented in this Appendix, some pertinent observations can be made regarding the performance of New Zealand residential structures when subjected to surface fault rupture deformation of varying levels of strain and amounts of displacement.

1. Single-storey, regular-shaped, timber-framed residential structures with light roofs and of modest dimensions (floor area of ≤~200 m^2) subjected to low/moderate surface fault rupture deformation (i.e. shear strains ≤10^{-2} and discrete displacements of decimetre-scale or less) do not appear to pose a collapse hazard.
2. At those levels of deformation, the prospects of damage control and repairability (and therefore post-event functionality) appear to be improved for such residential structures if the cladding contributes to the robustness to the superstructure (e.g. plywood, timber weatherboard) and is not brittle.
3. This favourable behaviour is enhanced if building systems moderate the direct transmission of ground deformation into the superstructure (either by decoupling or by other means) and allow for re-levelling of the structure post-event. For additional discussion regarding the mitigation of surface fault rupture hazard via the decoupling of ground deformation from the superstructure, see, for example, Lazarte et al. (1994), Murbach et al. (1999), Bray (2001, 2009), Bray and Kelson (2006), Van Dissen et al. (2011) and Oettle and Bray (2013).
4. For residential structures with the above-mentioned attributes, non-collapse performance can be achieved at even higher levels of strain (~10^0) and larger discrete displacements (metre-scale) in a predominantly horizontal displacement setting (i.e. strike-slip) if the superstructure decouples from (is isolated from) the underlying ground deformation. Our New Zealand dataset does not contain examples of the performance of residential structures subjected to such large surface fault rupture strains and displacements in a predominantly vertical displacement setting. In a horizontal displacement setting, the decoupled superstructure still rests on (and is supported by) the ground. This may not be the case in a predominantly vertical displacement setting where there is the possibility that fault rupture will leave a significant portion of the decoupled superstructure un-supported and this may lead, if not to collapse, then at least to significant tilting and angular distortions. In addition, in a reverse/thrust vertical displacement setting, there is the potential for a 'bulldozer zone' to develop at the base of the scarp where fault displacement forces the scarp to thrust horizontally across the ground surface, and this too can severely impact structures (Kelson et al. 2001).

In New Zealand, the primary document providing guidance with regards to the mitigation of surface fault rupture hazard is the Ministry for the Environment (MfE) report titled 'Planning for development of land on or close to active faults: A guideline to assist resource management planners in New Zealand' (Kerr et al. 2003; see also Van Dissen et al. 2006). In this guidance document, with its life-safety focus, a distinction is made between single-storey timber-framed residential structures (Building Importance Category 2a structures – i.e. BIC 2a structures) and other normal structures (BIC 2b structures), with more permissive resource consent categories applied to the former. The non-collapse performance of single-storey timber-framed structures when subjected to surface fault rupture in the 2010 Darfield and 2016 Kaikōura earthquakes strongly supports this distinction. In addition, the MfE document makes a distinction between *well-defined* (i.e. concentrated) deformation and *distributed* deformation, with more restrictive resource consent categories applied to the former. Our observations that the severity of damage, in general, increases with both increasing total displacement and increasing strain supports this distinction.

The MfE guidance document also recommends that the siting and construction of a BIC 2a structure (i.e. single-storey timber-framed house) in a greenfield setting within a distributed deformation zone of an active fault with a recurrence interval ≤3500 years be considered a *Discretionary* activity. However, given the life-safety focus of the MfE guidance document, and the non-collapse performance of BIC 2a structures – especially when subjected to distributed lower-strain surface fault rupture deformation, consideration could be given to adopting a more permissive resource consent category such as *Controlled*. Nevertheless, we must stress that consideration of more permissive resource consent categories is only germane from a life-safety perspective. From a damage-control perspective, or a post-event-functionality perspective, application of more permissive resource consent categories will, in general, run counter to those objectives.

A2.6 Conclusions

About two dozen buildings, typically single-storey timber-framed houses, barns and woolsheds with regular shaped floor plans and lightweight roofing materials, have been directly impacted by surface fault rupture in recent New Zealand earthquakes. The amount and style of surface rupture deformation varied considerably, ranging from decimetre-scale distributed folding with estimated shear strains in the order of $\leq 10^{-2}$, to metre-scale discrete rupture with estimated shear strains up to 10^{0}. While the severity of damage generally increased with both increasing total displacement and increasing strain, none of these buildings collapsed. From a life-safety standpoint, all of these buildings performed well and provide insight into construction styles that could best be employed to facilitate non-collapse performance resulting from surface fault rupture and, in certain instances, post-event functionality.

A2.7 Appendix 2 References

Anderson H, Webb T. 1989. The rupture process of the 1987 Edgecumbe earthquake, New Zealand. *New Zealand Journal of Geology and Geophysics*. 32(1):43–52. doi:10.1080/00288306.1989.10421387.

Bastin SH, Ogden M, Wotherspoon LM, van Ballegooy S, Green RA, Stringer M. 2018. Geomorphological influences on the distribution of liquefaction in the Wairau Plains, New Zealand, following the 2016 Kaikōura earthquake. *Bulletin of the Seismological Society of America*. 108(3B):1683–1694. doi:10.1785/0120170248.

Beanland S, Berryman KR, Blick GH. 1989. Geological investigations of the 1987 Edgecumbe earthquake, New Zealand. *New Zealand Journal of Geology and Geophysics*. 32(1):73–91. doi:10.1080/00288306.1989.10421390.

Beavan J, Samsonov S, Motagh M, Wallace L, Ellis S, Palmer N. 2010. The Darfield (Canterbury) earthquake: geodetic observations and preliminary source model. *Bulletin of the New Zealand Society for Earthquake Engineering*. 43(4):228–235. doi:10.5459/bnzsee.43.4.228-235.

Bradley BA, Razafindrakoto HNT, Ahsan Nazer M. 2017. Strong ground motion observations of engineering interest from the 14 November 2016 M_W 7.8 Kaikōura, New Zealand earthquake. *Bulletin of the New Zealand Society for Earthquake Engineering*. 50(2):85–93. doi:10.5459/bnzsee.50.2.85-93.

Bray JD. 2001. Developing mitigation measures for the hazards associated with earthquake surface fault rupture. In: *A Workshop on Seismic Fault-Induced Failures: possible remedies for damage to urban facilities, Tokyo, Japan, 11–12 January 2001*. Tokyo (JP): Japan Society for the Promotion of Science. p. 55–79.

Bray JD. 2009. Designing buildings to accommodate earthquake surface fault rupture. In: Goodno B, editor. *ATC and SEI Conference on Improving the Seismic Performance of Existing Buildings and Other Structures*. 2009 Dec 9–11; San Francisco (CA). Reston (VA): American Society of Civil Engineers. p. 1269–1280.

Bray JD, Kelson KI. 2006. Observations of surface fault rupture from the 1906 earthquake in the context of current practice. *Earthquake Spectra*. 22(2-suppl):69–89. doi:10.1193/1.2181487.

Clark KJ, Nissen E, Howarth JD, Hamling I, Mountjoy J, Ries W, Jones K, Goldstien S, Cochran U, Villamor P, et al. 2017. Highly variable coastal deformation in the 2016 M_W7.8 Kaikōura earthquake reflects rupture complexity along a transpressional plate boundary. *Earth and Planetary Science Letters*. 474:334–344. doi:10.1016/j.epsl.2017.06.048.

Cubrinovski M, Bray JD, de la Torre C, Olsen MJ, Bradley BA, Chiaro G, Stocks E, Wotherspoon L. 2017. Liquefaction effects and associated damages observed at the Wellington CentrePort from the 2016 Kaikoura earthquake. *Bulletin of the New Zealand Society for Earthquake Engineering*. 50(2):152–173. doi:10.5459/bnzsee.50.2.152-173.

Dellow S, Massey C, Cox S, Archibald G, Begg J, Bruce Z, Carey J, Davidson J, Della Pasqua F, Glassey P, et al. 2017. Landslides caused by the Mw7.8 Kaikōura earthquake and the immediate response. *Bulletin of the New Zealand Society for Earthquake Engineering*. 50(2):106–116. doi:10.5459/bnzsee.50.2.106-116.

Downes GL, Dowrick DJ. 2014. Atlas of isoseismal maps of New Zealand earthquakes: 1843–2003. 2nd ed. (revised). Lower Hutt (NZ): GNS Science. 1 DVD. (GNS Science monograph; 25).

Duffy B, Quigley M, Barrell DJA, Van Dissen R, Stahl T, Leprince S, McInnes C, Bilderback E. 2013. Fault kinematics and surface deformation across a releasing bend during the 2010 M_W 7.1 Darfield, New Zealand, earthquake revealed by differential LiDAR and cadastral surveying. *GSA Bulletin*. 125(3–4):420–431. doi:10.1130/b30753.1.

Forsyth PJ, Barrell DJA, Jongens R, compilers. 2008. Geology of the Christchurch area [map]. Lower Hutt (NZ): GNS Science. 67 p. + 1 folded map, scale 1:250,000. (GNS Science 1:250,000 geological map; 16).

Gledhill KR, Ristau J, Reyners ME, Fry B, Holden C. 2010. The Darfield (Canterbury) earthquake of September 2010: preliminary seismological report. *Bulletin of the New Zealand Society for Earthquake Engineering*. 43(4):215–221. doi:10.5459/bnzsee.43.4.215-221.

Hamling IJ, Hreinsdóttir S, Clark K, Elliott J, Liang C, Fielding E, Litchfield N, Villamor P, Wallace L, Wright TJ, et al. 2017. Complex multifault rupture during the 2016 Mw 7.8 Kaikōura earthquake, New Zealand. *Science*. 356(6334):eaam7194. doi:10.1126/science.aam7194.

Holden C, Beavan RJ, Fry B, Reyners ME, Ristau J, Van Dissen RJ, Villamor P, Quigley M. 2011. Preliminary source model of the M_W 7.1 Darfield earthquake from geological, geodetic and seismic data. In: *Ninth Pacific Conference on Earthquake Engineering: building an earthquake resilient society, April 14–16, 2011, University of Auckland, Auckland, New Zealand*. Auckland (NZ): 9PCEE. Paper 164.

Holden C, Kaiser AE, Van Dissen RJ, Jury R. 2013. Sources, ground motion and structural response characteristics in Wellington of the 2013 Cook Strait earthquakes. *Bulletin of the New Zealand Society for Earthquake Engineering*. 46(4):188–195. doi:10.5459/bnzsee.46.4.188-195.

Hornblow S, Quigley M, Nicol A, Van Dissen RJ, Wang N. 2014. Paleoseismology of the 2010 M_W 7.1 Darfield (Canterbury) earthquake source, Greendale Fault, New Zealand. *Tectonophysics*. 637:178–190. doi:10.1016/j.tecto.2014.10.004.

Kaiser A, Balfour N, Fry B, Francois-Holden C, Litchfield N, Gerstenberger M, D'Anastasio E, Horspool N, McVerry G, Ristau J, et al. 2017. The 2016 Kaikōura, New Zealand, earthquake: preliminary seismological report. *Seismological Research Letters*. 88:727–739. doi:10.1785/0220170018.

Kearse J, Little TA, Van Dissen RJ, Barnes PM, Langridge R, Mountjoy J, Ries W, Villamor P, Clark KJ, Benson A, et al. 2018. Onshore to offshore ground-surface and seabed rupture of the Jordan–Kekerengu–Needles fault network during the 2016 Mw 7.8 Kaikōura earthquake, New Zealand. *Bulletin of the Seismological Society of America*. 108(3B):1573–1595. doi:10.1785/0120170304.

Kelson KI, Kang K-H, Page WD, Lee C-T, Cluff LS. 2001. Representative styles of deformation along the Chelungpu Fault from the 1999 Chi-Chi (Taiwan) Earthquake: geomorphic characteristics and responses of man-made structures. *Bulletin of the Seismological Society of America*. 91(5):930–952. doi:10.1785/0120000741.

Kerr J, Nathan S, Van Dissen RJ, Webb P, Brunsdon D, King AB. 2003. Planning for development of land on or close to active faults: a guideline to assist resource management planners in New Zealand. Wellington (NZ): Ministry for the Environment; [accessed 2020 May]. https://www.mfe.govt.nz/sites/default/files/media/RMA/planning-development-faults-graphics-dec04%20(1).pdf.

Langridge RM, Ries WF, Litchfield NJ, Villamor P, Van Dissen RJ, Barrell DJA, Rattenbury MS, Heron DW, Haubrock S, Townsend DB, et al. 2016. The New Zealand Active Faults Database. *New Zealand Journal of Geology and Geophysics*. 59(1):86–96. doi:10.1080/00288306.2015.1112818.

Langridge R, Rowland J, Villamor P, Mountjoy J, Townsend D, Nissen E, Madugo C, Ries W, Gasston C, Canva A, et al. 2018. Coseismic rupture and preliminary slip estimates for the Papatea Fault and its role in the 2016 Mw 7.8 Kaikōura, New Zealand, earthquake. *Bulletin of the Seismological Society of America*. 108(3B):1596–1622. doi:10.1785/0120170336.

Lazarte CA, Bray JD, Johnson AM, Lemmer RE. 1994. Surface breakage of the 1992 Landers earthquake and its effects on structures. *Bulletin of the Seismological Society of America*. 84(3):547–561.

Litchfield NJ, Villamor P, Dissen RJV, Nicol A, Barnes PM, A. Barrell DJ, Pettinga JR, Langridge RM, Little TA, Mountjoy JJ, et al. 2018. Surface rupture of multiple crustal faults in the 2016 Mw 7.8 Kaikōura, New Zealand, earthquake. *Bulletin of the Seismological Society of America*. 108(3B):1496–1520. doi:10.1785/0120170300.

Massey C, Townsend D, Rathje E, Allstadt KE, Lukovic B, Kaneko Y, Bradley B, Wartman J, Jibson RW, Petley DN, et al. 2018. Landslides triggered by the 14 November 2016 Mw 7.8 Kaikōura earthquake, New Zealand. *Bulletin of the Seismological Society of America*. 108(3B):1630–1648. doi:10.1785/0120170305.

Murbach D, Rockwell TK, Bray JD. 1999. The relationship of foundation deformation to surface and near-surface faulting resulting from the 1992 Landers earthquake. *Earthquake Spectra*. 15(1):121–144. doi:10.1193/1.1586032.

Nairn IA, Beanland S. 1989. Geological setting of the 1987 Edgecumbe earthquake, New Zealand. *New Zealand Journal of Geology and Geophysics*. 32(1):1–13. doi:10.1080/00288306.1989.10421383.

Nicol A, Khajavi N, Pettinga JR, Fenton C, Stahl T, Bannister S, Pedley K, Hyland-Brook N, Bushell T, Hamling I, et al. 2018. Preliminary geometry, displacement, and kinematics of fault ruptures in the epicentral region of the 2016 Mw 7.8 Kaikōura, New Zealand, earthquake. *Bulletin of the Seismological Society of America*. 108(3B):1521–1539. doi:10.1785/0120170329.

Nissen E, Krishnan AK, Arrowsmith JR, Saripalli S. 2012. Three-dimensional surface displacements and rotations from differencing pre- and post-earthquake LiDAR point clouds. *Geophysical Research Letters*. 39(16):L16301. doi:10.1029/2012gl052460.

Oettle NK, Bray JD. 2013. Geotechnical mitigation strategies for earthquake surface fault rupture. *Journal of Geotechnical and Geoenvironmental Engineering*. 139(11):1864–1874. doi:10.1061/(ASCE)GT.1943-5606.0000933.

Pender MJ, Robertson TW. 1987. Edgecombe earthquake: reconnaissance report. *Bulletin of the New Zealand Society for Earthquake Engineering*. 20(3):201–249. doi:10.5459/bnzsee.20.3.201-249.

Power WL, Clark KJ, King DN, Borrero J, Howarth JD, Lane EM, Goring D, Goff J, Chagué-Goff C, Williams J, et al. 2017. Tsunami runup and tide-gauge observations from the 14 November 2016 M7.8 Kaikoura earthquake, New Zealand. *Pure and Applied Geophysics*. 174(7):2457–2473. doi:10.1007/s00024-017-1566-2.

Quigley M, Van Dissen RJ, Litchfield NJ, Villamor P, Duffy B, Barrell DJA, Furlong K, Stahl T, Bilderback E, Noble D. 2012. Surface rupture during the 2010 M_W 7.1 Darfield (Canterbury) earthquake: implications for fault rupture dynamics and seismic-hazard analysis. *Geology*. 40(1):55–58. doi:10.1130/g32528.1.

Quigley M, Van Dissen RJ, Villamor P, Litchfield NJ, Barrell DJA, Furlong K, Stahl T, Duffy B, Bilderback E, Noble D, et al. 2010. Surface rupture of the Greendale Fault during the Darfield (Canterbury) Earthquake, New Zealand: initial findings. *Bulletin of the New Zealand Society for Earthquake Engineering*. 43(4):236–242. doi:10.5459/bnzsee.43.4.236-242.

Stirling M, Litchfield N, Villamor P, Van Dissen RJ, Nicol A, Pettinga J, Barnes P, Langridge R, Little T, Barrell DJA, et al. 2017. The Mw7.8 Kaikōura earthquake: surface fault rupture and seismic hazard context. *Bulletin of the New Zealand Society for Earthquake Engineering*. 50(2):73–84.

Stringer ME, Bastin S, McGann CR, Cappellaro C, El Kortbawi M, McMahon R, Wotherspoon LM, Green RA, Aricheta J, Davis R, et al. 2017. Geotechnical aspects of the 2016 Kaikōura earthquake on the South Island of New Zealand. *Bulletin of the New Zealand Society for Earthquake Engineering*. 50(2):117–141. doi:10.5459/bnzsee.50.2.117-141.

Van Dissen RJ, Barrell DJA, Litchfield NJ, Villamor P, Quigley M, King AB, Furlong K, Begg JG, Townsend DB, Mackenzie H, et al. 2011. Surface rupture displacement on the Greendale Fault during the M_W 7.1 Darfield (Canterbury) Earthquake, New Zealand, and its impact on man-made structures. In: *Ninth Pacific Conference on Earthquake Engineering: building an earthquake resilient society, April 14–16, 2011, University of Auckland, Auckland, New Zealand*. Auckland (NZ): 9PCEE. 8p. Paper 186.

Van Dissen RJ, Heron DW, Becker JS, King AB, Kerr JE. 2006. Mitigating active fault surface rupture hazard in New Zealand: development of national guidelines, and assessment of their implementation. In: *8th US National Conference on Earthquake Engineering*; 2006 Apr 18–22; San Francisco, CA. Oakland (CA): Earthquake Engineering Research Institute. 10 p. Paper 633.

Van Dissen RJ, Stahl T, King A, Pettinga JR., Fenton C, Little TA, Litchfield NJ, Stirling MW, Langridge RM, Nicol A, et al. 2019. Impacts of surface fault rupture on residential structures during the 2016 Mw 7.8 Kaikōura earthquake, New Zealand. *Bulletin of the New Zealand Society for Earthquake Engineering*. 52(1):1–22. doi:10.5459/bnzsee.52.1.1-22.

APPENDIX 3 BUILDING IMPORTANCE CATEGORIES AND RELATIONSHIP WITH RECURRENCE INTERVALS

Table A3.1 Building Importance Categories from the MfE Active Fault Guidelines (Kerr et al. 2003).

Building Importance Category	Description	Examples
1	**Temporary structures** with low hazard to life and other property	• Structures with a floor area of <30 m^2 • Farm buildings, fences • Towers in rural situations
2a	**Timber-framed** residential construction	• Timber-framed single-storey dwellings
2b	**Normal structures** and structures not in other categories	• Timber-framed houses with area >300 m^2 • Houses outside the scope of NZS 3604 'Timber-Framed Buildings' • Multi-occupancy residential, commercial and industrial buildings accommodating <5000 people and <10,000 m^2 • Public assembly buildings, theatres and cinemas <1000 m^2 • Car parking buildings
3	**Important structures** that may contain people in crowds or contents of high value to the community or pose risks to people in crowds	• Emergency medical and other emergency facilities not designated as critical post-disaster facilities • Airport terminals, principal railway stations, schools • Structures accommodating >5000 people • Public assembly buildings >1000 m^2 • Covered malls >10,000 m^2 • Museums and art galleries >1000 m^2 • Municipal buildings • Grandstands >10,000 people • Service stations • Chemical storage facilities >500 m^2
4	**Critical structures** with special post-disaster functions	• Major infrastructure facilities • Air traffic control installations • Designated civilian emergency centres, medical emergency facilities, emergency vehicle garages, fire and police stations

Table A3.2 Relationship between fault recurrence interval and Building Importance Category, from the MfE Active Fault Guidelines.

<table>
<tr><th rowspan="2">Recurrence Interval Class</th><th rowspan="2">Average Recurrence Interval of Surface Rupture</th><th colspan="2">Building Importance (BI) Category Limitations (Allowable Buildings)</th></tr>
<tr><th>Previously Subdivided or Developed Sites</th><th>‘Greenfield’ Sites</th></tr>
<tr><td>I</td><td>≤2000 years</td><td>BI Category 1
Temporary buildings only</td><td rowspan="2">BI Category 1
Temporary buildings only</td></tr>
<tr><td>II</td><td>>2000–≤3500 years</td><td>BI Category 1 and 2a
Temporary and residential timber-framed buildings only</td></tr>
<tr><td>III</td><td>>3500–≤5000 years</td><td>BI Category 1, 2a and 2b
Temporary, residential timber-framed and normal structures</td><td>BI Category 1 and 2a
Temporary and residential timber-framed buildings only</td></tr>
<tr><td>IV</td><td>>5000–≤10,000 years</td><td rowspan="2">BI Category 1, 2a, 2b and 3
Temporary, residential timber-framed, normal and important structures (but not critical post-disaster facilities)</td><td>BI Category 1, 2a and 2b
Temporary, residential timber-framed and normal structures</td></tr>
<tr><td>V</td><td>>10,000–≤20,000 years</td><td>BI Category 1, 2a, 2b and 3
Temporary, residential timber-framed, normal and important structures (but not critical post-disaster facilities)</td></tr>
<tr><td>VI</td><td>>20,000–≤125,000 years</td><td colspan="2">BI Category 1, 2a, 2b, 3 and 4
Critical post-disaster facilities cannot be built across an active fault with a recurrence interval ≤20,000 years</td></tr>
</table>

Note: Faults with average recurrence intervals >125,000 years are not considered active.

www.gns.cri.nz

Principal Location

1 Fairway Drive, Avalon
Lower Hutt 5010
PO Box 30368
Lower Hutt 5040
New Zealand
T +64-4-570 1444
F +64-4-570 4600

Other Locations

Dunedin Research Centre
764 Cumberland Street
Private Bag 1930
Dunedin 9054
New Zealand
T +64-3-477 4050
F +64-3-477 5232

Wairakei Research Centre
114 Karetoto Road
Private Bag 2000
Taupo 3352
New Zealand
T +64-7-374 8211
F +64-7-374 8199

National Isotope Centre
30 Gracefield Road
PO Box 30368
Lower Hutt 5040
New Zealand
T +64-4-570 1444
F +64-4-570 4657